Time-dependent quantum transport: Causal superfermions, exact fermion-parity protected decay modes, and Pauli exclusion principle for mixed quantum states

R. B. Saptsov[1,2] and M. R. Wegewijs[1,2,3]
[1]*Peter Grünberg Institut, Forschungszentrum Jülich, 52425 Jülich, Germany*
[2]*JARA-Fundamentals of Future Information Technology*
[3]*Institute for Theory of Statistical Physics, RWTH Aachen, 52056 Aachen, Germany*
(Received 6 November 2013; revised manuscript received 22 May 2014; published 14 July 2014)

We extend the recently developed *causal* superfermion approach to the real-time diagrammatic transport theory to time-dependent decay problems. Its usefulness is illustrated for the Anderson model of a quantum dot with tunneling rates depending on spin due to ferromagnetic electrodes and/or spin polarization of the tunnel junction. This approach naturally leads to an exact result for one of the time-dependent decay modes for any value of the Coulomb interaction compatible with the wideband limit. We generalize these results to multilevel Anderson models and indicate constraints they impose on renormalization-group schemes in order to recover the exact noninteracting limit.(i) We first set up a second quantization scheme in the space of *density operators* constructing "causal" field superoperators using the fundamental physical principles of causality/probability conservation and fermion-parity superselection (univalence). The time-dependent perturbation series for the time evolution is renormalized by explicitly performing the wideband limit on the superoperator level. As a result, the occurrence of destruction and creation superoperators are shown to be tightly linked to the physical short- and long-time reservoir correlations, respectively. This effective theory takes as a reference a *damped* local system, which may also provide an interesting starting point for numerical calculations of memory kernels in real time. (ii) A remarkable feature of this approach is the natural appearance of a *fermion-parity protected* decay mode which can be measured using a setup proposed earlier [Phys. Rev. B 85, 075301 (2012)]. This mode can be calculated exactly in the fully Markovian, infinite-temperature limit by leading-order perturbation theory, but surprisingly persists unaltered for finite temperature, for any interaction and tunneling spin polarization. (iii) Finally, we show how a Liouville-space analog of the *Pauli principle* directly leads to an exact expression in the noninteracting limit for the time evolution, extending previous works by starting from an arbitrary initial mixed state including spin and pairing coherences and two-particle correlations stored on the quantum dot. This exact result is obtained already in finite-order renormalized perturbation theory, which surprisingly is not quadratic but *quartic* in the field superoperators, despite the absence of Coulomb interaction. The latter fact we relate to the time evolution of the two-particle component of the mixed state, which is just the fermion-parity operator, a cornerstone of the formalism. We illustrate how the super-Pauli-principle also simplifies problems with nonzero Coulomb interaction.

DOI: 10.1103/PhysRevB.90.045407 PACS number(s): 73.63.Kv, 03.65.Yz, 05.60.Gg, 71.10.−w

I. INTRODUCTION

A. Experimental motivation

Quantum dynamics of open systems is of interest in various research fields, ranging from transport through meso- and nanoscopic systems, quantum information processing, and quantum optics to physical chemistry and biology. Typically, the object of investigation is some smaller part of a larger system, e.g., a single molecule attached to macroscopically large contacts, which act as reservoirs and impose strong nonequilibrium boundary conditions. In the field of quantum transport a high degree of control has been achieved over *fermionic* subsystems, such as few-electron quantum dots coupled to various kinds of electrodes (e.g, metals, ferromagnets, or superconductors). This control relies mostly on the strong electrostatic effects, which for very small systems makes the theoretical description challenging. This progress has enabled detailed studies of not only stationary but also of time-dependent transport phenomena [1–9] down to the scale of atomic quantum dots [10,11]. Interaction effects in the time domain have been investigated early on, such as the SET oscillations in the weak tunnel coupling regime [12], and continue to be of interest [13]. Quantum fluctuations between such a strongly correlated dot and the electrodes lead to additional effects, such as level renormalization, inelastic tunneling effects, and Kondo physics in stationary transport and their nontrivial signatures in the time domain have also attracted interest. A problem that received quite some attention is the time-dependent response of a quantum dot in the Kondo regime [14–17]. Theoretically, it has been studied using various models and methods [18–26]. For instance, when starting from a Kondo model description [19,20,27], the real-time diagrammatic approach [24], which is at the focus of this paper, provides deep analytical insight into the renormalization of exchange interactions as well as the renormalization of the various dissipative effects that ultimately destroy the Kondo effect. On the other hand, recent numerical studies starting from an Anderson model [18,21,25,26,28] have investigated the development of the Kondo effect in time, in particular, the much debated splitting of the Kondo peaks [29]. Application of the real-time diagrammatic approach to the Anderson model at $T = 0$ is of high interest as it can provide analytical insight, especially regarding the time evolution towards stationarity. Outside the Kondo regime we recently reported some progress

in this direction in the stationary limit [30] and noted an interesting relation to the time-evolution decay modes that were studied before in the weak/moderate tunnel coupling limit [31]. In Ref. [31], motivated by experimental progress on single-electron sources [6,7], new measurement setups were suggested to probe the relaxation rates of a quantum dot [32] using a quantum point contact (QPC). This study and a more recent one [33] focused on the effect of the Coulomb interaction and surprisingly found that certain multiparticle correlators show a remarkable robustness with respect to most details of the setup (see below), in particular to the interaction. As argued there, this absence of interaction corrections is really an effect that can be measured. A key result of the present paper, expressed by Eq. (111), is that this conclusion holds beyond various of the approximations made in Ref. [31,33]. This result can be written as follows:

$$\langle (n_\uparrow - \tfrac{1}{2})(n_\downarrow - \tfrac{1}{2})\rangle(t) = e^{-\Gamma t}\langle (n_\uparrow - \tfrac{1}{2})(n_\downarrow - \tfrac{1}{2})\rangle(0) + \cdots . \tag{1}$$

Here n_σ, $\sigma = \downarrow, \uparrow$ are the spin-resolved occupations of the dot. The (equal-time) two-particle correlation function (1) contains a term that decays strictly Markovian with rate Γ. This function appears as a coefficient in the expansion of the mixed state of the quantum dot. It has been shown [31,33] that the experimental observation of the decay of the mixed *state* is possible: One can optimally choose the parameters that determine the initial and final states of the time-dependent decay such that on a well-separated time scale the current through a detector coupled to the quantum dot directly probes this part of the decay (1). This has been worked out in detail for a QPC detector in Ref. [31] and was recently extended to a quantum-dot detector [33]. It is therefore of interest to calculate the full mixed-state dynamics and not just focus on the current through the quantum dot itself, which does not reveal this effect. This is undertaken here: Motivated by the above experimental connection, we investigate the mixed-state dynamics and our conclusions strengthen the experimental importance of this effect. First, the decay is exactly exponential in the wideband limit; i.e., the Markovian assumption made in Refs. [31,33] continues to hold, but only for this special mode. Second, this form of the decay is valid for any tunnel coupling, including possible spin dependence: Still, Γ in Eq. (1) is simply given by the sum of the golden rule expressions for the spin-resolved tunnel rates of the various junctions $r = L,R$: $\Gamma = \sum_{r\sigma} \Gamma_{r\sigma}$; cf. Eq. (23). Finally, we show that any more realistic quantum-dot model taking into account multiple orbitals labeled by l has such a "protected" mode, the decay rate being $\Gamma = \sum_{rl\sigma} \Gamma_{rl\sigma}$. Notably, this is independent of the experimental details of the quantum dot as long as its energy scales are much below the electrode bandwidth. This can include more complex forms of the Coulomb interaction—including all local two-particle matrix elements, not just the charging part—or spin-orbit interaction, etc. The only crucial assumption is that the tunnel coupling is bilinear in the electron operators, a basic starting point of virtually all modeling of quantum transport through strongly interacting systems. In fact, even the simplifying assumption of collinear spin dependence of the tunneling made in this work turns out not to be crucial [34]. The interesting question is raised as to which physical principle can be responsible for this remarkable effect.

The theoretical importance of the key result (1) lies in the fact that it arises naturally in the real-time framework—by mere formulation, without real calculation—when using a particular kind of superfermion approach. This particular approach arose in the context of stationary-state transport problems [30] and further below we give an overview of other superfermion constructions. The experimental relevance of the striking result (1) thus *physically motivates* a reformulation of the general real-time framework. Perhaps the impact of this should be compared with that of second quantization in standard quantum mechanics and field theory, which by itself presents no new physical theory or prediction. That approach, however, had a big impact by making the general framework more intuitively accessible (e.g., by introducing field operators to represent quasiparticles), simplifying calculations to such an extent that their results become intuitively clear and often revealing their physical origin (e.g, particle exchange). Such a second quantization scheme is well established for closed quantum systems but is still under active study for open systems (see below). Only recently, this idea has been combined with the real-time diagrammatic theory targeting stationary transport [30]. By itself, the real-time diagrammatic theory is already a very successful framework for the calculation of transport properties of nanoscale, strongly interacting systems [35], allowing various levels of approximations to be systematically formulated and worked out, both analytically [36–38] and numerically [39–41], which have found application to transport experiments [42–47]. Any general progress in simplifying or clarifying the general structure of this theory is therefore ultimately of experimental relevance since more accurate approximations come within reach. For example, as mentioned above, the Anderson model and its generalizations present technical obstacles for gaining analytical insight into the low-T nonequilibrium physics. By combining it with a superfermion technique, we were able to make detailed predictions [30] at $T = 0$ for measurable stationary dI/dV maps, covering large parameter regimes for strong interactions. This includes level renormalization effects, energy-dependent broadening, charge-fluctuation renormalization of cotunneling peaks. The restriction of the approximations (only one plus two-loop renormalization-group diagrams), however, precluded a study of the Kondo regime for the Anderson model. Clearly, addressing the time-dependent problem for this model presents an even greater challenge. Therefore, the superfermion technique deserves further attention and development before such attempts are to be made.

Besides the aforementioned general indirect importance to experiments and the concrete nonperturbative predictions, (1) the present paper also reports an extensive discussion of the time dependence in the effectively noninteracting limit $U \ll \Gamma$. In contrast to previous works, we include spin coherence, electron-pair coherence (superconducting correlations [48]), and two-particle correlations in the initial state of the quantum dot. In addition to various theoretical motivations mentioned in the following, this limit is also of experimental relevance. For example, the mentioned highly controllable single-electron sources [6,7] can be understood very well in such a picture.

B. Theoretical motivation

The above-mentioned experimental progress thus motivates theoretical developments and in this paper we invest in a reexamination of the fundamental starting points of transport theory and show that they can be exploited more explicitly. As we now outline, this leads to the key physical principle underlying Eq. (1). To describe a quantum dot in the presence of the reservoirs one uses a mixed-state theoretical description. The mixed quantum state is described by the reduced density operator and can be conveniently considered as an element of a linear space of operators, referred to as Liouville space. The time evolution of the state is quite generally described by a kinetic or quantum master equation, whose time-nonlocal kernel or self-energy is a superoperator on this Liouville space. This picture is formally quite analogous to that of quantum mechanics of closed systems described in a Hilbert space. However, the Liouville-space self-energy describes dissipative/non-Hamiltonian dynamics, including non-Markovian memory effects.

Technically, the dynamics in Liouville space is more complicated because one needs to keep track of the evolution of state vectors (kets) as well as their adjoints (bras): In the language of Green's functions, the evolution on two Keldysh contours must be described. As a result, the usual concepts of quasiparticles corresponding to quantum field operators breaks down. For open *fermion* systems the anti-commutation sign presents additional problems in Liouville space [49–51].

To address such problems, Schmutz [49] introduced *superfermions*, i.e., analogs of quantum field operators that act on the many-particle Liouville space and obey a similar algebra. It was shown that these, in fact, generate the Liouville space starting from some vacuum supervector and can thus be used to construct mixed-state density operators. Following this analogy, insights from quantum field theory in Hilbert space could then also be applied to density-operator approaches to nonequilibrium systems [52–54]. In these works superfermions were applied mostly to Markovian quantum dynamics as described by a given self-energy or time-evolution kernel and were found to simplify the diagonalization of Lindblad time-evolution generators, in particular, finding their stationary eigenvectors [52].

In a recent work, Ref. [30], we have extended the application of superfermion techniques to the *derivation* of the reduced dynamics from a system-bath approach within the framework of the general real-time transport theory [55,56] formulated in Liouville-space [51]. This does not rely on Born and/or Markov approximations. Moreover, in contrast to the previous superfermion approaches [49,50,52,54,57], the special superfermions that are involved simultaneously incorporate the structure imposed by causality, [58,59] related to probability conservation [51], as well as the fermion-parity superselection rule of quantum mechanics [60]. The fermion-parity was already included by Schmutz [49], but turns out to play a far more prominent role. This causal structure furthermore exploits a Liouville-space analog of the "Keldysh rotation" [58], well-known from Green's function approaches. Although these particular *causal* superoperators were introduced earlier [51], their role as quantum fields in Liouville space was not recognized or taken advantage of. In this formulation of the real-time approach, the unit operator plays the special role of the vacuum state in Liouville-Fock space of the reduced system. However, physically this operator describes the *infinite-temperature* mixed quantum state of the reduced system with maximal von Neumann entropy. It was realized that there is a corresponding natural decomposition of the self-energy into an infinite-temperature part and non-trivial *finite-temperature* corrections. The causal superfermion operators are constructed in such a way to maximally simplify and emphasize this fundamental structure of the perturbation theory for self-energy kernels, for time-evolution, and for arbitrary observables. This is a general feature of open fermionic quantum systems which other superfermion formulations do not explicitly reveal. The causal superfermions, furthermore, translate other fundamental properties of the underlying Hilbert-Fock space fields in a particularly clear way [30], such as their irreducible transformation under spin and particle-hole symmetry transformations, as well as fluctuation-dissipation relations (related to the Liouville-space Wick theorem [51]).

One of the aims of this paper is to highlight simple applications of causal superfermions and illustrate the physical insight they convey into nonequilibrium transport through an Anderson quantum dot, sketched in Fig. 1. These particular quantum-field superoperators were introduced in the admittedly rather complicated context of Ref. [30], which constituted one of its major technical applications: Only by exploiting the properties of the causal superfermions the two-loop real-time renormalization-group (RG) calculation of the $T = 0$ transport could be kept tractable, even when using the minimalistic Anderson model for the quantum dot. This may convey the incorrect impression that superfermions are not useful in simpler calculations or that they even rely

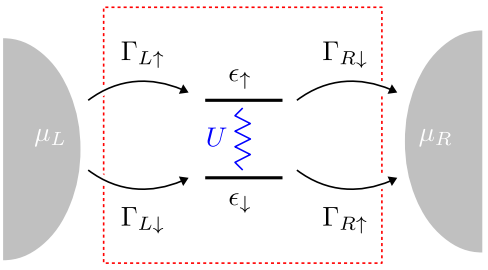

FIG. 1. (Color online) Anderson model with spin-dependent tunneling of electrons from reservoirs $r = L, R$ into orbitals with energy ϵ_σ and local Coulomb interaction U. The dependence of the tunneling on the spin $\sigma = \uparrow, \downarrow$ can arise either from the tunnel barriers or from a spin polarization of the density of states in the electrodes (e.g., ferromagnets) or from both. For simplicity, the magnetic field $\mathbf{B} = B\mathbf{e}_z$ that causes the Zeeman splitting $\epsilon_\uparrow - \epsilon_\downarrow = B$ and the axes of spin-polarization of the tunneling are assumed to coincide. The sum of all tunnel rates $\Gamma = \sum_{r,\sigma} \Gamma_{r\sigma}$ that connect the quantum dot to the electrodes turns out to be an *exact* decay rate in the interacting ($U \neq 0$) nonequilibrium Anderson model. The corresponding decay mode is the fermion-parity operator $(-1)^n$, a central quantity in the construction of the causal superfermions.

on the advanced RG machinery. Indeed, in Ref. [30] we already outlined how various aspects of the Liouville-space real-time approach are further clarified, independent of the RG formulated "on top" of it [61]. These more formal insights have already found useful applications to real-time calculations in several works [62–65] dealing with simpler problems and/or approximations. The superfermion approach also allowed an *exact* result to be found that is more specific to the Anderson model: [30] two complex-valued eigenvalues of the exact self-energy superoperator lie symmetric with respect to an average value depending on known, bare parameters. This implies a nonperturbative sum rule for the level positions *and* broadenings of nonequilibrium excitations of the quantum dot in the presence of coupling to the reservoirs and interaction. It was indeed noted earlier in real-time perturbation theory [66] and more recently in a Liouville-space Green's function study [67].

Time-dependence and fermion parity. Another exact result obtained using the causal superfermions provided more concrete physical insights into another previous work: We showed that generically the *exact* effective self-energy has an eigenvalue that is protected by the fermion-parity superselection rule of quantum mechanics. This eigenvalue corresponds to the experimentally measurable decay mode, the key result (1) mentioned in the previous section. Surprisingly, this decay mode depends only on the sum of all tunnel rate constants but not on any of the remaining parameters, *including the Coulomb interaction* U. Using the superfermion approach this result, first obtained perturbatively in Ref. [31], could be shown [30] to hold nonperturbatively in the tunnel coupling. However, our study, Ref. [30], did not consider spin-dependent tunneling, in contrast to Ref. [31], a restriction that we lift in this paper. Moreover, this result can be easily generalized for an arbitrary number of spin orbitals and, in fact, is independent of the details of the interaction on the quantum dot (i.e., the concrete form of the quantum-dot model Hamiltonian): only the wideband limit and the bilinear form of the tunnel Hamiltonian matter. This striking result motivates another aim of this paper, namely, to illustrate the usefulness of causal superfermions for time-dependent decay problems, rather than the stationary-state problems at the focus of Ref. [30]. The first part of the paper is concerned with formulating the general time-dependent perturbation theory using causal superfermions and discusses several insights offered into interacting problems. For instance, we show that the exact time-evolution superoperator has an effective expansion involving only causal "*creation* superoperators" with intermediate propagators which are exponentially *damped* in time, i.e., dissipative. This physical picture emerges when we integrate out Markovian correlations, leaving only that part of the bath dynamics that leads to the nontrivial, low-temperature phenomena in the Anderson model. This applies generally, i.e., also to interacting systems, and may be an interesting starting point for direct numerical simulation schemes of reduced dynamics [25,26,68–72], since it eliminates some "Markovian overhead" from the start. Throughout the paper we highlight such connections of admittedly formal expressions to physical insights, which is important for effectively applying the technique to more complex problems that have motivated this work.

Noninteracting limit: Super-Pauli principle. To most clearly highlight applications of causal superfermions, the second part of this paper focuses on the simplest case, the noninteracting limit ($U = 0$) of the Anderson model. Importantly, we include the spin—distinguishing it from the spinless noninteracting resonant level model (NRLM)—and we also include a magnetic field and spin dependence of the tunneling.

First, our study provides a clear illustration of how the causal field superoperators allow one to deal with large fermionic Liouville spaces encountered in transport problems. (Already for the very simplistic single-level Anderson model the dimension of this space equals 16.) We show by direct calculation that in the noninteracting limit the perturbation theory—after a simple skeleton resummation that exploits the wideband limit (a *discrete* renormalization step [51])—naturally terminates at the second loop order. Moreover, the lack of interactions on the quantum dot results in an additional simplification, namely, that the two-loop part of the time-evolution superoperator factorizes. As we show, this is less clear when considering the two-loop self-energy in Laplace space as is often done when focusing on stationary-state properties [39–41]. Most importantly, we show that this termination and factorization directly follow from the fundamental anticommutation relations of the causal fermionic superoperators. The termination is, in fact, a consequence of the *super-Pauli principle*, the Liouville-space analog of the corresponding principle in the Hilbert-space of the quantum mechanics of closed systems, which additionally relies on the independent principle of fermion-parity superselection (this principle is discussed in Sec. II A). Interaction effects bring additional complications, and also here the causal superfermions bring about simplifications, some of which were not yet noted in Ref. [30] and are pointed out here.

Second, the analysis of the noninteracting limit provides an important benchmark for studies employing the real-time transport theory. This approach is tailored to deal with strongly interacting problems, but it has proven difficult to see on a general level how the exact solution of the noninteracting limit is recovered, in particular, when including the effect of multiple spin orbitals. Without spin, the exact solutions were checked to be reproduced explicitly by nonperturbative diagrammatic summation [73,74], but the simplifications due to the vanishing of interactions arise only after a detailed analysis of cancellations. In the presence of spin and orbital degeneracies, this is even less obvious when working with explicit, model-dependent matrix representations of superoperators in large Liouville spaces required for interacting systems. Our application of the causal superfermion approach to the real-time formalism shows immediately how the noninteracting limit is correctly reached on the general *superoperator* level. This illustrates that it may actually pay off to understand the noninteracting limit in the best possible way, when one is interested in addressing interacting problems and even when one is not expanding around the noninteracting limit. So far this aspect has not been given much attention within the real-time framework.

Third, the causal superfermion formulation also facilitates comparison of the real-time transport theory with other approaches, which usually take the noninteracting limit as a reference (using, e.g., path integrals or Green's functions) and

therefore always contain its solution explicitly on a general level.

Our previous study, Ref. [30], provides an example for which the stationary, noninteracting limit of the Anderson model—exhaustively analyzed here—functions as a benchmark. The one- plus two-loop real-time RG approach worked out there has the important property that it includes the exact solution for the noninteracting limit $U = 0$, while for large U it still provides a good approximation that is nonperturbative in Γ. It was found that even for the noninteracting limit one still needs a full one- plus *two*-loop RG to obtain the exact density operator. Reformulated, the exact effective Liouvillian of the quantum dot turns out to be *quartic* (instead of quadratic) in the field superoperators. This may seem to be surprising at first in view of the absence of interactions. As mentioned above, in the present paper we show that although the renormalized perturbation theory terminates, it does so only at the *second* loop order (i.e., terms quartic in the fields), finding explicit agreement with the stationary RG results [30] for the full density matrix, self-energy, and charge current. The time-dependent solution for the current in the spinless noninteracting Anderson model was also used as a benchmark for another real-time RG study [75], dealing with the interacting resonant level model in the limit where the nonlocal interaction coupling between the quantum dot and the reservoirs vanishes. The benchmark result of the present paper provides the complete time-dependent propagator, density operator, as well as the current and also includes the spin.

Combined with the second quantization tools of causal superfermions, the real-time Liouville-space approach becomes a more accessible tool for dealing with noninteracting problems. Such problems continue to attract attention [76,77], especially regarding non-Markovian effects that arise beyond the wideband limit, for which no general analytic solution seems to be known. In the wideband limit, noninteracting problems can be solved by means of various other techniques, for both the stationary limit [78] and the transient approach [79]. However, we demonstrate how in the real-time approach the full time-evolution can be calculated quite straightforwardly in this limit, i.e., avoiding a self-energy calculation and without transforming to Laplace space and back. In the description of the noninteracting decay we include the effects of spin and pairing coherence and of two-particle correlations in the initial quantum-dot state that have been ignored so far. Solving such problems with the real-time approach has the additional advantage of directly allowing one to gauge the effect of interactions and to include them in either a perturbative or a nonperturbative way. A case in point is the key result for fermion-parity protected decay mode [Eq. (1)]. Finally, our formulation also provides a framework for calculating corrections beyond the wideband limit.

Outline. The paper is organized as follows. In Sec. II, we directly formulate the model in Liouville-space notation, introduce the causal superfermion fields, construct the Liouville-Fock space, and formulate the super-Pauli principle. In Sec. III, we formulate the time-dependent Liouville-space perturbation theory and derive a renormalized series that explicitly incorporates the wideband limit on the superoperator level. We give general rules for the simplifications that arise in the noninteracting ($U = 0$) limit. This critically relies on the causal structure which is made explicit by the causal superfermions. Importantly, in this limit the renormalized series naturally terminates at the second loop, and higher-order corrections are identically equal to zero. This analysis also reveals the special importance of the physical infinite-temperature limit $T \to \infty$, serving as a reference point for both the construction of Liouville-Fock space and the renormalized perturbation theory. In Sec. IV, we perform the explicit one- and two-loop calculations, giving the exact, full time-evolution propagator, the density operator, and the charge current in the noninteracting limit ($U = 0$). To better understand the stationary limits of these results and to directly compare with the real-time RG results of Ref. [30], we additionally perform the calculation directly in Laplace space. We summarize our results in Sec. V and discuss their generalization to multiple orbitals, the implications for real-time RG schemes, and possible further application of the developed ideas.

II. ANDERSON MODEL IN LIOUVILLE-FOCK SPACE

A. Fermion-parity superselection rule

In this paper, we make explicit use of the postulate of fermion-parity (or univalence) superselection in quantum mechanics and quantum field theory [60,80]. It is a part of quantum kinematics and can therefore be discussed before any model of the dynamics is formulated. Here we briefly illustrate the main substance of this postulate and discuss one of its aspects, which is crucial for starting up the formulation of our approach in the following. For example, for a single-level quantum dot with field operators d_σ and $d_\sigma^\dagger$, where $\sigma = \pm$ corresponds to spin up ($\uparrow$) and down ($\downarrow$) along the z axis, the fermion-parity operator, recurring at many crucial steps in the paper, is defined as

$$(-1)^n := e^{i\pi n} = \prod_\sigma (1 - 2n_\sigma), \tag{2}$$

where $n = \sum_\sigma n_\sigma$ is the fermion number operator. For this simple case, the fermion-parity superselection rule can be phrased as follows [81]: The density operator and the operator of any physical observable A must commute with the total fermion-parity operator of the system,

$$[(-1)^n, A]_- = [(-1)^n, \rho]_- = 0. \tag{3}$$

This excludes the possibility of interference (superpositions of) states with even and odd number of fermions. The operator $(-1)^n$ has been applied in Ref. [82] to make field operators for different fermion species commute (rather than anticommute), and it plays a key role in setting up the second quantization in Liouville space.

Here and in the following, it is convenient to introduce an additional particle-hole index η:

$$d_{\eta\sigma} = \begin{cases} d_\sigma^\dagger, & \eta = +, \\ d_\sigma, & \eta = -. \end{cases} \tag{4}$$

Throughout the paper we denote the inverse value of a two-valued index with a bar, e.g.,

$$\bar{\eta} = -\eta. \tag{5}$$

We combine all indices into a multi-index variable written as a number,

$$1 = \eta,\sigma, \quad \bar{1} = \bar{\eta},\sigma, \tag{6}$$

where, by way of exception, the bar denotes inversion of the particle-hole index only. If we have more than one multi-index, we distinguish their components by using the multi-index number as a subscript: $1 = \eta_1,\sigma_1,r_1,\omega_1, 2 = \eta_2,\sigma_2,r_2,\omega_2$ and use a multi-index Kronecker symbol

$$\delta_{12} = \delta_{\eta_1,\eta_2}\delta_{\sigma_1,\sigma_2}. \tag{7}$$

For clarity, we usually omit these subscripts if there is only one multi-index as in Eq. (6). Then $d_1 = d_{\eta\sigma}$ and $d_{\bar{1}} = d_{-\eta\sigma}$, and we can summarize all fundamental relations simply by $(d_1)^\dagger = d_{\bar{1}}$ and $[d_1,d_2]_+ = \delta_{1\bar{2}}$. Throughout the paper, we denoted the (anti)commutators by $[A,B]_- = AB - BA$ and $[A,B]_+ = AB + BA$.

A first application of the fermion parity arises when we connect the quantum dot to reservoirs with field operators $a_{\sigma rk}$, where σ is the spin index, k the orbital index, and the reservoir index $r = \pm$ corresponds to left/right. We have to make a *choice* for commutation relations of $a_{\eta\sigma rk}$ relative to $d_{\eta'\sigma'}$: In setting up the second quantization, one is free to choose either commutation or anticommutation relations for fermions of different states/particles, whereas one *must* have anticommutation relations for fermions in the same state [83]. Both choices produce identical, correctly antisymmetrized multiparticle states. Usually, the most elegant choice, indicated here by a prime on the field operators, is to let them all anticommute,

$$[a'_1,d'_2]_+ = 0, \tag{8a}$$

$$[d'_1,d'_2]_+ = \delta_{1\bar{2}}, \tag{8b}$$

$$[a'_1,a'_2]_+ = \delta_{1\bar{2}}. \tag{8c}$$

The fields are pairwise Hermitian adjoints, $(d'_1)^\dagger = d'_{\bar{1}}$ and $(a'_1)^\dagger = a'_{\bar{1}}$. The fermion number operator of the dot is expressed as $n = \sum_\sigma {d'_\sigma}^\dagger d'_\sigma$ and the corresponding fermion-parity operator anticommutes with the dot fields d'_1 (using $[(-1)^n]^2 = e^{2i\pi n} = 1$),

$$(-1)^n d'_1 (-1)^n = e^{i\pi n} d'_1 e^{-i\pi n} = -d'_1, \tag{9}$$

but commutes with the reservoir operators a'_1 (like any operator local to the dot),

$$a'_1(-1)^n = (-1)^n a'_1. \tag{10}$$

In approaches where the reservoir degrees of freedom are eliminated by a partial trace operation, it is much more convenient to let reservoir and dot fields *commute* by definition, allowing operators of different subsystems to be separated easily. By doing this from the start many unnecessary canceling sign factors can be avoided. Such fields are used throughout this paper and are indicated by leaving out the prime. The fields on the different (the same) systems mutually (anti)commute:

$$[a_1,d_2]_- = 0, \tag{11a}$$

$$[a_1,a_2]_+ = \delta_{1\bar{2}}, \tag{11b}$$

$$[d_1,d_2]_+ = \delta_{1,\bar{2}}, \tag{11c}$$

with $d_{\bar{1}}^\dagger = d_{\bar{1}}$ and $a_{\bar{1}}^\dagger = a_{\bar{1}}$. This choice of commutation relations was used in Refs. [51] and [30] and will be used here as well, unless stated otherwise.

The fermion-parity operator now appears as the formal device relating the above two choices, which is convenient to have at hand for a direct comparison with other approaches, e.g., the Green's function approach, [84] starting from the choice Eq. (8). One way of obtaining the choice in Eq. (11) from the fields satisfying Eq. (8) is the following change of variables:

$$a_1 = (-1)^n a'_1, \quad = a'_1(-1)^n, \tag{12a}$$

$$d_1 = -\eta_1(-1)^n d'_1 = \eta_1 d'_1(-1)^n. \tag{12b}$$

Here $(a_1)^\dagger = a_{\bar{1}}$ and the η sign ensures that the adjoint relation $(d'_1)^\dagger = d'_{\bar{1}}$ is also preserved: using Eq. (9) $(d_1)^\dagger = \eta_1(-1)^n(d'_1)^\dagger = -\eta_1(d'_1)^\dagger(-1)^n = \eta_{\bar{1}} d'_{\bar{1}}(-1)^n = d_{\bar{1}}$. A key point, needed later, is that when tracing out the reservoirs only averages of products of an even number of reservoir fermions can appear, and the quantum-dot operator $(-1)^n$ in Eq. (12a) cancels out in $\mathrm{Tr}_R a_1 \cdots a_{2k} = \mathrm{Tr}_R a'_1 \cdots a'_{2k}$ since $(-1)^{2kn} = 1$. The transformation (12) is only canonical *locally* on the quantum dot and on the reservoirs. Since it is not globally canonical we must check how observable operators are transformed. This is done in Sec. II B once we have specified the dynamics and the physical operators of interest.

B. Anderson model

The model that we consider was already sketched in Fig. 1. The usual formulation of the single-level Anderson model specifies the Hamiltonian

$$H = \epsilon n + BS_z + Un_\uparrow n_\downarrow, \tag{13}$$

where ϵ denotes the energy of the orbital and

$$n = \sum_\sigma n_\sigma, \quad n_\sigma = d_\sigma^\dagger d_\sigma, \tag{14}$$

is the fermion number operator [85]. Furthermore, $S_z = \frac{1}{2}\sum_\sigma \sigma n_\sigma$ is the z component of the spin vector operator $\mathbf{S} = \sum_{\sigma\sigma'} \frac{1}{2}\boldsymbol{\sigma}_{\sigma,\sigma'} d_\sigma^\dagger d_{\sigma'}$ along the external magnetic field $\mathbf{B} = B\mathbf{e}_z$ (in units $g\mu_B = 1$) and $\boldsymbol{\sigma}$ is the vector of Pauli matrices. The dot is attached to electrodes, which are treated as free electron reservoirs:

$$H^R = \sum_{\sigma,r,k} \epsilon_{\sigma rk} a^\dagger_{\sigma rk} a_{\sigma rk}. \tag{15}$$

The reservoir electron number and spin

$$n^R = \sum_r n^r, \quad \mathbf{s}^R = \textstyle\sum_r \mathbf{s}^r, \tag{16}$$

respectively, can be decomposed into their contributions $n^r = \sum_{\sigma,k} a^\dagger_{\sigma rk} a_{\sigma rk}$ and $\mathbf{s}^r = \sum_{\sigma,k} \frac{1}{2}\boldsymbol{\sigma}_{\sigma,\sigma'} a^\dagger_{\sigma rk} a_{\sigma' rk}$. Before we introduce the coupling, we introduce the notation of Ref. [30] to conveniently deal with the continuum limit. The reservoirs are described by a density of states $\nu_{r\sigma}(\omega) = \sum_k \delta(\omega - \epsilon_{\sigma rk} + \mu_r)$ and we go to the energy representation of the fermionic

operators,

$$a_{\sigma r}(\omega) = \frac{1}{\sqrt{\nu_r(\omega)}} \sum_k a_{\sigma r k} \delta(\omega - \epsilon_{\sigma r k} + \mu_r), \tag{17}$$

with the anticommutation relations:

$$[a_{\sigma r}(\omega), a^\dagger_{\sigma' r'}(\omega')]_+ = \delta_{\sigma,\sigma'} \delta_{r,r'} \delta(\omega - \omega'), \tag{18}$$

$$[a_{\sigma r}(\omega), a_{\sigma' r'}(\omega')]_+ = 0. \tag{19}$$

Here we denote (anti)commutators by $[A,B]_\mp = AB \mp BA$. The continuous reservoir Hamiltonian is thus

$$H^R = \sum_{\sigma,r} \int d\omega (\omega + \mu_r) a^\dagger_{\sigma r}(\omega) a_{\sigma r}(\omega), \tag{20}$$

with the electron energy ω taken relative to μ_r for reservoir r. The junctions connecting the dot and reservoirs are modeled by the tunneling Hamiltonian

$$V = \textstyle\sum_r V^r, \tag{21}$$

$$V^r = \sum_\sigma \int d\omega \sqrt{\nu_{r\sigma}(\omega)} [t_{r\sigma}(\omega) a^\dagger_{\sigma r}(\omega) d_\sigma + \text{H.c.}], \tag{22}$$

with real spin-dependent amplitudes $t_{r\sigma}(\omega)$. Using the spectral density

$$\Gamma_{r\sigma}(\omega) = 2\pi \nu_{r\sigma}(\omega) |t_{r\sigma}(\omega)|^2, \tag{23}$$

it is convenient to rescale the field operators:

$$b_{\sigma r}(\omega) = \sqrt{\frac{\Gamma_{r\sigma}(\omega)}{2\pi}} a_{\sigma r}(\omega). \tag{24}$$

We thus incorporate two sources of spin polarization of the tunneling rates: Either the attached electrodes are ferromagnetic [$\nu_{r\sigma}(\omega)$] or the tunnel junctions are magnetic [$t_{r\sigma}$], or both. We made the simplifying assumption that the magnetizations of the electrodes are collinear (either parallel or antiparallel) and also collinear with the spin-polarization axes of the tunnel junctions. Moreover, the external magnetic field **B** is assumed to be collinear with this axis.

As before, we introduce an additional particle-hole index,

$$b_{\eta\sigma r}(\omega) = \begin{cases} b^\dagger_{\sigma r}(\omega), \eta = +, \\ b_{\sigma r}(\omega), \eta = -, \end{cases} \tag{25}$$

and combine all indices into a multi-index variable written as a number, which now includes an additional continuous index ω [86]:

$$1 = \eta,\sigma,r,\omega, \quad \bar{1} = \bar{\eta},\sigma,r,\omega. \tag{26}$$

Then $b_1 = b_{\eta\sigma r}(\omega)$ and $b_{\bar{1}} = b_{-\eta,\sigma r}(\omega)$ and the (anti)commutation relations are

$$[d_1, b_2]_- = 0, \tag{27}$$

$$[d_1, d_2]_+ = \delta_{1\bar{2}}, \tag{28}$$

$$[b_1, b_2]_+ = \frac{\Gamma_1}{2\pi} \delta_{1\bar{2}}, \tag{29}$$

where $\Gamma_1 = \Gamma_{r\sigma}(\omega)$. In Eq. (29), it is left implicit that the multi-index δ function $\delta_{1\bar{2}}$ contains an additional δ function $\delta(\omega_1 - \omega_2)$ relative to the Kronecker δ (7) in Eq. (28).

Since we formulated our model in terms of fields obtained by a noncanonical transformation, we should now check the form of the model in terms of the (primed) anticommuting fields [Eq. (8)]. First, any local reservoir observable has the same form in terms of b_1 operators as in terms of b'_1. This immediately follows from the fermion-parity superselection rule: By Eq. (3) local reservoir observables always contain products of even numbers of the primed reservoir field operators. Second, any operator local to the quantum dot also has the same form due to fermion-parity superselection rule *if* it conserves the fermion number n [87]. Locally, we can thus express everything in terms of b_1 and d_1 by simply omitting the primes. However, the interaction operator $V = \sum_{\sigma,r} \int d\omega (b'^\dagger_{\sigma r\omega} d'_\sigma + d'^\dagger_\sigma b'_{\sigma r\omega}) = \sum_1 \eta b'^\dagger_1 d'_1$ now changes its form. In fact, it simplifies by losing its η sign:

$$V = b^\dagger_{\bar{1}} d_1. \tag{30}$$

Here we implicitly sum over all discrete parts of the multi-index 1 (i.e., η,σ,r) and integrate over its continuous part (ω). An alternative discussion of the above not explicitly referring to the fermion parity can be found in Ref. [51]

Finally, the reservoirs are assumed to be in thermal equilibrium with temperature T, each described by its own grand-canonical density operator,

$$\rho^R = \prod_r \rho^r, \quad \rho^r = \frac{1}{Z^r} e^{-\frac{1}{T}(H^r - \mu^r n^r)}, \tag{31}$$

where $Z^r = \operatorname{Tr}_r e^{-\frac{1}{T}(H^r - \mu^r n^r)}$. For the example setup shown in Fig. 1 one can give the electrochemical potentials by, e.g., assuming a symmetrically applied bias voltage, i.e., $\mu_{L,R} = \pm V_b/2$. However, most of our results apply to any number of electrodes and do not depend on this.

Together with the the Hamiltonian of the total system,

$$H^{\text{tot}} = H + H^R + V, \tag{32}$$

this specifies the model. The NRLM is obtained by setting $U = 0$ in the dot Hamiltonian Eq. (13) in Eq. (32) and discarding the spin.

C. Reduced time-evolution propagator

In order to calculate the dynamics of the reduced density operator of the quantum dot, we first need to consider the evolution of the total system density operator. It is generated by the Liouville-von Neumann equation,

$$\partial_t \rho^{\text{tot}}(t) = -i[H^{\text{tot}}, \rho^{\text{tot}}(t)]_- = -i L^{\text{tot}} \rho^{\text{tot}}(t), \tag{33}$$

with the Liouvillian superoperator $L^{\text{tot}} \bullet = [H^{\text{tot}}, \bullet]_-$. Superoperators are linear transformations of operators and throughout the paper (if needed) we let the solid bullet $\bullet$ indicate the operator on which a superoperator acts. In the following, we make the common assumption that the initial state of the total system at time t_0 is a direct product,

$$\rho^{\text{tot}}(t_0) = \rho^R \rho(t_0). \tag{34}$$

However, some of the developments reported in the following do not depend on this assumption. In a forthcoming work [84] we will show that the causal superfermion approach is useful also when initial reservoir-dot correlations are present. The formal solution of Eq. (33) is

$$\rho^{\rm tot}(t) = e^{-iL^{\rm tot}(t-t_0)}\rho^{\rm tot}(t_0). \tag{35}$$

The reduced dot density operator is obtained by integrating out of reservoirs degrees of freedom:

$$\rho(t) = \mathop{\rm Tr}_R \rho^{\rm tot}(t) = \mathop{\rm Tr}_R (e^{-iL^{\rm tot}(t-t_0)}\rho^R)\rho(t_0). \tag{36}$$

Equation (36) is the starting point for a perturbation theory for the propagator superoperator,

$$\Pi(t,t_0) = \mathop{\rm Tr}_R (e^{-iL^{\rm tot}(t-t_0)}\rho^R)\bullet\,. \tag{37}$$

Decomposing $L^{\rm tot} = L + L^R + L^V$, with $L = [H,\bullet]_-$, $L^R = [H^R,\bullet]_-$ we expand in the tunnel coupling $L^V = [V,\bullet]_- \sim \sqrt{\Gamma}$. Usually two additional steps are taken, in either order. First, one derives a Dyson equation for the exact propagator and introduces a self-energy $\Sigma(t,t')$,

$$\Pi(t,t_0) = e^{-iL(t-t_0)} - i\int\limits_{t\geqslant t_2\geqslant t_1\geqslant t_0} dt_2 dt_1 e^{-iL(t-t_2)}\Sigma(t_2,t_1)\Pi(t_1,t_0). \tag{38}$$

The reduced density operator is then found to satisfy Nakajima-Zwanzig/generalized master/kinetic equation

$$\partial_t\rho(t) = -i\int_{t_0}^{t} dt' L(t,t')\rho(t'), \tag{39}$$

where

$$L(t,t') = L\bar\delta(t-t') + \Sigma(t,t') \tag{40}$$

is the so-called *effective Liouvillian* for the quantum dot. We introduced $\bar\delta(t-t') := 2\delta(t-t')$ such that

$$\int_{t_0}^{t} dt'\bar\delta(t-t') = 1 \tag{41}$$

to absorb the factor 2 that is required to recover the Liouville equation for $\partial_t\rho(t) = -iL\rho(t')$ from Eq. (39) for $\Sigma(t,t') = 0$ [since $\int_{t_0}^{t}\delta(t-t')dt' = 1/2$]. See Refs. [88] and [41] for a discussion of the equivalence of the Nakajima-Zwanzig and real-time approaches and Ref. [77] for a derivation using Feynman path integrals in Keldysh space in the context of relaxation dynamics of the NRLM. The problem is then reduced to the calculation of the self-energy and the subsequent solution of the kinetic equation (39). In many cases, this step is indeed advantageous. Second, if one is mostly interested in the stationary state of the dot, it is more convenient to change to a Laplace representation [51]. Equation (39) in the Laplace representation is then the starting point for the calculation of stationary quantities using different approximate calculation schemes, e.g., perturbative [40,55,89] and RG approaches [30,51,90]. The time evolution can be obtained by calculating the full Laplace image of the reduced density operator by means of perturbation theory or RG approaches [24,75,91,92] and then performing the inverse Laplace transformation.

However, a direct approach in the time representation is of interest. For instance, even if one is interested in stationary properties in the end, some manipulations may be easier or clearer in the time representation, for instance, in problems of noise and counting statistics [93–96], Markovian approximations [97], and adiabatic driving corrections [98–100] or simplifications for higher-order tunnel rates in the stationary limit [41]. Whereas the above-cited works mostly deal with strongly interacting (Anderson) quantum dots, here the noninteracting limit of the Anderson model ($U = 0$) has our interest. We show that for this case it is convenient to work directly with the propagator $\Pi(t,t_0)$ in the time representation. The self-energy is only used in an intermediate renormalization step of the perturbation series for $\Pi(t,t_0)$ to deal with the wideband limit. For now, however, we make no assumption on U unless stated otherwise.

Although we only calculate Schrödinger picture quantities, it is useful to extend the standard interaction representation [101] to the Liouville space [102]. The solution of the von Neumann equation (35) for the total density operator has a form familiar from the Hamiltonian time evolution of the state vector in Hilbert-space quantum mechanics,

$$\rho^{\rm tot}(t) = e^{-i(L+L^R)(t-t_0)}\hat T e^{-i\int_{t_0}^{t} L^V(\tau)d\tau}\rho^{\rm tot}(t_0), \tag{42}$$

where $\hat T$ denotes the time ordering of superoperators and $L^V(\tau)$ are the tunnel Liouvillians in the interaction picture:

$$L^V(\tau) = e^{i(L+L^R)(\tau-t_0)}L^V e^{-i(L+L^R)(\tau-t_0)}. \tag{43}$$

Expanding Eq. (42) in $L^V(t)$, one obtains the time-dependent perturbation expansion

$$\rho^{\rm tot}(t) = e^{-i(L+L^R)(t-t_0)}\Big[1 - i\int_{t_0}^{t} dt_1 L^V(t_1) + (-i)^2\int_{t_0}^{t} dt_2\int_{t_0}^{t_2} dt_1 L^V(t_2)L^V(t_1) + \cdots\Big]\rho^{\rm tot}(t_0). \tag{44}$$

Making use of $\mathrm{Tr}_R L^R = 0$, the perturbation expansion for the time-dependent reduced density operator in powers of L^V reads as

$$\rho(t) = e^{-iL(t-t_0)}\mathop{\rm Tr}_R[1 + \sum_{m=0}^{\infty}(-i)^m \times\int_{t\geqslant t_m\cdots\geqslant t_1\geqslant t_0} dt_1\cdots dt_m L^V(t_m)\cdots L^V(t_1)]\rho^{\rm tot}(t_0) \tag{45a}$$

$$= e^{-iL(t-t_0)}\rho(t_0) + \sum_{m=0}^{\infty}(-i)^m\int_{t\geqslant t_m\cdots\geqslant t_1\geqslant t_0} dt_1\cdots dt_m e^{-iL(t-t_m)} \times\mathop{\rm Tr}_R\big[L^V e^{-i(L+L^R)(t_m-t_{m-1})}\cdots L^V e^{-i(L+L^R)(t_1-t_0)}\rho^{\rm tot}(t_0)\big]. \tag{45b}$$

A direct analysis of the series Eq. (45a) is cumbersome, even for the noninteracting case. To derive a manageable series, we now introduce the *causal* fermionic superoperators in the next section.

D. Second quantization in Liouville-Fock space

The above Liouville-space formulation of quantum mechanics is well known [103] and has found many applications

[104]. However, when applied to quantum many-particle systems, it becomes more powerful if analogs of field-theoretical techniques are introduced, in particular, field *super*operators and Liouville-Fock space [30,49,50,52,53,57,105].

1. Causal superfermions

Special *causal* field superoperators may be constructed [106]: For the quantum dot they read as

$$G_1^q \bullet = \frac{1}{\sqrt{2}}\{d_1 \bullet + q(-1)^n \bullet (-1)^n d_1\}, \tag{46}$$

and for the reservoir

$$J_1^q \bullet = \frac{1}{\sqrt{2}}\{b_1 \bullet - q(-1)^{n^R} \bullet (-1)^{n^R} b_1\}. \tag{47}$$

Here $q = \pm$ labels the components obtained after a "Keldysh rotation" of simpler superoperators defined by left and right multiplication with a Hilbert-Fock space field. Moreover, $(-1)^n = e^{i\pi n}$ and $(-1)^{n^R} = e^{i\pi n^R}$ are the fermion-parity operators of the dot and reservoirs, respectively [cf. Eqs. (14) and (16)]. The additional minus sign in the second term of the definition of J_1^q, relative to the definition of G_1^q is purely conventional but is advantageous later [cf. Eqs. (89) and (90)]. The tunneling Liouvillian L^V can be written compactly as

$$L^V = \sum_{q=\pm} G_1^q J_{\bar{1}}^q = \bar{G}_1 \bar{J}_{\bar{1}} + \tilde{G}_1 \tilde{J}_{\bar{1}}, \tag{48}$$

where in the second equality we used "bar-tilde" notation of Refs. [51] and [30] for the $q = \pm$ components, respectively,

$$\begin{aligned} \bar{G}_1 &= G_1^+, \quad \bar{J}_1 = J_1^+, \\ \tilde{G}_1 &= G_1^-, \quad \tilde{J}_1 = J_1^-, \end{aligned} \tag{49}$$

which is sometimes more convenient. We note that in the rewriting of L^V as Eq. (48) the fermion-parity superselection rule is already used; see Ref. [30] for a discussion. The superoperators G_1^q and J_1^q obey fermionic anticommutation relations,

$$[\bar{G}_1, \tilde{G}_2]_+ = \delta_{1,\bar{2}}, \quad [\bar{G}_1, \bar{G}_2]_+ = [\tilde{G}_1, \tilde{G}_2]_+ = 0, \tag{50}$$

$$[\bar{J}_1, \tilde{J}_2]_+ = \frac{\Gamma_1}{2\pi}\delta_{1,\bar{2}}, \quad [\bar{J}_1, \bar{J}_2]_+ = [\tilde{J}_1, \tilde{J}_2]_+ = 0, \tag{51}$$

where $[\ ,\ ]_+$ now denotes the anticommutator of superoperators. The superoperators of the dot and the reservoirs commute with each other,

$$[\tilde{J}_1, \tilde{G}_2]_- = [\bar{J}_1, \bar{G}_2]_- = [\bar{J}_1, \tilde{G}_2]_- = [\tilde{J}_1, \bar{G}_2]_- = 0. \tag{52}$$

This follows from our assumption that the dot and the reservoir *operators* commute [see Sec. II A]. Furthermore, the field superoperators are pairwise related by the super-Hermitian conjugation (which is defined shortly hereafter) [107]:

$$\bar{G}_1^\dagger = \tilde{G}_{\bar{1}}, \quad \bar{J}_1^\dagger = \tilde{J}_{\bar{1}}. \tag{53}$$

In this relation, note the reversal of the causal index ($\bar{q}$) as well as the multi-index ($\bar{1}$): $(G_1^q)^\dagger = G_{\bar{1}}^{\bar{q}}$ and $(J_1^q)^\dagger = J_{\bar{1}}^{\bar{q}}$.

The crucial properties of the *causal* fermionic field superoperators (46) and (47), distinguishing them from previously introduced field superoperators (see Ref. [30] for a detailed comparison), are

$$\underset{D}{\mathrm{Tr}} \bar{G}_1 \bullet = 0, \quad \underset{R}{\mathrm{Tr}} \tilde{J}_1 \bullet = 0, \tag{54}$$

$$\bar{G}_1 (-1)^n = 0, \quad \tilde{J}_1 (-1)^{n^R} = 0, \tag{55}$$

for *all* values of the multi-index 1. In the following, we see that Eq. (54) relates to the fundamental causal structure of the correlation functions expressed in these superfields and plays a key role in maximally simplifying them [cf. Eq. (89) and (90)]. Equation (55) arises since the fermion-parity operator is used to ensure that the field superoperators anticommute. This property leads to an interesting exact result for the interacting Anderson model discussed in Sec. III C 2.

It is of interest to also give the superoperators G_1^q in terms of the anticommuting dot fields d_1' [Eq. (12b)]:

$$G_1^q \bullet = \eta \frac{1}{\sqrt{2}}[d_1', (-1)^n \bullet]_{-q} \tag{56a}$$

$$= \eta (-1)^{n+1} \frac{1}{\sqrt{2}}(d_1' \bullet + q \bullet d_1'). \tag{56b}$$

The causal field superoperators in Liouville-Fock space are thus simply the commutator and anticommutator of these Hilbert-Fock space field operators (cf. Ref. [50]), but only after the fermion-parity has been applied to its argument. In Eq. (56a), taking the commutator and anticommutator of an operator is the superoperator equivalent of performing the Keldysh rotation [30]. One useful aspect of the form (56a) is that for $q = +$ the two fundamental properties (54) and (55) are immediately clear: The property (54) follows from the vanishing of the trace of a commutator and (55) from the vanishing of any commutator with the unit operator [108]. These are dual properties with respect to the scalar product in Liouville-Fock space; see Sec. II D 2. The form (56a) is also convenient for a direct comparison with expressions which occur in formalisms using the local dot Green's functions [109].

2. Causal basis for Liouville-Fock space: Super-Pauli principle

As was shown in Ref. [30], the causal field superoperators $G^\pm$ [Eq. (46)] generate a basis for the Liouville space of the quantum dot, in close analogy with the construction of the usual fermion Fock basis in the many-particle Hilbert space. The four-dimensional Hilbert-Fock space of the quantum dot is spanned by the orthogonal-state vectors

$$|0\rangle, \quad |\uparrow\rangle = d_\uparrow^\dagger |0\rangle, \quad |\downarrow\rangle = d_\downarrow^\dagger |0\rangle, \quad |2\rangle = d_\uparrow^\dagger d_\downarrow^\dagger |0\rangle. \tag{57}$$

Operators $A = \sum_{k,l=0,\uparrow,\downarrow,2} A_{k,l} |k\rangle\langle l|$ acting on this space themselves form a 16-dimensional linear space $\mathfrak{L}$ with the inner product $(A|B) = \mathrm{Tr}_D A^\dagger B$, which we refer to as the *Liouville space* of the quantum dot. By $|A)$ we denote an operator A considered as a supervector in $\mathfrak{L}$, and use the rounded bracket notation to avoid possible confusion with Hilbert-space state vectors $|\psi\rangle$. A set of mutually orthogonal supervectors, i.e., operators $A_i, i = 1, \ldots, 16$ satisfying

$$(A_i|A_j) = \underset{D}{\mathrm{Tr}} A_i^\dagger A_j = \delta_{i,j}, \tag{58}$$

form an orthonormal basis in the quantum-dot Liouville space. Superoperators are linear maps $S : \mathfrak{L} \to \mathfrak{L}$ and can be expressed in this basis as

$$S = \sum_{i,j} S_{i,j} |A_i)(A_j|, \quad i,j = 0,\ldots,16, \tag{59}$$

where $(A|\bullet = \mathrm{Tr}_D A^\dagger \bullet$ denotes the linear function on operators $\bullet$ built from the operator A. The super-Hermitian conjugation Eq. (53) is defined with respect to the Liouville-space inner product, i.e., $(A|S^\dagger|B) = (B|[SA])^*$.

For a Liouville space of a many-particle system, a *Liouville-Fock space*, a super-Fock basis can be constructed starting from some operator defining a vacuum superstate. (In Sec. II D 3, we indicate that some care must taken when using the term "superstate".) For the causal field superoperators (46) the vacuum superstate of the quantum dot is given by

$$|Z_L) = \tfrac{1}{2}\mathbb{1}, \tag{60a}$$

which is indeed destroyed by the annihilation superoperators $G_1^- = \tilde{G}_1$: $\tilde{G}_{\eta\sigma}|Z_L) = 0$ for all η, σ by the super-Hermitian conjugate of the identity (54). From this vacuum another seven *bosonic* operators are created by application of all possible products of an *even* number of fermionic creation superoperators $G_1^+ = \bar{G}_{\eta\sigma}$. The doubly occupied superstates are

$$|\chi_\sigma) = \bar{G}_{+\sigma}\bar{G}_{-\sigma}|Z_L) = -\tfrac{1}{2}e^{i\pi n_\sigma}, \tag{60b}$$

$$|T_+) = \bar{G}_{+\uparrow}\bar{G}_{+\downarrow}|Z_L) = d_\uparrow^\dagger d_\downarrow^\dagger, \tag{60c}$$

$$|T_-) = -\bar{G}_{-\uparrow}\bar{G}_{-\downarrow}|Z_L) = d_\downarrow d_\uparrow, \tag{60d}$$

$$|S_\sigma) = \bar{G}_{+\sigma}\bar{G}_{-\bar{\sigma}}|Z_L) = d_\sigma^\dagger d_{\bar{\sigma}}, \tag{60e}$$

where $\sigma = \pm = \uparrow, \downarrow$, cf. Eq. (14). The operators χ_σ are proportional to the fermion-parity operator for a single spin-σ orbital of the dot, $e^{i\pi n_\sigma} = 1 - 2n_\sigma$. The "most filled" superstate $|Z_R)$ (quadruply occupied) equals the total fermion-parity operator of the dot $e^{i\pi n} = \prod_\sigma e^{i\pi n_\sigma} = (1-2n_\uparrow)(1-2n_\downarrow)$, normalized to the Liouville-space scalar product:

$$|Z_R) = \bar{G}_{+\uparrow}\bar{G}_{-\uparrow}\bar{G}_{+\downarrow}\bar{G}_{-\downarrow}|Z_L) = \tfrac{1}{2}e^{i\pi n}. \tag{60f}$$

In addition, another eight *fermionic* superoperators are created by the action of products of *odd* numbers of fermionic creation superoperators $\bar{G}_{\eta\sigma}$, either with one excitation,

$$|\alpha^+_{\eta\sigma}) = \sigma^{\frac{1-\eta}{2}}\bar{G}_{\eta,(\sigma\eta)}|Z_L) = \tfrac{1}{\sqrt{2}}\sigma^{\frac{1-\eta}{2}} d_{\eta,(\sigma\eta)}, \tag{61a}$$

or with three ($\bar{\sigma}\eta = \sigma\bar{\eta} = -\sigma\eta$),

$$\begin{aligned}|\alpha^-_{\eta\sigma}) &= \sigma^{\frac{1-\eta}{2}}\bar{G}_{\eta,(\sigma\eta)}\bar{G}_{\eta,(\bar{\sigma}\eta)}\bar{G}_{\bar{\eta},(\sigma\bar{\eta})}|Z_L) \\ &= e^{i\pi n}\tfrac{1}{\sqrt{2}}\sigma^{\frac{1-\eta}{2}} d_{\eta,(\sigma\eta)}.\end{aligned} \tag{61b}$$

Using the anticommutation relations (50), one shows that the above 16 supervectors (operators) (60) and (61) form a complete, orthonormal basis in the sense of Eq. (58) for the Liouville-Fock space. For the central applications of this paper, we do not need the fermionic part of this basis except for the next Sec. II D 3. However, since second-quantized expressions for superoperators act on the entire Liouville space, one must be aware of this linear subspace, as we illustrate in several cases in the following.

In the above construction of Liouville-Fock space, the fermion-parity operator $(-1)^n = 2Z_R$ plays a fundamental role. First, it was included into the definition of the field superoperators to ensure fermionic anticommutation relation. This, in particular, results in

$$(\bar{G}_1)^2 = 0, \tag{62}$$

which expresses that one cannot doubly occupy a superstate (labeled by $1 = \eta,\sigma$). We refer to Eq. (62) as the *super-Pauli exclusion principle* by analogy with the Pauli principle for fermionic fields in Hilbert-Fock space, for which $(d_\sigma^\dagger)^2 = 0$. A consequence of central importance to the paper is that any product of more than four creation (or destruction) superoperators necessarily contains at least one duplicate and therefore vanishes:

$$\bar{G}_m \cdots \bar{G}_1 = 0 \quad \text{for } m > 4. \tag{63}$$

This is to be compared with the vanishing of products of more than two field creation operators in Hilbert-Fock space, i.e., $d^\dagger_{\sigma_m}\cdots d^\dagger_{\sigma_1} = 0$ for $m > 2$. Equation (63) can be generalized to an Anderson model with N spin orbitals by replacing the condition with $m > 2N$. Second, the singly and triply occupied superstates are constructed from the same set of four Hilbert-Fock field operators $d_{\eta\sigma}$, but they differ by the application of the parity operator, $|\alpha^-_{\eta\sigma}) = (-1)^n|\alpha^+_{\eta\sigma})$. It is this factor that ensures their orthogonality [110]. Finally, the left multiplication by the fermion-parity operator implements a superoperator analog of a particle-hole transformation, mapping basis supervectors with $\mathcal{N}$ superparticles onto those with $4 - \mathcal{N}$ superparticles [111].

In analogy to the usual second quantization, one can introduce a superoccupation operator [cf. Eq. (53)] [112]:

$$\mathcal{N}_{\eta\sigma} = \bar{G}_{\eta\sigma}\tilde{G}_{\bar{\eta}\sigma} = \bar{G}_{\eta\sigma}\bar{G}^\dagger_{\eta\sigma}. \tag{64}$$

By construction, due to the anticommutation relations, it satisfies

$$[\mathcal{N}_{\eta\sigma}, \bar{G}_{\eta\sigma}] = \bar{G}_{\eta\sigma}. \tag{65}$$

It therefore simply counts the number of times that the creation superoperators $\bar{G}_{\eta\sigma}$ appears in a basis superket, which is restricted to 0 or 1 by Eq. (62): With $\mathcal{N}_1 := \mathcal{N}_{\eta\sigma}$,

$$\mathcal{N}_i \bar{G}_m \cdots \bar{G}_1|Z_L) = (\delta_{i,m} + \cdots + \delta_{i,1})\bar{G}_m \cdots \bar{G}_1|Z_L). \tag{66}$$

Finally, we note that operators Eqs. (60b)–(60e) are closely related to the group generators of the spin- (S) and charge-rotation (T) symmetry of the Anderson model (they transform as irreducibly under the symmetry group). By working in the causal Liouville-Fock space basis (60) and (61), one thus not only profits from the fundamental causal properties of interest here, but one also maximally exploits these model-specific symmetries; see the study Ref. [30], where this was of crucial importance.

3. *Examples of second quantization in Liouville space*

Before we move on, we first illustrate the above-introduced second quantization in Liouville-Fock space using causal superfermions. We discuss the expansion of a supervector, using the density operator as an example, and the expansion of a superoperator, the Liouvillian L.

(a) Mixed-state supervector ρ. We can construct the most general form of the reduced density operator for the quantum dot by accounting for the restrictions on a physical mixed state: The operator ρ must (i) be positive, (ii) be self-adjoint, (iii) have unit trace, and (iv) satisfy the fermion-parity superselection rule (univalence) [30,60,80]. The latter requires that any density operator ρ has no off-diagonal matrix elements with respect to the fermion-parity quantum number [cf. Eq. (3)]:

$$[\rho,(-1)^n]_- = 0. \tag{67}$$

The linear space containing such operators satisfying (ii)-(iv) is spanned by the bosonic operators in Eqs. (60). The reduced density operator is a supervector in this space and is thus generated by application of products of an *even* number of creation superfields from the vacuum superket with, in general, seven coefficients $\Omega_\pm(t), \Phi_\pm(t), \Upsilon_\pm(t)$, and $\Xi(t)$:

$$\begin{aligned}\rho(t) &= \Big\{\frac{1}{2} + \sum_\sigma \Phi_\sigma(t)\bar{G}_{+\sigma}\bar{G}_{-\sigma} + \sum_\sigma \Omega_\sigma(t)\bar{G}_{+\sigma}\bar{G}_{-\bar{\sigma}} \\ &\quad + \sum_\eta \eta\Upsilon_\eta(t)\bar{G}_{\eta\uparrow}\bar{G}_{\eta\downarrow} + \Xi(t)\bar{G}_{+\uparrow}\bar{G}_{-\uparrow}\bar{G}_{+\downarrow}\bar{G}_{-\downarrow}\Big\}|Z_L) \\ &= \frac{1}{2}|Z_L) + \sum_\sigma \Phi_\sigma(t)|\chi_\sigma) + \Xi(t)|Z_R) \\ &\quad + \sum_\eta \Upsilon_\eta(t)|T_\eta) + \sum_\sigma \Omega_\sigma(t)|S_\sigma).\end{aligned} \tag{68}$$

With appropriate restrictions imposed by the positivity condition (i), these coefficients thus parametrize an arbitrary dot state, e.g., the complicated time-dependent density operator $\rho(t)$ of the $U \neq 0$ Anderson model [Eq. (45b)]. The coefficients are the nonequilibrium averages $\langle\bullet\rangle(t) = \mathrm{Tr}_D[\bullet\rho(t)]$ of the complete set of local observable operators (60). The coefficient

$$\Phi_\sigma(t) = (\chi_\sigma|\rho(t)) = -\tfrac{1}{2}\langle e^{i\pi n_\sigma}\rangle(t) \tag{69}$$

gives the average occupation: $\langle n_\sigma\rangle(t) = 1/2 + \Phi_\sigma(t)$ by using $e^{i\pi n_\sigma} = (1 - 2n_\sigma)$. The coefficient

$$\Xi(t) = (Z_R|\rho(t)) = \tfrac{1}{2}\langle e^{i\pi n}\rangle(t), \tag{70}$$

the average of the fermion-parity operator, $\Xi(t) = \frac{1}{2}\langle\prod_\sigma e^{i\pi n_\sigma}\rangle(t) = 2\langle n_\uparrow n_\downarrow\rangle(t) - \langle n\rangle(t) + 1/2$, takes into account the correlations of the occupancies: $\langle n_\uparrow n_\downarrow\rangle(t) \neq \langle n_\uparrow\rangle(t)\langle n_\downarrow\rangle(t)$ is equivalent to $\Xi(t) \neq 2\prod_\sigma \Phi_\sigma(t)$. Furthermore, the average of an "anomalous" and a spin-flip combination of Hilbert-Fock space field operators,

$$\Upsilon_{\bar{\eta}}(t) = (T_{\bar{\eta}}|\rho(t)) = \eta\langle d^\eta_\uparrow d^\eta_\downarrow\rangle(t), \tag{71}$$

$$\Omega_{\bar{\sigma}}(t) = (S_{\bar{\sigma}}|\rho(t)) = \langle d^\dagger_\sigma d_{\bar{\sigma}}\rangle(t), \tag{72}$$

describes the transverse spin ($\uparrow$-$\downarrow$) coherence and the electron-pair (0-2) coherence of the state at time t. At the initial time t_0 such coherences can be prepared: the transverse spin coherence by contact with a ferromagnet with a polarization transverse to the magnetic field B and the electron-pair coherence by contact with a superconductor. At finite times t such coherences will persist, but in the stationary limit $t \to \infty$ they must vanish since the Anderson model has spin-rotation symmetry (with respect to the magnetic field axis) and charge-rotation symmetry [30]. Likewise, two-particle correlations can be initially present on the quantum dot if it has been in contact with an interacting system. These will decay, in the sense that $\lim_{t\to\infty}\Xi(t) = 2\prod_\sigma \lim_{t\to\infty}\Phi_\sigma(t)$, if the quantum dot is noninteracting ($U = 0$).

Of the eight bosonic operators (60), only Z_L has a nonzero trace, and the physical requirement $\mathrm{Tr}\rho = 1$ completely fixes its coefficient in Eq. (68). By itself, the operator

$$\rho_\infty := \tfrac{1}{2}|Z_L) = \tfrac{1}{4}\mathbb{1} \tag{73}$$

represents the physical stationary state of the quantum dot coupled to reservoirs at infinite temperature (i.e., T much larger than any other energy scale, i.e., U, $\epsilon - \mu_r$, B). In any finite-temperature mixed state (68), there are, in general, two- and four-superfermion excitations. In our formalism, such superexcitations correspond to a "cooling" relative to the infinite-temperature supervacuum (73). Although this point of view is opposite to that in the Hilbert-Fock space (where excitations rather describe a "heating" of the zero-temperature vacuum $|0\rangle$), the causal superfermion approach is thus entirely physical and brings definite insights and advantages in the study of open quantum systems. However, care must be taken to import physical concepts from second quantization in Hilbert-Fock space. For instance, it should be noted that of the basis supervectors only $|Z_L)$ can represent a physical state *on its own*: The other 15 basis supervectors, such as $\bar{G}_1|Z_L)$, are traceless by construction [Eq. (54)] and cannot fulfill the probability normalization condition $\mathrm{Tr}_D\rho = 1$ by themselves. Moreover, the fermionic basis vectors (61), such as $\bar{G}_1|Z_L)$, do not have the right fermion parity. It is only in superpositions with $|Z_L)$ of the form (68) that the bosonic basis supervectors (60) take part in real mixed states described by a density operator, whereas the fermionic basis vectors (61) only play a role in *virtual* intermediate mixed states; see discussion of Eq. (76) in the following. This should be kept in mind when speaking formally about "superstates," "superparticles," or "superexcitations," a terminology which we do consider to be useful.

(b) Liouvillian superoperator L. As a next illustration, we discuss the second quantized form of the Liouvillian superoperator of the isolated Anderson model in terms of the field superoperators,

$$L = \sum_{\eta,\sigma}\eta([\epsilon + U/2] + \sigma B/2)\bar{G}_{\eta\sigma}\tilde{G}_{\bar{\eta}\sigma} \tag{74a}$$

$$+ \frac{U}{2}\sum_{\eta,\sigma}(\bar{G}_{\eta\sigma}\tilde{G}_{\bar{\eta}\sigma}\tilde{G}_{\eta\bar{\sigma}}\tilde{G}_{\bar{\eta}\bar{\sigma}} + \bar{G}_{\eta\sigma}\bar{G}_{\bar{\eta}\sigma}\bar{G}_{\eta\bar{\sigma}}\tilde{G}_{\bar{\eta}\bar{\sigma}}), \tag{74b}$$

which is verified by substitution of Eq. (46) to give $L = [H,\bullet]_-$ with H given by Eq. (13). Similar to the usual second quantization technique, this expression directly reveals a number of general properties. For instance, particle number conservation is expressed by the fact that in the field superoperators only conjugate pairs of η, $\bar{\eta}$ appear. Furthermore, since only products of an *even* number of field superoperators appear, the superoperator L preserves the fermion-parity superselection rule of the density operator [Eq. (67)]: The off-diagonal supermatrix elements between a bosonic [$|B$), Eq. (60)] and a fermionic [$|F$), Eq. (61)] basis operator vanish, $(B|L|F) = (F|L|B) = 0$, simply because these are created

from $|Z_L)$ by the action of an even and an odd number of field superoperators, respectively. As a result, if initially $\rho(t_0)$ satisfies Eq. (67), then so does $\rho(t) = e^{-iL(t-t_0)}\rho(t_0)$ at later times $t > t_0$ for a closed system. A property more specific to the use of *causal* superfermions in the second quantized form Eq. (74), is that the conservation of probability is immediately obvious *term by term*: Each term ends with a destruction superoperator $\tilde{G}$ on the left, ensuring by Eq. (54) that the trace is preserved, $\mathrm{Tr}_D e^{-iL(t-t_0)}\rho(t_0) = \mathrm{Tr}_D\rho(t_0)$.

More specific to the Anderson model is that Eq. (74) automatically achieves an interesting decomposition of the interaction term. In particular, the *quartic* term (74b) $\propto U$ commutes with the simple quadratic term (74a), which also contains U. Importantly, the quartic term acts *only* in the fermionic sector of the Liouville-Fock space [spanned by the superkets (61)]: For any two bosonic operators B and B' we have $(B|L|_{\mathrm{quartic}}|B') = 0$. This follows from

$$(B|\sum_{\eta,\sigma}\bar{G}_1\tilde{G}_{\bar{1}}\tilde{G}_2\tilde{G}_{\bar{2}}|B') = 0, \tag{75}$$

where $1 = \eta,\sigma$ and $2 = \eta,\bar{\sigma}$ and the same for the second term in Eq. (74b) (which is the Hermitian superadjoint of this). Equation (75) immediately follows from the structure of the quartic term using reasoning very similar to that used in the usual second quantization in Hilbert-Fock space. The result (75), together with the fermion-parity superselection rule (67), now implies that in the time-evolution expansion Eq. (45b) the quartic interaction term Eq. (74b) *plays no role* in the free quantum-dot propagator $e^{-iL(t_{k+1}-t_k)}$ when it occurs after an *even* number (k) of tunneling Liouvillians L^V. For example, inserting in the fourth-order expression of Eq. (45b) a complete set of superstates (expansion of the unit superoperator) for the quantum dot between $L^V(t_3)$ and $L^V(t_2)$ and substituting Eq. (48), we obtain the structure [113]

$$\begin{aligned}&\cdots G_4^{q_4}\cdots G_3^{q_3}e^{-iL(t_3-t_2)}G_2^{q_2}\cdots G_1^{q_1}\cdots\rho(t_0)\\ &\quad=\sum_{B,B'}\cdots G_4^{q_4}\cdots G_3^{q_3}|B)(B|e^{-iL(t_3-t_2)}|B')\\ &\qquad\times(B'|G_2^{q_2}\cdots G_1^{q_1}\cdots\rho(t_0),\end{aligned} \tag{76}$$

where only the quantum-dot part of the expressions are shown. The sums over $|B)$, $|B')$ are restricted to the bosonic superkets [Eq. (60)]: Since $\rho(t_0)$ is a bosonic operator, application of an even number of superfields brings us back to the bosonic sector. Now the quartic U term drops out in the matrix elements $(B|e^{-iL(t_3-t_2)}|B')$ due to Eq. (75). The propagation of the bosonic *virtual intermediate* states in Eq. (45b) is thus defined entirely by the *quadratic* part of the dot Liouvillian, Eq. (74a), and is thus *effectively noninteracting*, with a renormalized single-particle energy level: $\epsilon \to \epsilon + U/2$. This general rule leads to very useful simplifications in perturbative [84] and nonperturbative [64] studies of the interacting Anderson model that will not be explored further here.

Another point revealed by the second quantization of L, Eq. (74), is that the the essential two-particle operator to which the interaction couples in the *Hamiltonian* H, Eq. (13), is the fermion-parity operator $(-1)^n = 2Z_R$:

$$L|_{\mathrm{quartic}} = \left[\frac{1}{4}U(-1)^n,\ \bullet\ \right]_- = \frac{U}{2}\sum_{\nu,\eta,\sigma}|\alpha^{\nu}_{\eta\sigma})(\alpha^{\bar{\nu}}_{\eta\sigma}|. \tag{77}$$

The term (77) captures the essential many-particle effect of the interaction U since in the quadratic term Eq. (74a) the *effect* of U can be compensated by tuning the level position to the particle-hole symmetry point $\epsilon = -U/2$. The first rewriting in Eq. (77) shows that the quartic term corresponds to the operator $\frac{U}{4}(-1)^n$ contained in H. This also shows that it acts only in the Liouville-Fock space spanned by fermionic operators Eq. (61), again leading to Eq. (75), since the fermion-parity operator, by construction, (anti)commutes with all bosonic (fermionic) operators by Eq. (60) [Eq. (61)]. The second rewriting in terms the fermionic superbras and superkets [Eq. (61)] explicitly confirms this.

Finally, we emphasize that a particularly useful aspect of the above reasoning, based *directly* on the Liouville-Fock representation, Eq. (74), is that it also allows one to infer general physical properties of a superoperator describing an open fermionic system, even when it does not have the commutator form which L has.

4. *Interaction picture of causal superfermions*

Using the second quantization, we can also easily work out the explicit form of interaction Liouvillian L^V [Eq. (48)] in the interaction picture, $L^V(t) = \sum_q e^{i(L+L^R)(t-t_0)}G_1^q J_{\bar{1}}^q e^{-i(L+L^R)(t-t_0)}$, which is required in the next section. For a noninteracting quantum dot ($U = 0$) we have the following simplifying property: For $1 = \eta,\sigma$,

$$\left[L, G_1^q\right]_- = \eta\epsilon_\sigma G_1^q \quad \text{for} \quad U = 0, \tag{78}$$

$$\epsilon_\sigma = \epsilon + B\sigma/2, \tag{79}$$

which follows from the quadratic part (74a) of L using the superfermion commutation relations (50). Note that the right-hand side is independent of q, i.e., the creation and annihilation superoperators have the same frequency $\eta\epsilon_\sigma$, in contrast to Hilbert-Fock space fields. The interaction-picture field superoperators,

$$G_1^q(t) := e^{iL(t-t_0)}G_1^q e^{-iL(t-t_0)} \tag{80a}$$

$$= e^{i\eta\epsilon_\sigma(t-t_0)}G_1^q \quad \text{for} \quad U = 0, \tag{80b}$$

in the noninteracting case ($U = 0$) are then simply proportional to those in the Schrödinger picture, G_1^q, since we can commute $e^{-iL(t-t_0)}$ through G_1^q using Eq. (78), resulting only in a phase factor. This is the crucial simplification, which allows the exact solution of the noninteracting problem to be obtained quite simply once we have taken the wideband limit, as discussed in the next section. The field superoperators of the noninteracting reservoirs have the same simple time dependence as those of the dot for $U = 0$. Since by our definitions in Eq. (46) and (47) $J_1^{\bar{q}}$ and G_1^q with opposite q index play the same role, one can write analogous to Eq. (74), accounting for a factor due to the rescaling (24),

$$L^R = [H^R,\bullet]_- = \frac{2\pi}{\Gamma_1}\eta(\omega+\mu_r)\tilde{J}_1\tilde{J}_{\bar{1}} \tag{81}$$

(with the usual implicit integration over the index ω and summation over indices η,σ,r of the multi-index $1 = \eta,\sigma,\omega,r$)from which it follows that

$$\left[L^R, J_1^q\right]_- = \eta(\omega+\mu_r)J_1^q. \tag{82}$$

As a result, for $\bar{1} = -\eta,\sigma,\omega,r$,

$$J_{\bar{1}}^q(t) := e^{iL^R(t-t_0)}J_{\bar{1}}^q e^{-iL^R(t-t_0)} \tag{83a}$$

$$= e^{-i\eta(\omega+\mu_r)(t-t_0)}J_{\bar{1}}^q. \tag{83b}$$

Therefore, implicitly summing (integrating) over discrete (continuous) indices,

$$L^V(t) = e^{-i\eta(\omega+\mu_r)(t-t_0)}J_{\bar{1}}^q G_1^q(t) \tag{84a}$$

$$= e^{-i\eta(\omega+\mu_r-\eta\epsilon_\sigma)(t-t_0)}J_{\bar{1}}^q G_1^q \quad \text{for} \quad U=0. \tag{84b}$$

III. TIME EVOLUTION AND CAUSAL SUPERFERMIONS

We now first set up the time-dependent perturbation theory for the general, *interacting* case ($U \neq 0$), explicitly incorporating the wideband limit from the start on the level of *superoperators*. This leads to a renormalized version of the perturbation series [51] for which the crucial result Eq. (80b) can be directly exploited to solve the noninteracting problem ($U = 0$) exactly by a next-to-leading-order perturbative calculation.

A. Real-time perturbation expansion for the reduced propagator

We are now in a position to exploit the causal superoperator second quantization technique to the expansion for the propagator $\Pi = \sum_{m=0}^{\infty}\Pi_m$ defined by Eq. (45a). For each term in the expansion of order m in L_V, denoted by Π_m, one can collect all reservoir superoperators by commuting them to the left through the G^q's,

$$\Pi_m = (-i)^m e^{-iL(t-t_0)}\operatorname*{Tr}_R[L^V(t_m)\cdots L^V(t_1)\rho^{\rm tot}(t_0)]$$

$$= (-i)^m\left\langle J_{\bar{m}}^{q_m}(t_m)\cdots J_{\bar{1}}^{q_1}(t_1)\right\rangle_R$$

$$\times e^{-iL(t-t_0)}G_m^{q_m}(t_m)\cdots G_1^{q_1}(t_1), \tag{85}$$

where we implicitly perform a time-ordered integration such that $t \geqslant t_m \geqslant \cdots \geqslant t_1 \geqslant t_0$, as well as a summation over all dummy indices $m,\ldots,1$. Here, $\langle S\rangle_R$ denotes the reservoir average of a *super* operator S:

$$\langle S\rangle_R = \operatorname*{Tr}_R(S\rho^R). \tag{86}$$

To eliminate the reservoirs, we need the multiparticle correlation functions of the reservoirs. Their time dependence amounts to a simple phase factor by Eq. (83b), $\langle J_{\bar{m}}^{q_m}(t_m)\cdots J_{\bar{1}}^{q_1}(t_1)\rangle_R = \prod_{i=1}^m e^{-i\eta_i(\omega_i+\mu_{r_i})(t_i-t_0)}\langle J_{\bar{m}}^{q_m}\cdots J_{\bar{1}}^{q_1}\rangle_R$, and the remaining equal-time correlation functions follow from the Wick theorem [51] for the J_1^q superoperators [30]: For even m,

$$\left\langle J_m^{q_m}\cdots J_1^{q_1}\right\rangle_R = \sum_{\rm contr}(-1)^P\prod_{\langle i,j\rangle}\left\langle J_i^{q_i}J_j^{q_j}\right\rangle_R. \tag{87}$$

Here $(-1)^P$ denotes the usual fermionic sign of the permutation P that disentangles the contractions over which we sum, $\langle i,j\rangle$ denoting the product over contracted pairs. For odd m the average vanished by the fermion-parity superselection rule. The Wick theorem (87) was shown in Ref. [30] to follow from the standard derivation of Gaudin [114] when using the superoperator expression for the equilibrium fluctuation-dissipation theorem for the reservoirs:

$$\bar{J}_1|\rho^R) = \tanh(\eta_1\omega_1/2T)\tilde{J}_1|\rho^R). \tag{88}$$

The field superoperators (47) are called "causal" since they make the constraints imposed by causality [58,59] explicit: There are only two possible types of contraction functions $\langle J_2^{q_2}J_1^{q_1}\rangle_R$ in the expansion Eq. (87) that are nonzero. These are [30] the retarded function,

$$\tilde{\gamma}_{2,1}(\eta_1\omega_1) := \langle\bar{J}_2\tilde{J}_1\rangle_R = \frac{\Gamma_1}{2\pi}\delta_{2,\bar{1}}, \tag{89}$$

and the Keldysh function,

$$\bar{\gamma}_{2,1}(\eta_1\omega_1) := \langle\bar{J}_2\bar{J}_1\rangle_R = \frac{\Gamma_1}{2\pi}\tanh(\eta_1\omega_1/2T)\delta_{2,\bar{1}}, \tag{90}$$

while all other possible pair contractions are equal to zero. These properties of the contractions give a corresponding *causal structure* to the perturbation theory which is revealed only when using the causal field superoperators (46), as we see in the following. We have thus explicitly integrated out the reservoir degrees of freedom and obtained the real-time perturbation theory [40,51] for the reduced-time evolution superoperator:

$$\Pi_m = (-i)^m\left(\sum_{\rm contr}(-1)^P\prod_{\langle i,j\rangle}\gamma_{i,j}^{q_i}(t_i-t_j)\right)e^{-iL(t-t_1)}$$

$$\times G_m^{q_m}e^{-iL(t_m-t_{m-1})}G_{m-1}^{q_{m-1}}\cdots G_1^{q_1}e^{-iL(t_1-t_0)}. \tag{91}$$

An individual term consists of a sequence of free dot evolutions, generated by L [Eq. (74)], interrupted by the pairwise action of quantum-dot field superoperators G^q [Eq. (80a)], which is weighted by the time-dependent reservoir correlation function (Fourier transform)

$$\gamma_{i',j'}^{q_i}(t_i-t_j) := \int d\omega_i e^{-i\eta_i(\omega_i+\mu_i)(t_i-t_j)}\gamma_{i,j}^{q_i}(\eta_i\omega_i). \tag{92}$$

On the right-hand side, we also make use of both the q index, as well as the bar-tilde notation, as in Eq. (49):

$$\gamma_{i,j}^{q_j} := \left\langle J_i^+J_j^{q_j}\right\rangle = \tilde{\gamma}_{i,j}\delta^{q_j,-} + \bar{\gamma}_{i,j}\delta^{q_j,+}. \tag{93}$$

We note that the initial time t_0 cancels out in the reservoir dynamical phase factor since $\gamma_{i,j}^{q_j} \propto \delta_{1\bar{2}} \propto \delta(\omega_i-\omega_j)\delta_{\bar{\eta}_i,\eta_j}$ [by Eqs. (89) and (90)]. The primed multi-indices i', j' on the left-hand side of Eq. (92) indicate that we leave out the reservoir frequencies ω_i and ω_j from the multi-indices i, j, respectively. At this stage these frequencies have been integrated out of the theory, and from here on we omit the primes; i.e., the multi-indices [1, $\bar{1}$, etc., in Eq. (91)] do not contain ω_i anymore, unless stated otherwise.

In Fig. 2, we represent individual terms in Eq. (91) diagrammatically [30,51] and the total evolution is the sum of such terms over all possible Wick pairings of an even number of discrete indices $m,\ldots,1$, integrated over ordered times, i.e., $t \geqslant t_m \cdots \geqslant t_1 \geqslant t_0$. We refer to an mth-order diagram

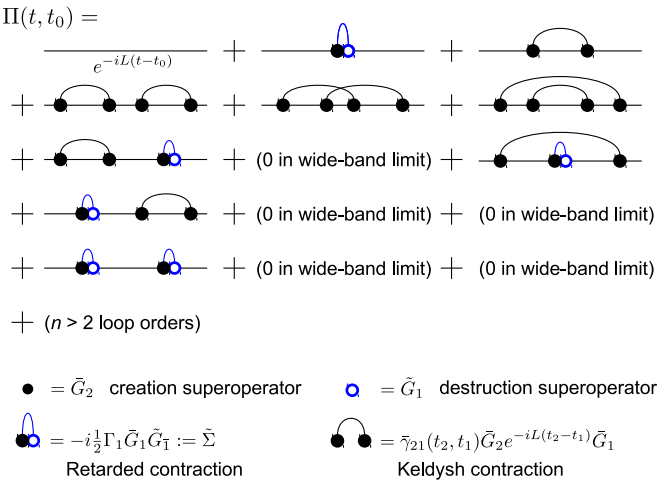

FIG. 2. (Color online) Real-time perturbation expansion in the wideband limit: Diagrams contributing to the full time-evolution propagator $\Pi(t,t_0)$ in the first three loop orders of perturbation theory as given by Eq. (85), $\Pi_0 = e^{-iL(t-t_0)}$, Π_2 and Π_4. Within each column, the two-loop diagrams have the same contraction configuration but differ by the contraction functions involved ($\bar{\gamma}$ or $\tilde{\gamma}$). Diagrams and expressions for the corresponding terms for the self-energy $\Sigma(t,t_0) = \Sigma_2 + \Sigma_4 + \cdots$ are obtained by (i) retaining only the diagrams in the second and third column and (ii) discarding from these diagrams the free time-evolution parts before the first and after the last vertex. The full evolution $\Pi(t,t_0)$ is then generated by $\Sigma(t_2,t_1)$ through the Dyson equation (38). As indicated, the retarded contractions are "Markovian"; i.e., in the wideband limit they act *instantaneously* and do not allow for internal time integrations (δ-function constraint); cf. Eq. (94). We indicate the number of two-loop diagrams that give zero due to this constraint, but do not draw them. These are the only contractions that survive in the $T \to \infty$ limit and are considered further in Fig. 3(a).

contributing to Π_m with $m/2$ contractions (γ) as a $m/2$-loop diagram. Importantly, due to the structure of the reservoir correlation function Eq. (93), each term in (91) has a *causal structure*: The destruction superoperator $G^-_{\bar{1}} = \tilde{G}_{\bar{1}}$ can never appear on the left of the field superoperator (either $G^{\pm} = \bar{G}$ or $\tilde{G}$) with which it is contracted. One implication of this structure is that $\bar{G}$ always stands on the far left, at the latest time t_m. This ensures by Eq. (54) that, *term-by-term*, $\mathsf{Tr}\Pi(t,t_0) = \mathsf{Tr}$ and therefore probability is conserved, $\mathsf{Tr}\rho(t) = \mathsf{Tr}\rho(t_0) = 1$, since $\mathsf{Tr}\Pi_0 = \mathsf{Tr}$ and $\mathsf{Tr}\Pi_m = 0$ for $m \geqslant 1$. We now turn to further implications of this causal structure in the wideband limit.

B. Wideband limit

The perturbation theory Eq. (91) applies generally without further assumptions to the interacting Anderson model ($U \neq 0$). However, even when considering the noninteracting limit ($U = 0$) in combination with the wideband limit (WBL) for the stationary state ($t \to \infty$) it is not directly obvious how to explicitly evaluate Eq. (91). To obtain the exact solution in that case, one needs to identify which contributions vanish in each loop order of the time-evolution superoperator, and then sum up the remaining ones from all orders [73,74]. We now show how in the WBL the time-dependent perturbation series (91) for the interacting case ($U \neq 0$) can be transformed with the help of our causal superoperators. In this new formulation, the solution of the noninteracting limit ($U = 0$) also becomes obvious, even allowing for the direct calculation of the full time evolution $\Pi(t,t_0)$.

1. Retarded reservoir correlations: Elimination of annihilation superfields

The key simplification in the WBL, in which the rates $\Gamma_{r\sigma}$ are constant, is that the retarded contraction function becomes energy independent, corresponding to a δ function in time [cf. Eq. (41)] (see also Refs. [77,79,115]),

$$\tilde{\gamma}_{2,1}(t_2,t_1) = \frac{\Gamma_1}{2\pi}\delta_{1,\bar{2}}\int d\omega_1 e^{-i\eta_1(\omega_1+\mu_{r_1})(t_2-t_1)}$$
$$= \Gamma_1\delta(t_2-t_1)\delta_{2,\bar{1}} = \frac{\Gamma_1}{2}\bar{\delta}(t_2-t_1)\delta_{2,\bar{1}}, \quad (94)$$

where $\Gamma_1 = \Gamma_{r\sigma}$ does not depend on the frequency ω_1 or time t_1. By working with causal field superoperators, we thus automatically collect a Markovian part of the dynamics: The "Markovian contraction" $\tilde{\gamma}$ appears only when a *destruction* superoperator $\tilde{G}$ is contracted with a $\bar{G}$ (necessarily so by the causal structure). This allows one to easily eliminate the $\tilde{G}$ from the perturbation series (85), thereby isolating the remaining, nontrivial part of the time evolution. To do this, we note that "processes" described by $\tilde{\gamma}$ occur instantly in time [116]. Therefore, all Π_m diagrams vanish in which one or more vertices appear between any two vertices connected by a $\tilde{\gamma}$ contraction: There is no phase space left for the integration of the time variable of such vertices due to the δ function constraint (94) [117]. This means that in the surviving diagrams the $\tilde{\gamma}$ contractions form a ladder series [see Fig. 3(a)], which can be summed up. The skeleton diagram for this resummation is shown in Fig. 3(b) and consists of a single term: With Eq. (94),

$$\tilde{\Sigma}(t_1-t_2) = -i\sum_r \bar{G}_1\Gamma_1\delta(t_1-t_2)e^{-iL(t_1-t_2)}\tilde{G}_{\bar{1}} \quad (95a)$$
$$= 2\tilde{\Sigma}\,\delta(t_1-t_2) = \tilde{\Sigma}\,\bar{\delta}(t_1-t_2), \quad (95b)$$

with the time-independent superoperator,

$$\tilde{\Sigma} = -i\sum_1 \frac{1}{2}\Gamma_1\bar{G}_1\tilde{G}_{\bar{1}} = -i\sum_\sigma \frac{1}{2}\Gamma_\sigma\sum_\eta \bar{G}_{\eta\sigma}\tilde{G}_{\bar{\eta}\sigma}. \quad (96)$$

Note that in the sum over $1 = \eta,\sigma,r$, $\Gamma_1 = \Gamma_{r\sigma}$ does not depend on η and we again introduced the function $\bar{\delta}$ of Eq. (41). The sum of the spin-resolved tunnel rates over the reservoirs is denoted by

$$\Gamma_\sigma = \sum_r \Gamma_{r\sigma}. \quad (97)$$

The superoperator (96) is just the (constant) Laplace transform of $\tilde{\Sigma}(t_1-t_2)$ and is skew adjoint, $\tilde{\Sigma}^\dagger = -\tilde{\Sigma}$, since $\tilde{G}_{\bar{1}} = \bar{G}_1^\dagger$. By resumming diagrams as illustrated in Fig. 3(b), we can now simply leave out all terms with retarded contractions $\tilde{\gamma}$ from the series and we can incorporate their effect into a simple renormalization of the bare dot Liouvillian by the skeleton term (95)

$$L \to \bar{L} = L + \tilde{\Sigma}. \quad (98)$$

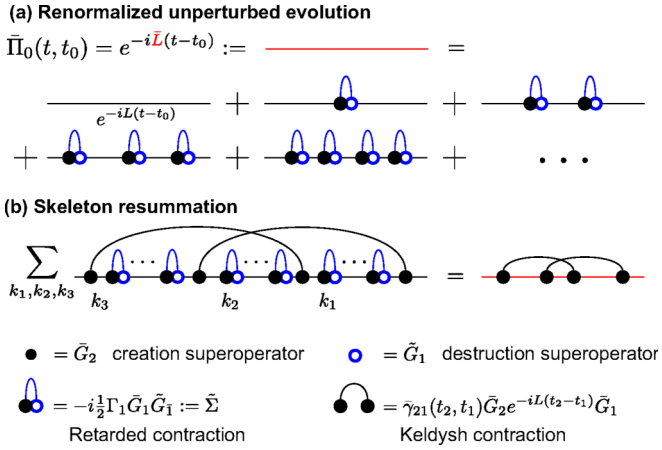

FIG. 3. (Color online) Wideband limit. (a) Free dot evolutions (the black horizontal lines) interrupted by a sequence of k retarded contractions $\tilde{\gamma}$ (the blue curved lines) are resummed to define a renormalized Liouvillian $\bar{L} := L + \tilde{\Sigma}$ [Eq. (98)]. The retarded "Markovian" contractions give rise to instantaneous $\tilde{\Sigma}$ blocks [Eq. (95)]; cf. Fig. 2. The sum defines a *renormalized* unperturbed evolution $\bar{\Pi}_0$ (the red horizontal line) which is *dissipative* [see Eq. (116)] and provides a starting point for a new perturbation theory. (b) Next, diagrams with a fixed configuration of Keldysh contractions $\bar{\gamma}$ (the black curved lines) are summed over all possible insertions of retarded contractions, here illustrated for two Keldysh loops. What remains is a renormalized perturbation theory in which only $\bar{L}$ and creation superoperators $\bar{G}$ appear explicitly with Keldysh contractions $\bar{\gamma}$; see Fig. 4.

In this way, we have eliminated the *annihilation* field superoperators $\tilde{G}$ of the quantum dot which enter only through the retarded reservoir correlation function $\tilde{\gamma}$ [cf. Eq. (89)]. This elimination was first pointed out in the more general framework of the real-time RG as formulated in Ref. [51] (where it is referred to a discrete RG step), which is not limited to the WBL and which explicitly constructs the corrections due to the frequency dependence (e.g., vertex renormalization). However, the above simpler derivation [118] may be of broad practical interest since in most studies the WBL is assumed from the start anyway. Also, the use of δ restrictions on time integrations reveals a mathematical analogy to the theory of disordered metals where spatial δ correlations of the disorder suppress crossing impurity contractions [119].

2. *Renormalized perturbation theory for finite temperature*

Having eliminated the destruction superoperators $\tilde{G}$ and the retarded reservoir correlation functions $\tilde{\gamma}$ by the replacement Eq. (98), we obtain a new time-ordered expansion for the propagator, $\Pi(t,t_0) = \sum_{m=0}^{\infty} \bar{\Pi}_m(t,t_0)$, for which the mth-order term is analogous to Eq. (85),

$$\begin{aligned}\bar{\Pi}_m &= (-i)^m \langle \bar{J}_{\bar{m}}(t_m)\cdots\bar{J}_{\bar{1}}(t_1)\rangle_R e^{-i\bar{L}(t-t_0)}\bar{G}'_m(t_m)\cdots\bar{G}'_1(t_1)\\ &= (-i)^m \sum_{\text{contr}}(-1)^P \prod_{\langle i,j\rangle}\bar{\gamma}_{i,j}(t_i-t_j)\\ &\quad\times e^{-i\bar{L}(t-t_0)}\bar{G}'_m(t_m)\cdots\bar{G}'_1(t_1) \qquad (99a)\end{aligned}$$

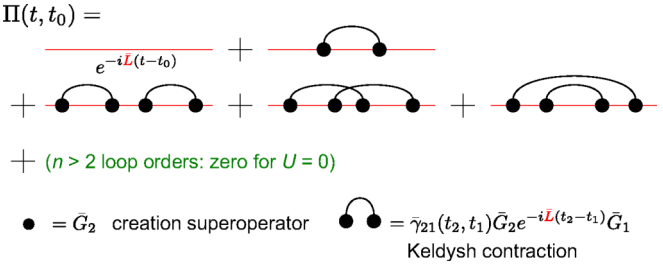

FIG. 4. (Color online) *Renormalized* real-time perturbation expansion in the WBL: contributing to the full time-evolution propagator $\Pi(t,t_0)$ in the first few loop orders of *renormalized* expansion (99b), $\bar{\Pi}_0 = e^{-i\bar{L}(t-t_0)}$, $\bar{\Pi}_2$, and $\bar{\Pi}_4$. Diagrams and expressions for the *renormalized* self-energy $\bar{\Sigma}(t,t_0) = \bar{\Sigma}_2 + \bar{\Sigma}_4 + \cdots$ are obtained by the same steps indicated in Fig. 2. The full evolution $\Pi(t,t_0)$ is now obtained by $\bar{\Sigma}(t,t_0)$ from the alternative Dyson equation (104), in which the unperturbed evolution is generated by the renormalized Liouvillian $\bar{L} = L + \bar{\Sigma}$; see Fig. 3(a). In contrast to the series in Fig. 2, the renormalized series for both $\Pi(t,t_0)$ and $\bar{\Sigma}(t,t_0)$, and therefore also for $\Sigma(t,t_0) = \tilde{\Sigma}(t,t_0) + \bar{\Sigma}(t,t_0)$, *terminates* at loop order *two* for the noninteracting Anderson model ($U = 0$), due to the super-Pauli principle (62) and (63); see Eqs. (122) and (123).

$$\begin{aligned}&= (-i)^m \sum_{\text{contr}}(-1)^P \prod_{\langle i,j\rangle}\bar{\gamma}_{i,j}(t_i-t_j)\\ &\quad\times e^{-i\bar{L}(t-t_m)}\bar{G}_m e^{-i\bar{L}(t_m-t_{m-1})}\cdots\bar{G}_1 e^{-i\bar{L}(t_1-t_0)}, \qquad (99b)\end{aligned}$$

with the same conventions as in Eq. (91), but with a *renormalized* interaction picture for the causal creation superoperators,

$$\bar{G}'_j(t) = e^{i\bar{L}(t-t_0)}\bar{G}_j e^{-i\bar{L}(t-t_0)}, \qquad (100)$$

whose difference from Eq. (80a) is indicated by the prime.

The renormalized perturbation theory for $\Pi(t,t_0)$ is expressed entirely in terms of the WBL form of Keldysh contraction function (90) (see Appendix B),

$$\begin{aligned}\bar{\gamma}_{2,\bar{1}}(t_2-t_1) &= \delta_{2,\bar{1}}\frac{\Gamma_2}{2\pi}\int d\omega_2 e^{-i\eta_2(\omega_2+\mu_{r_2})(t_2-t_1)}\tanh(\eta_2\omega_2/2T)\\ &= \delta_{2,\bar{1}}\frac{-i\Gamma_2 T}{\sinh[\pi T(t_2-t_1)]}e^{-i\eta_2\mu_{r_2}(t_2-t_1)}, \qquad (101)\end{aligned}$$

the *creation* field superoperators $\bar{G}$, and the renormalized Liouvillian $\bar{L}$ generating the *renormalized* free evolution $\bar{\Pi}_0(t,t_0) = e^{-i\bar{L}(t-t_0)}$. The diagrammatic expansion, shown in Fig. 4, is much simpler than the original one in Fig. 2. Since all appearing creation superoperators $\bar{G}$ anticommute, the key difficulty in the superoperator structure of Eq. (99b) lies in the failure of the $\bar{G}$ to commute with the renormalized Liouvillian, more precisely, $[\bar{G},L]_- \not\propto \bar{G}$, due to the quartic interaction term (74b) in L for $U \neq 0$.

The expansion (99b) captures the time-dependent, finite-temperature effects. For $T \to \infty$ the renormalized perturbation theory is exact already in zeroth order: In this limit, all higher-order $m \geqslant 1$ corrections (99b) vanish since the Keldysh contraction (101) goes to zero for $T \to \infty$ [even without taking the WBL; cf. Eq. (90)]. Thus, $\bar{L}$ generates the exact, dissipative, Markovian effective Liouvillian [cf. Eq. (40)] in

the infinite-temperature limit,

$$\lim_{T\to\infty} L(t,t') = \bar{L}\bar{\delta}(t-t'), \tag{102}$$

$$\lim_{T\to\infty} \Pi(t,t_0) = e^{-i\bar{L}(t-t_0)}, \tag{103}$$

with $\bar{L} = L + \tilde{\Sigma}$. Since this renormalized time evolution serves as a reference for the renormalized perturbation theory (99b), it is considered in more detail in the next section.

Although the causal superfermion approach is crucial in setting up the renormalized series (99b), one can calculate $\tilde{\Sigma}$, and therefore $\bar{L}$, using any equivalent density operator technique [40,41,88,120] (Nakajima-Zwanzig, etc.) simply by taking the leading order in the tunnel coupling in the WBL and then letting $T \to \infty$.

C. Infinite-temperature limit and fermion parity

Before we continue our analysis of the renormalized perturbation theory (99b) for the noninteracting limit ($U = 0$) in Sec. III D, we point out an interesting immediate consequence of the above general structure of (99b) which applies to the interacting Anderson model ($U \neq 0$). In fact, it applies to a broad class of quantum-dot models, i.e., for other model Hamiltonians instead of H [Eq. (13)], coupled to the reservoirs by a bilinear, particle-conserving H_T.

We have taken the $T \to \infty$ limit to define the starting point for both the construction of Liouville-Fock space [namely, the vacuum superket $|Z_L) = \frac{1}{2}\mathbb{1}$] and for the renormalization of the perturbation theory (99b) [$\tilde{\Sigma}\bar{\delta}(t-t') = \lim_{T\to\infty}\Sigma(t,t')$]. The result for $\tilde{\Sigma}$ holds nonperturbatively in all parameters in the limit $T \to \infty$ even though it results from the leading term in the perturbation theory in $\Gamma_{r\sigma}$. It is all the more surprising that it has observable implications in a *finite*-temperature experiment [31], for arbitrary values of $\Gamma_{r\sigma}$, the interaction U, applied voltages, and magnetic field (only restricted by the WBL). This result was first noted in the perturbative study Ref. [31] and subsequently related to the $T \to \infty$ limit and the fermion parity, generalizing it nonperturbatively in Γ and arbitrary Anderson-type models [30]. We now analyze this fermion-parity protected decay mode within the time-dependent perturbation theory in order to directly compare with the analysis in Sec. IV, which avoids the Laplace space analysis of Ref. [30] altogether. Moreover, we now also include the spin-dependent tunneling which Ref. [31] also considered. For this discussion and that following in Sec. III C 2, it is useful to elaborate more on the self-energy, although most parts of this work emphasize the possibility of calculating the time-evolution propagator $\Pi(t,t_0)$ directly from Eq. (99b) by using field superoperators. The self-energy also facilitates comparison with results from real-time RG and other density operator approaches.

1. Renormalized self-energy

The self-energy superoperator is defined either by the kinetic equation (39) for $\rho(t)$ or the equivalent Dyson equation for $\Pi(t,t_0)$ [Eq. (38)]. Diagrammatically, it is defined by collecting those parts of diagrams of $\Pi(t,t_0)$ that are *irreducibly* contracted (i.e., diagrams pieces obtained by *only* cutting through free time evolutions, without cutting contractions) and summing these. The perturbation theory for the self-energy superoperator is then simply obtained from the perturbation theory for $\Pi(t,t_0)$ by (i) restricting the sum to irreducible contractions and (ii) omitting the initial ($t_0 \to t_1$) and final ($t_m \to t$) free time evolutions. The perturbation theory can then be resummed in terms of these self-energy diagram blocks. If this is done for the original perturbation theory Eq. (85), taking $e^{-iL(t-t_0)}$ as the free time evolution, we obtain the Dyson Eq. (38) with self-energy $\Sigma(t,t_0)$ (equal to the Nakajima-Zwanzig kernel). However, the renormalized perturbation theory Eq. (99b) takes $e^{-i\bar{L}(t-t_0)}$ as a reference. This series can be resummed as well in terms of different self-energy diagram blocks, now denoted by $\bar{\Sigma}(t,t')$. This gives an equivalent Dyson equation for the same superoperator $\Pi(t,t_0)$,

$$\Pi(t,t_0) = e^{-i\bar{L}(t-t_0)} - i\int_{t\geqslant t_2\geqslant t_1\geqslant t_0} dt_2 dt_1 e^{-i\bar{L}(t-t_2)}\bar{\Sigma}(t_2,t_1)\Pi(t_1,t_0). \tag{104}$$

The renormalized self-energy superoperator $\bar{\Sigma}(t,t_0)$ [30,51] is obtained from Eq. (99b) by keeping *irreducible* Keldysh contractions. This corresponds to a decomposition of the effective dot Liouvillian,

$$L(t,t') = \bar{L}\bar{\delta}(t-t') + \bar{\Sigma}(t,t'), \tag{105}$$

alternative to Eq. (40). Since the kinetic equation (39) only depends on the *sum* of the reference Liouvillian $L\bar{\delta}(t-t')$ [$\bar{L}\bar{\delta}(t-t')$] and the self-energy $\Sigma(t,t')$ [$\bar{\Sigma}(t,t')$] appearing in the Dyson equation Eq. (38) [Eq. (104)], this results in the same time evolution $\Pi(t,t_0)$ in the WBL.

2. Fermion-parity protected decay mode

We now discuss how the infinite-temperature self-energy $\tilde{\Sigma}$ affects the *finite-temperature* time evolution of the density operator $\rho(t)$. The key observation is that by the causal structure [cf. Sec. III A] of Eq. (99b), also the renormalized self-energy $\bar{\Sigma}$ always has a creation superoperator $\bar{G}_1$ standing on the *far right*, i.e., at the time t_1 of the initial tunnel "process." An immediate consequence of our Liouville-Fock space construction using *causal* superfermions is that the maximally filled superket, i.e., the fermion-parity operator $|Z_R) = \frac{1}{2}(-1)^n$, is an exact right zero eigenvector of the nontrivial self-energy since $\bar{G}_m|Z_R) = 0$ [Eq. (55)],

$$\bar{\Sigma}(t,t_0)|Z_R) = 0 \quad \text{for any} \quad t,t_0. \tag{106}$$

This a consequence of the super-Pauli principle in Liouville space, Eq. (62). The time-evolution of the excitation mode $|Z_R)$ is then completely determined by $\tilde{\Sigma}$ which we obtained exactly in the WBL. We emphasize that it is determined *completely* by the *leading-order* term in Γ in the limit $T \to \infty$. The action of $\tilde{\Sigma}$ on this mode follows directly from the superfermion anticommutation relation

and $\bar{G}_1|Z_R) = 0$ [Eq. (55)],

$$\begin{aligned}\tilde{\Sigma}(t,t')|Z_R) &= -i\bar{\delta}(t-t')\sum_1 \frac{1}{2}\Gamma_1\bar{G}_1\tilde{G}_{\bar{1}}|Z_R)\\ &= -i\bar{\delta}(t-t')\sum_1 \frac{1}{2}\Gamma_1(1-\tilde{G}_{\bar{1}}\bar{G}_1)|Z_R)\\ &= -i\bar{\delta}(t-t')\Gamma|Z_R) \quad \text{for all} \quad t\geqslant t'\geqslant t_0.\end{aligned} \tag{107}$$

The *fermion-parity eigenvalue* is simply the sum of all tunnel rates over both reservoirs and spins,

$$\Gamma = \textstyle\sum_\sigma \Gamma_{\sigma r} = \sum_\sigma \Gamma_\sigma, \tag{108}$$

times $-i$. The renormalized time-dependent perturbation theory directly shows that for the fermion-parity mode $|Z_R)$ the $T\to\infty$ evolution remains exact at *all finite temperatures*:

$$\Pi(t,t_0)|Z_R) = e^{-\Gamma(t-t_0)}|Z_R) \quad \text{for all} \quad t\geqslant t_0. \tag{109}$$

All higher-order corrections given by Eq. (99b), responsible for dependence on U, ϵ, B, μ_r, and T, vanish: $\bar{\Pi}_m(t,t_0)|Z_R) = 0$ for $m\geqslant 1$. This follows since $|Z_R)$ is a supereigenvector of $\bar{L}$ and $\bar{G}_m|Z_R) = 0$ by the super-Pauli principle. The former follows from $L|Z_R) \propto [H,(-1)^n]_- = 0$ by the superselection rule (3) and Eq. (107). The exact result (109) can be also formulated for the original self-energy: Σ has $|Z_R)$ as an exact eigenmode with eigenvalue $-i\Gamma$,

$$\Sigma(t,t')|Z_R) = -i\Gamma|Z_R) \quad \text{for all} \quad t\geqslant t'\geqslant t_0. \tag{110}$$

For multiorbital models this generalizes to $\Gamma = \sum_{r\sigma l}\Gamma_{r\sigma l}$ and $|Z_R) = \prod_{\sigma l} e^{i\pi n_{\sigma l}}/N$ for N spin orbitals, where l is the orbital quantum number [30].

It should be noted that Eqs. (109) and (110) hold nonperturbatively both in the tunneling Γ as well as in Coulomb interaction U and down to zero temperature $T = 0$: Only the WBL is used here. Due to the fundamental fermion-parity superselection principle, the eigenvalue is thus prevented from picking up any dependence on energies other than $\Gamma = \sum_{r\sigma}\Gamma_{r\sigma}$ [Eq. (108)] and the decay remains strictly exponential. Since only the sum of spin-dependent rates enters, the spin-polarization of the tunneling also has no influence. Because we explicitly used this fermion-parity superselection principle in the construction of the causal field superoperators [cf. Eq. (55) and following discussion], the property (109) becomes directly clear on the superoperator level once the WBL has been taken [Eq. (99b)].

We note that $\bar{G}_1$ has only one nontrivial zero right eigenvector, $|Z_R)$, for all values of the multi-index 1: In analogy to usual the second quantization, only the maximally filled state is a common zero eigenvector of *all* creation superoperators. Therefore, the above argument applies only to the special fermion-parity superket $|Z_R)$.

The exact result (109) implies for the time-evolution of $\rho(t) = \Pi(t,t_0)\rho(t_0)$, starting from an initial state $\rho(t_0)$ with the general form Eq. (68) at $t = t_0$, that

$$\rho(t) = [\Xi(t_0)e^{-\Gamma(t-t_0)} + \cdots]|Z_R) + \cdots; \tag{111}$$

see the introductory discussion of Eq. (1) and Fig. 1. The decay of the initial two-particle correlation $\Xi(t_0)$ on the quantum dot thus happens on a time scale $t - t_0 \lesssim \Gamma^{-1}$ which is independent of all further energy scales mentioned above. As pointed out in Ref. [31], the appearance of the sum of all rates (108) in the decay rate of the the two-particle correlation seems to have a simple origin in the noninteracting limit ($U = 0$): Using a Markovian approximation, $\langle n_\uparrow n_\downarrow\rangle = \langle n_\uparrow\rangle\langle n_\downarrow\rangle \propto \prod_\sigma e^{-\Gamma_\sigma(t-t_0)} = e^{-\Gamma(t-t_0)}$. However, as emphasized there, it is all the more surprising that the decay maintains this exponential form and the value of the decay rate in the interacting limit, even when attaching a ferromagnet or superconductor or when the dot is initially in a correlated state, where this factorization breaks down. Also, note that the Markovian approximation remains exactly valid for this decay mode.

The real-time RG approach [30], was found to be consistent with the eigenvalue equation (107), even without any truncations of the exact hierarchy of RG equations or any approximations other than the WBL (as it should). In the continuous RG flow of the effective Liouvillian towards low energies, the coefficient of $|Z_R)(Z_R|$ is given by the eigenvalue $-i\Gamma$ and this coefficient does not flow.

Finally, we recall that the superket $|Z_R)$ in Eq. (109) on its own does not represent a physical state, only in linear combination with the vacuum superket $|Z_L)$ of the form Eq. (68) it does. Measurement setups that can target specifically the fermion-parity protected decay mode contained in this mixed state were analyzed in Refs. [31] and [121]. In the next section we calculate the full time dependence of such physical states for $T = \infty$ and finite interaction U and in Sec. IV for finite T but $U = 0$.

3. *Infinite-temperature limit and Markovian relaxation*

As mentioned in Sec. III B 2, the decay of all modes is Markovian and exponential in the infinite-temperature limit, which surprisingly continues to hold for the special fermion-parity mode $|Z_R)$ at any finite T as we have just seen. To calculate the $T\to\infty$ time evolution, $\bar{\Pi}(t,t_0) = e^{-i\bar{L}(t-t_0)}$ [Eq. (103)], which serves as a reference for the renormalized perturbation theory (99b), we need (some of) the supereigenvectors of $\bar{L} = L + \tilde{\Sigma}$. These follow easily from the second quantized forms (96) and (74) of the superoperators, as we now show.

First, the self-energy $\tilde{\Sigma} = -i\frac{1}{2}\sum_{\eta\sigma}\Gamma_\sigma\mathcal{N}_{\eta\sigma}$ [Eq. (96)] simply counts the mode occupation through the superoperator $\mathcal{N}_{\eta\sigma}$ [Eq. (64)] and multiplies it with the half of the spin-resolved decay rate (97), $\Gamma_\sigma = \sum_r\Gamma_{r\sigma}$. The bosonic basis superkets Eqs. (60) are thus supereigenvectors of $\tilde{\Sigma}$, and the latter can be expressed in projectors onto the bosonic part of the basis (60),

$$\tilde{\Sigma} = -i\sum_\sigma \Gamma_\sigma|\chi_\sigma)(\chi_\sigma| \tag{112a}$$

$$-i\Gamma|Z_R)(Z_R| \tag{112b}$$

$$-i\frac{1}{2}\Gamma\left[\sum_\sigma|S_\sigma)(S_\sigma| + \sum_\eta|T_\eta)(T_\eta|\right] + F, \tag{112c}$$

where again $\Gamma = \sum_\sigma\Gamma_\sigma$ [Eq. (108)] and F denotes the irrelevant fermionic part [cf. Sec. II D 2]. Since $\tilde{\Sigma}^\dagger = -\tilde{\Sigma}$ [cf. Eq. (95)], the eigenvalues are necessarily imaginary or zero

[bosonic eigenvector $|Z_L)$], and the left supereigenvectors are the superadjoints of the right ones with the same eigenvalues.

Similarly, we can rewrite the Liouvillian,

$$L = \sum_{\eta,\sigma} \eta(\epsilon + U/2 + \sigma B/2)\mathcal{N}_{\eta\sigma} + L|_{\text{quartic}} \tag{113a}$$

$$= \sum_{\sigma} \sigma B |S_\sigma)(S_\sigma| + \sum_{\eta} \eta(2\epsilon + U)|T_\eta)(T_\eta| + F, \tag{113b}$$

where F again denotes the irrelevant fermionic part. [122] In writing Eq. (113b) we used that the quartic part of L [Eq. (74b)] acts *only* on the fermionic part of the Liouville-Fock space [cf. Eq. (77)], whereas the quadratic part has a component in both the bosonic and the fermionic parts.

For the particular case of the Anderson model, the bosonic blocks of L and $\tilde{\Sigma}$ commute, as Eqs. (113b) and (112) explicitly show [123]. Therefore, when working in the basis naturally provided by the causal superfermions, we obtain the diagonal form for (bosonic part of) $\bar{L} = L + \tilde{\Sigma}$ when simply adding [124] Eqs. (112) and (113b), which we quote here for future reference:

$$\bar{L} = -i \sum_{\sigma} \Gamma_\sigma |\chi_\sigma)(\chi_\sigma| \tag{114a}$$

$$- i\Gamma |Z_R)(Z_R| \tag{114b}$$

$$+ \sum_{\sigma} \left(\sigma B - i\frac{1}{2}\Gamma\right) |S_\sigma)(S_\sigma| \tag{114c}$$

$$+ \sum_{\eta} \left(\eta(2\epsilon + U) - i\frac{1}{2}\Gamma\right) |T_\eta)(T_\eta| + F. \tag{114d}$$

Notably, this implies that for the time evolution in the limit $T \to \infty$—fully determined by the bosonic part of $\bar{L} = L + \tilde{\Sigma}$—the nontrivial quartic part (77) has no influence: The interaction parameter U only enters via the quadratic part of the interaction Liouvillian [125].

From the diagonal form (114) we immediately obtain the $T \to \infty$ time evolution of the reduced density operator expressed in terms of the coefficients of the initial dot density operator $\rho(t_0)$ [cf. Eq. (68)]:

$$\lim_{T\to\infty} \rho(t) = e^{-i\bar{L}(t-t_0)}\rho(t_0) \tag{115}$$

$$= \frac{1}{2}|Z_L) + \sum_{\sigma} e^{-\Gamma_\sigma(t-t_0)}\Phi_\sigma(t_0)|\chi_\sigma)$$

$$+ e^{-\Gamma(t-t_0)}\Xi(t_0)|Z_R)$$

$$+ \sum_{\eta} e^{-\left[i\eta(2\epsilon+U)+\frac{1}{2}\Gamma\right](t-t_0)}\Upsilon_\eta(t_0)|T_\eta)$$

$$+ \sum_{\sigma} e^{-\left[i\sigma B+\frac{1}{2}\Gamma\right](t-t_0)}\Omega_\sigma(t_0)|S_\sigma). \tag{116}$$

The result (116) explicitly illustrates that renormalized free evolution dissipative, involving exponential decay with rates Γ_σ, $\Gamma/2$, and Γ. The oscillations during the decay (116) indicate the presence of coherent spin $\uparrow$-$\downarrow$ excitations (frequency B) or coherent electron-pair 0-2 excitations (frequency $2\epsilon + U$) in the initial state $\rho(t_0)$.

At infinite temperature, we obtain from Eq. (116) in the stationary limit the maximum von Neumann entropy state (73), $\lim_{T\to\infty}\rho(\infty) = \rho_\infty = \frac{1}{4}\mathbb{1} = \frac{1}{2}|Z_L)$, the vacuum superket (60a) in our Liouville-Fock space construction. Indeed, $|Z_L)$ is the right zero eigenvector of $\bar{L}$ since $|Z_L)(Z_L|$ is missing in Eq. (114), a point that will be important later on [cf. discussion of Eq. (156)]. Generally, the left zero supereigenvector $(Z_L|$ guaranteeing probability conservation $(Z_L|\bar{L} = 0$ only implies the *existence* of at least one right zero supervector, the stationary state $|\rho_{\text{st}})$ (assuming it is unique). However, in general, this stationary state is not equal to the (properly normalized) superadjoint of $(Z_L|$. The above discussion now shows that, in general, the deviation of $|\rho_{\text{st}})$ from $\frac{1}{2}|Z_L)$ is generated by the finite-temperature corrections described by $\bar{\Pi}_m$ for $m \geqslant 1$ (and $\bar{\Sigma}$), which makes good physical sense.

D. Noninteracting limit

Nearly all considerations of the perturbation series Eq. (85) and (99b) so far apply to the interacting Anderson model ($U \neq 0$) and, where mentioned, its generalizations. We now identify the simplifications that the noninteracting limit $U = 0$ brings.

In Sec. II D 4, we found that the interaction-picture field superoperators $G_1^q(t) = e^{iL(t-t_0)}G_1^q e^{-iL(t-t_0)}$ [Eq. (80b)] simplify for $U = 0$ since in this case L is quadratic in these fields. However, even in this simple limit, the original perturbation theory (85) still contains an infinite series of terms. Although this series can be resummed, this can be avoided if one instead starts from the physically motivated renormalized perturbation series (99), as we now show. For $U = 0$ the renormalized interaction picture of the creation superfields $\bar{G}_1'(t) = e^{i\bar{L}(t-t_0)}\bar{G}_1 e^{-i\bar{L}(t-t_0)}$ [Eq. (100)] with respect to the quadratic renormalized Liouvillian,

$$\bar{L} = \sum_{\eta,\sigma} \left(\eta\epsilon_\sigma - i\frac{1}{2}\Gamma_\sigma\right)\bar{G}_{\eta\sigma}\tilde{G}_{\bar{\eta}\sigma}, \tag{117}$$

simplifies, since now

$$[\bar{L}, \bar{G}_1]_- = \left(\eta\epsilon_\sigma - i\frac{1}{2}\Gamma_\sigma\right)\bar{G}_1, \tag{118}$$

which follows from the anticommutation relations (50). Analogous to Eq. (80b) we obtain

$$\bar{G}_1'(t) = e^{(i\eta\epsilon_\sigma + \frac{1}{2}\Gamma_\sigma)(t-t_0)}\bar{G}_1, \tag{119}$$

and therefore these field superoperators also anticommute,

$$[\bar{G}_2'(t_2), \bar{G}_1'(t_1)]_+ = 0. \tag{120}$$

Inserting Eq. (119) into (99b), we obtain the key result

$$\bar{\Pi}_m = (-i)^m \sum_{\text{contr}} (-1)^P \prod_{\langle i,j\rangle} \bar{\gamma}_{i,j}(t_i - t_j) e^{i\eta_i\epsilon_{\sigma_i}(t_i - t_j)} \tag{121a}$$

$$\times \prod_{k=1}^{m} e^{\frac{1}{2}\Gamma_{\sigma_k}(t_k - t_0)} \tag{121b}$$

$$\times e^{-i\bar{L}(t-t_0)}\bar{G}_m \cdots \bar{G}_1. \tag{121c}$$

Note that the dissipative factors (121b) depend explicitly on t_0, in contrast to the coherent phase factors (121a), in which

t_0 cancels out [cf. Eq. (92)]. Their exponential increase leads to no problems as it is always dominated by the exponentially decaying term $e^{-i\bar{L}(t-t_0)}$ in Eq. (121c).

The result (121) shows that all terms of order $m > 4$ are *identically zero* due to their *superoperator structure*. Like Eq. (106), this is another manifestation of the super-Pauli principle (62) and (63). The exact result for the case $U = 0$ is thus obtained in just the first two nonvanishing loop orders of the renormalized perturbation theory, represented by precisely those diagrams shown in Fig. 4,

$$\Pi(t,t_0) = \bar{\Pi}_0(t,t_0) + \bar{\Pi}_2(t,t_0) + \bar{\Pi}_4(t,t_0), \quad (122)$$

$$\bar{\Sigma}(t,t_0) = \bar{\Sigma}_2(t,t_0) + \bar{\Sigma}_4(t,t_0), \quad (123)$$

and the exact total self-energy follows from $\Sigma(t,t_0) = \tilde{\Sigma}(t,t_0) + \bar{\Sigma}(t,t_0)$. The super-Pauli principle also shows that the renormalized Dyson equation can be solved exactly, relating Eq. (122) to Eq. (123) [126],

$$\bar{\Pi}_2(t,t_0) = \bar{\Pi}_0 * \bar{\Sigma}_2 * \bar{\Pi}_0(t,t_0), \quad (124)$$

$$\bar{\Pi}_4(t,t_0) = \bar{\Pi}_0 * [\bar{\Sigma}_4 + \bar{\Sigma}_2 * \bar{\Pi}_0 * \bar{\Sigma}_2] * \bar{\Pi}_0(t,t_0), \quad (125)$$

where by $A * B(t,t_0) = \int_{t_0}^{t} dt_1 A(t,t_1)B(t_1,t_0)$ we denote the time convolution. This illustrates the computational advantage of working with field superoperators directly in Liouville space, in particular, when incorporating the causal structure into these fields. Equations (122) and (123) show that it becomes practical to avoid the calculation of the self-energy in the limit $U = 0$, since the structure of the time propagator Π is no less complicated. In fact, as we see explicitly in the next section [Eq. (138), Fig. 5, and Eq. (164b)], the inclusion of the second reducible term in $\bar{\Pi}_4$ on the right-hand side in Eq. (125) makes it a simpler object than $\bar{\Sigma}_4$ in the $U = 0$ limit. We emphasize that the simple structure of the noninteracting problem appears only in the *renormalized* series, i.e., after explicitly exploiting the WBL. Similar, but less drastic, simplifications on the *superoperator level* can be exploited for interacting problems as well [84].

We emphasize that the truncation in Eqs. (122) and (123) does not rely on the spin- and charge-rotation [30] symmetry of the Anderson model: only the number of spin orbitals of the model (=2) and the absence of quartic terms and higher in L matter ($U = 0$). The crucial observation for this was that in Eq. (121) we were able to commute $\bar{L}$ through all the $\bar{G}$ fields to the left side, thereby only generating c-number factors, without changing the structure of the appearing field superoperators. For the interacting Anderson model, however, the expansion (91) must be used: Here $\bar{L}$ cannot be commuted through the fields $\bar{G}$ without generating additional, higher-order terms. Then even the renormalized perturbation theory has nonzero terms beyond the two-loop order. (Note however, that the self-energy $\tilde{\Sigma}$ remains quadratic even for finite U due to the WBL.) Yet even in this case the causal superfermions bring simplifications; cf. Eq. (76) [127].

The result, Eqs. (122) and (123), thus explicitly shows that the higher-order terms in the renormalized perturbation theory are *generated* by the nontrivial part of the Coulomb interaction, Eq. (74b), which is the part that couples U to the fermion-parity operator, Eq. (77). The real-time RG in the one- plus two-loop approximation [30] encodes these higher-order terms into a renormalization of $\bar{L}$ and $\bar{G}$. An important property of this approach is that, while it provides a good approximation for large U as well, it exactly includes the solution for the noninteracting limit $U = 0$. The above simple analysis explains why *at least* the one- and two-loop orders must be included to exactly recover the noninteracting limit (i.e., for the full self-energy and the full density operator, not just selected quantities [128]).

Finally, we note that Eq. (123) shows that the quantum-dot self-energy Σ and therefore the effective Liouvillian (105) is *quartic* [129] in the field superoperators, even in the noninteracting limit ($U = 0$). This is to be contrasted with, e.g., Green's function and path-integral approaches, where only quadratic expressions appear for noninteracting problems. To understand better how this difference arises, we turn to the explicit evaluation of all contributions in Eq. (122) for $U = 0$, which will reveal a further simplification.

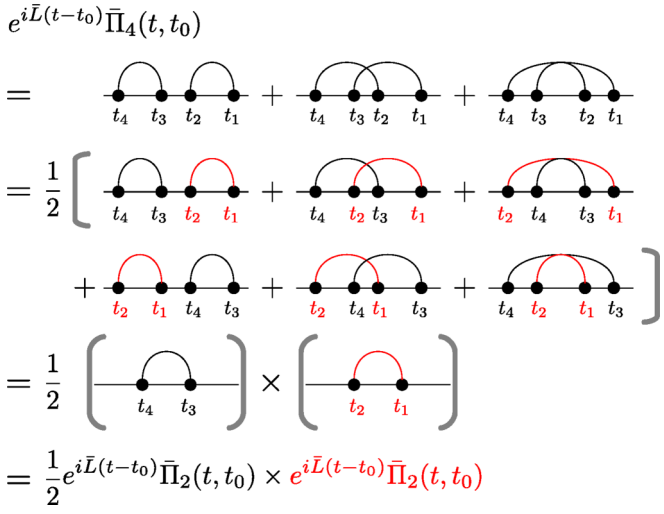

FIG. 5. (Color online) Factorization (138) of the renormalized two-loop propagator $\bar{\Pi}_4(t,t_0)$: diagrammatic proof; see Appendix E for explicit expressions. We use the modified convention that diagrams represent the same expressions Eq. (121) as in Fig. 4 but now without the overall renormalized unperturbed propagator $e^{-i\bar{L}(t-t_0)}$ in Eq. (121c). First equality: Two loop terms in Fig. 4 with the time-ordered integrations $t \geqslant t_4 \geqslant t_3 \geqslant t_2 \geqslant t_1 \geqslant t_0$. Second equality: We first duplicated the terms while compensating with a factor $1/2$ and then relabeled the dummy time variables as indicated. The dummy multi-indices, are relabeled correspondingly: A vertex with time t_i thus stands for $\bar{G}_i(t_i)$ with multi-index $i = \eta_i,\sigma_i$. In each term the integrations are such that vertices maintain their order; e.g., in the second term we integrate over $t \geqslant t_4 \geqslant t_2 \geqslant t_3 \geqslant t_1 \geqslant t_0$. Since the vertex superoperators anticommute [Eq. (120)], we can factorize the *integrand* superoperators and bring together the black and the red parts. For the second and fifth diagrams (crossed contraction), this introduces a quantum-dot fermion sign (-1) that exactly cancels the Wick sign of the reservoir $[(-1)^P$ in Eq. (137)]. As a result, all integrands are given by the same superoperator. Third equality: By summing all the integrals with all possible time orderings, the resulting *integral* also factorizes. The resulting expression in the factors is precisely the one-loop propagator (i.e., the one-loop terms in Fig. 4, again using the mentioned convention). Multiplying the equation by $e^{-i\bar{L}(t-t_0)}$ gives Eq. (138).

IV. EXACT NONINTERACTING TIME EVOLUTION

In this section, we specialize to the noninteracting limit $U = 0$, unless stated otherwise.

A. Time evolution

1. Time-evolution propagator

We now calculate the one- and two-loop corrections to the renormalized free propagator (103), which is defined by the time-local renormalized Liouvillian (114)

$$\begin{aligned}\bar{\Pi}_0(t,t_0) &= \lim_{T\to\infty}\Pi(t,t_0) = e^{-i\bar{L}(t-t_0)}\\ &= e^{-\Gamma(t-t_0)}|Z_R)(Z_R| + \sum_\sigma e^{-\Gamma_\sigma(t-t_0)}|\chi_\sigma)(\chi_\sigma|\\ &\quad + \sum_\sigma e^{-\left(i\sigma B+\frac{1}{2}\Gamma\right)(t-t_0)}|S_\sigma)(S_\sigma|\\ &\quad + \sum_\eta e^{-\left(i\eta 2\epsilon+\frac{1}{2}\Gamma\right)(t-t_0)}|T_\eta)(T_\eta| \qquad (126)\end{aligned}$$

(the fermionic part is omitted) and then discuss the time-dependent density operator $\rho(t)$.

(a) One-loop propagator. The one-loop ($m = 2$) contribution to Eq. (99b) can be written as

$$\bar{\Pi}_2(t,t_0) = -e^{-i\bar{L}(t-t_0)}\sum_{21}\int_{t\geqslant t_2\geqslant t_1\geqslant t_0} dt_2dt_1\bar{G}'_2(t_2)\bar{G}'_1(t_1)\bar{\gamma}_{21}(t_2-t_1) \qquad (127)$$

$$= -e^{-i\bar{L}(t-t_0)}\sum_{r,\sigma,\eta}\bar{G}_2\bar{G}_{\bar{2}} \times\int_{t\geqslant t_2\geqslant t_1\geqslant t_0} dt_2dt_1\bar{\gamma}_{2,\bar{2}}(t_2-t_1)e^{i\eta\epsilon_\sigma(t_2-t_1)}e^{\frac{1}{2}\Gamma_\sigma(t_2+t_1-2t_0)}, \qquad (128)$$

making use of the factor $\delta_{2,\bar{1}}$ in the contraction $\bar{\gamma}_{2,1}$ and writing $2 = \eta,\sigma,r$. The one-loop contributions only generate transitions which increase the superfermion number by two. This is expected since in Eq. (128) only *creation* superoperators appear. In the bosonic sector (60) these transitions proceed from the supervacuum state $|Z_L)$ to the doubly excited superkets $|\chi_\sigma)$ and from there to the most occupied superket $|Z_R)$. The corresponding matrix elements of the superoperator $\bar{G}_2\bar{G}_{\bar{2}}$ are again easily determined using the algebra of superfermions: First, we note that $\bar{G}_{\eta\sigma}\bar{G}_{\bar{\eta}\sigma} = \eta\bar{G}_{+\sigma}\bar{G}_{-\sigma}$ since the fields anticommute. Next, we see that for transitions between 0 and 2 superparticles, by definition $\bar{G}_{+\sigma}\bar{G}_{-\sigma}|Z_L) = |\chi_\sigma)$, and between 2 and 4 superparticles, $(Z_R|\bar{G}_{+\sigma}\bar{G}_{-\sigma} = [\bar{G}_{+\sigma}\bar{G}_{-\sigma}|Z_R)]^\dagger = [\bar{G}_{+\bar{\sigma}}\bar{G}_{-\bar{\sigma}}|Z_L)]^\dagger = [|\chi_{\bar{\sigma}})]^\dagger = (\chi_{\bar{\sigma}}|$, using Eq. (53) [130]. As a result,

$$\bar{G}_{\eta\sigma}\bar{G}_{\bar{\eta}\sigma} = \eta[|\chi_\sigma)(Z_L| + |Z_R)(\chi_{\bar{\sigma}}|] + F, \qquad (129)$$

where F is again an irrelevant fermionic part. Inserting this in Eq. (128), we obtain after summing over η

$$\begin{aligned}\bar{\Pi}_2(t,t_0) &= -e^{-i\bar{L}(t-t_0)}\sum_\sigma[|\chi_\sigma)(Z_L| + |Z_R)(\chi_{\bar{\sigma}}|]\\ &\quad\times\sum_r 2\Gamma_{r\sigma}\int_{t\geqslant t_2\geqslant t_1\geqslant t_0} dt_2dt_1\frac{T\sin[\epsilon_{r\sigma}(t_2-t_1)]}{\sinh[\pi T(t_2-t_1)]}\\ &\quad\times e^{\frac{1}{2}\Gamma_\sigma(t_2+t_1-2t_0)}, \qquad (130)\end{aligned}$$

where we denote the quantum-dot energies $\epsilon_\sigma = \epsilon + \sigma B/2$ relative to the electrochemical potential μ_r by

$$\epsilon_{r\sigma} = \epsilon_\sigma - \mu_r. \qquad (131)$$

Next, the diagonal form (114) of the renormalized free propagator is used

$$\bar{L}|\chi_\sigma) = -i\Gamma_\sigma|\chi_\sigma), \quad \bar{L}|Z_R) = -i\Gamma|Z_R), \qquad (132)$$

and we change variables, $\Theta = t_2 + t_1 - 2t_0$ and $\tau = t_2 - t_1$ in the integration, $\int_{t_0}^{t}\int_{t_0}^{t_2} dt_2dt_1 = \frac{1}{2}\int_0^\Delta d\tau\int_\tau^{2\Delta-\tau} d\Theta$, denoting $\Delta = t - t_0$, and then perform the Θ integral,

$$\begin{aligned}\bar{\Pi}_2(t,t_0) &= \sum_\sigma\{|\chi_\sigma)(Z_L| + e^{-\Gamma_{\bar{\sigma}}\Delta}|Z_R)(\chi_{\bar{\sigma}}|\}\\ &\quad\times\sum_r\frac{2\Gamma_{r\sigma}}{\Gamma_\sigma}[F^+_{r\sigma}(\Delta) + F^-_{r\sigma}(\Delta)]. \qquad (133)\end{aligned}$$

The explicit expressions for the time-dependent coefficients (see Appendix D),

$$\begin{aligned}F^+_{r\sigma}(\Delta) &:= -\int_0^\Delta d\tau\frac{T\sin(\epsilon_{r\sigma}\tau)}{\sinh(\pi T\tau)}e^{-\frac{1}{2}\Gamma_\sigma\tau}\\ &= \frac{1}{\pi}\operatorname{Im}\Psi\left(\frac{1}{2} - \frac{i\epsilon_{r\sigma}-\frac{1}{2}\Gamma_\sigma}{2\pi T}\right)\\ &\quad + \frac{1}{\pi}\operatorname{Im}e^{(-\pi T+i\epsilon_{r\sigma}-\frac{1}{2}\Gamma_\sigma)\Delta}\\ &\quad\times\Phi\left(e^{-2\pi T\Delta};1;\frac{1}{2}+\frac{i\epsilon_{r\sigma}-\frac{1}{2}\Gamma_\sigma}{2\pi T}\right), \qquad (134a)\\ F^-_{r\sigma}(\Delta) &:= e^{-\Gamma_\sigma\Delta}\int_0^\Delta d\tau\frac{T\sin(\epsilon_{r\sigma}\tau)}{\sinh(\pi T\tau)}e^{\frac{1}{2}\Gamma_\sigma\tau}\\ &= -e^{-\Gamma_\sigma\Delta}\cdot F^+_{r\sigma}(\Delta)\Big|_{\Gamma_\sigma\to-\Gamma_\sigma}, \qquad (134b)\end{aligned}$$

can be expressed through the digamma function $\Psi(z)$, with $\operatorname{Im}\Psi(z) = -\operatorname{Im}\sum_{n=0}^\infty 1/(n+z)$ and the Lerch transcendent function [131] $\Phi(z;s;\nu) = \sum_{n=0}^{+\infty}\frac{z^n}{(n+\nu)^s}$. The asymptotic values are

$$F^+_{r\sigma}(\infty) = \frac{1}{\pi}\operatorname{Im}\Psi\left(\frac{1}{2} - \frac{i\epsilon_{r\sigma}-\frac{1}{2}\Gamma_\sigma}{2\pi T}\right), \qquad (135a)$$

$$F^-_{r\sigma}(\infty) = 0. \qquad (135b)$$

The decay to these stationary values, given by the second term on the right-hand side of Eq. (134a), has the asymptotic

form

$$F^+_{r\sigma}(\Delta) - F^+_{r\sigma}(\infty) = \sin\left[\epsilon_{r\sigma}\Delta + \arctan\left(\frac{\epsilon_{r\sigma}}{\varsigma_\sigma}\right)\right] \begin{cases} \frac{T}{\sqrt{(\pi T)^2+(\epsilon_{r\sigma})^2}} 2e^{-\pi T\Delta} & \Delta \gg \Gamma_\sigma^{-1} \gg T^{-1}, \\ \frac{T}{\sqrt{(\Gamma_\sigma/2)^2+(\epsilon_{r\sigma})^2}} \frac{e^{-\frac{1}{2}\Gamma_\sigma\Delta}}{\sinh(\pi T\Delta)} & \Delta \gtrsim T^{-1} \gg \Gamma_\sigma^{-1}, \end{cases} \tag{136}$$

where $\varsigma_\sigma = \max\{\frac{1}{2}\Gamma_\sigma, \pi T\}$. Thus, for low-temperature $T \ll \Gamma_{r\sigma}$, the oscillatory decay of both $F^+_{r\sigma}(\Delta)$ and $F^-_{r\sigma}(\Delta)$ [following from Eq. (134b)] is at least as fast as $e^{-(\Gamma_\sigma/2)\Delta}$.

(b) Two-loop propagator. The two-loop ($m = 4$) contribution to Eq. (99a) reads as

$$\bar{\Pi}_4(t,t_0) = e^{-i\bar{L}(t-t_0)} \int_{t\geqslant t_4\geqslant t_3\geqslant t_2\geqslant t_1\geqslant t_0} dt_4 dt_3 dt_2 dt_1 \bar{G}'_4(t_4)\bar{G}'_3(t_3)\bar{G}'_2(t_2)\bar{G}'_1(t_1) \times \sum_{\langle i,j,k,l\rangle} (-1)^P \bar{\gamma}_{ij}(t_i - t_j)\bar{\gamma}_{kl}(t_k - t_j), \tag{137}$$

where $\langle i,j,k,l\rangle$ denotes the sum over the following possible contractions: $i,j,k,l = 4,3,2,1$ (reducible), 4,2,3,1, and 4,1,3,2 (both irreducible). The second major simplification occurring in the noninteracting limit ($U = 0$), besides the truncation (122) is that this contribution can be factorized as (see Appendix E and Fig. 5)

$$\bar{\Pi}_4(t,t_0) = \tfrac{1}{2}\bar{\Pi}_2(t,t_0)e^{i\bar{L}(t-t_0)}\bar{\Pi}_2(t,t_0). \tag{138}$$

This general insight is again readily obtained by making use of the causal superfermions: Since without interaction, the time-dependent interaction-picture fields anticommute [Eq. (120)], relabeling of dummy indices and integration variables in Eq. (137) directly leads to the factorization (138) on the superoperator level. This is shown diagrammatically in Fig. 5 and written out in Appendix E. Our approach thus clarifies how in the *many-body* Liouville-space simplification arises for $U = 0$, which is important since interacting theories are necessarily formulated in this large space. Clearly, when making use of the collinearity of the spin dependence of the tunneling and due to the magnetic field, the Liouville spaces of superfermions with different spin can be considered independently and one arrives also at Eq. (138). However, this consideration, formulated in Appendix F, does not make clear how in the formalism applicable to interacting cases this factorization comes about. Moreover, it is unnecessary when one makes use of the causal superfermions. Independent of the result Eq. (138), the structure of the superoperator (137) can also be determined easily using the Liouville-space second quantization. Inserting Eq. (119), the superoperator part of the expression (137) is $\propto e^{-i\bar{L}(t-t_0)}\bar{G}_4\bar{G}_3\bar{G}_2\bar{G}_1$. The product of four creation superoperators can only be nonzero if all multi-indices 1,2,3,4 are different and it is therefore *always* proportional to the transition superoperator taking the vacuum superket $|Z_L)$ into the most filled fermion-parity superket $|Z_R)$ [Eq. (60f)]:

$$\bar{\Pi}_4(t,t_0) = \vartheta(t-t_0)|Z_R)(Z_L|. \tag{139}$$

All that remains is to calculate the coefficient ϑ as a function of $\Delta = t - t_0$ by substituting Eq. (133) into Eq. (138):

$$\vartheta(\Delta) = 2\sum_\sigma \sum_{r,r'} \frac{\Gamma_{r\sigma}}{\Gamma_\sigma}[F^+_{r\sigma}(\Delta) + F^-_{r\sigma}(\Delta)] \times \frac{\Gamma_{r'\bar{\sigma}}}{\Gamma_{\bar{\sigma}}}[F^+_{r'\bar{\sigma}}(\Delta) + F^-_{r'\bar{\sigma}}(\Delta)] \tag{140a}$$

$$= 4\sum_r \frac{\Gamma_{r\uparrow}}{\Gamma_\uparrow}[F^+_{r\uparrow}(\Delta) + F^-_{r\uparrow}(\Delta)] \times \sum_{r'} \frac{\Gamma_{r'\downarrow}}{\Gamma_\downarrow}[F^+_{r'\downarrow}(\Delta) + F^-_{r'\downarrow}(\Delta)]. \tag{140b}$$

That the fourfold, time-ordered integral Eq. (137) reduces to the simple product of the two spin-resolved functions depending only on the difference $\Delta = t - t_0$ is expected from the considerations in Appendix F . However, without the renormalized formulation of the perturbation theory in the causal superfermion framework the origin of such simplifications in real-time calculations remain unclear.

Finally, we note that the superoperator form (139) as well as the truncation of the perturbation series (122) both remain valid for the case of the *noncollinear* magnetizations of the (ferromagnetic) reservoirs and/or of tunnel junctions. They are based on the very general causal structure of the perturbation series, which is independent of the spin rotation and other symmetries of the problem. Summarizing, the full time-evolution propagator reads as

$$\begin{aligned} \Pi(t,t_0) &= [\bar{\Pi}_0(t,t_0) + \bar{\Pi}_2(t,t_0) + \bar{\Pi}_4(t,t_0)] \\ &= \lim_{T\to\infty}\Pi(t,t_0) + \sum_{r,\sigma}\frac{2\Gamma_{r\sigma}}{\Gamma_\sigma}[F^+_{r\sigma}(t-t_0) + F^-_{r\sigma}(t-t_0)] \\ &\quad \times \{|\chi_\sigma)(Z_L| + e^{-\Gamma_{\bar{\sigma}}(t-t_0)}|Z_R)(\chi_{\bar{\sigma}}|\} + \vartheta(t-t_0)|Z_R)(Z_L|, \end{aligned} \tag{141}$$

where the first term is given by Eq. (126), $F^\pm_{r\sigma}$ by Eq. (134), and ϑ by Eq. (140).

2. Time-dependent density operator

Evaluating [132] $\rho(t) = \Pi(t,t_0)\rho(t_0)$, where the initial state $\rho(t_0)$ has the general form (68) with $t = t_0$, we obtain the exact time-dependent density operator for $U = 0$ in the WBL:

$$\rho(t) = \lim_{T\to\infty}\rho(t) + \sum_{r,\sigma}\frac{\Gamma_{r\sigma}}{\Gamma_\sigma}[F^+_{r\sigma}(t-t_0) + F^-_{r\sigma}(t-t_0)]|\chi_\sigma) \tag{142a}$$

$$+ \left\{\sum_{r,\sigma} e^{-\Gamma_{\bar{\sigma}}(t-t_0)}\frac{2\Gamma_{r\sigma}}{\Gamma_\sigma}[F^+_{r\sigma}(t-t_0) + F^-_{r\sigma}(t-t_0)] \times \Phi_{\bar{\sigma}}(t_0) + \frac{1}{2}\vartheta(t-t_0)\right\}|Z_R). \tag{142b}$$

Here, the first term on the right-hand side of Eq. (142a) is the exact $T \to \infty$ result (116) discussed in Sec. III C 3.

(a) Electron-pair and spin coherence. We first note the absence of corrections to the $T \to \infty$ decay as given by Eq. (116) of the electron-pair coherence [Eq. (71)] and transverse spin coherence coefficients [Eq. (72)] of the initial state $\rho(t_0)$. For $U = 0$ these therefore decay exponentially to zero with rates which are independent of temperature and equal: $\Upsilon_\eta(t) = e^{-(\Gamma/2)(t-t_0)}\Upsilon_\eta(t_0)$ and $\Omega_\sigma(t) = e^{-(\Gamma/2)(t-t_0)}\Omega_\sigma(t_0)$, respectively. This is much like the fermion parity discussed below, but in contrast to the latter, here the decay is altered when $U \neq 0$. The stationary values are zero by charge- and spin-rotation symmetry, see Sec. IV B [133]. The finite temperature gives rise to corrections to both the stationary values and to the decay, which we now discuss.

(b) Spin-orbital occupancies. The second term in (142a) modifies the decay of the level occupancies:

$$\begin{aligned}\Phi_\sigma(t) &= \langle n_\sigma\rangle(t) - \frac{1}{2}\\ &= e^{-\Gamma_\sigma(t-t_0)}\Phi_\sigma(t_0)\\ &\quad + \sum_r \frac{\Gamma_{r\sigma}}{\Gamma_\sigma}[F^+_{r\sigma}(t-t_0) + F^-_{r\sigma}(t-t_0)].\end{aligned} \tag{143}$$

Our result (143) for a single spin agrees with the one obtained in Ref. [77] for spin-independent tunneling, i.e., $\Gamma_{r\sigma} = \tilde{\Gamma}_r$ and zero magnetic field, $B = 0$, after calculating the ω-integral expression left unevaluated in Ref. [77]. Additionally switching off the reservoir dependence of the tunnel coefficients, i.e., $\tilde{\Gamma}_r = \tilde{\Gamma}$, in Eq. (143) and assuming that initially the dot is unoccupied, $\langle n_\sigma\rangle(t_0) = 0$, we find agreement with the result of Ref. [134] obtained within these assumptions. The stationary value, obtained using Eq. (135a),

$$\begin{aligned}\Phi_\sigma(\infty) &:= \langle n_\sigma\rangle(\infty) - \frac{1}{2}\\ &= \frac{1}{\pi}\sum_r \frac{\Gamma_{r\sigma}}{\Gamma_\sigma}\,\mathrm{Im}\,\Psi\left(\frac{1}{2} + \frac{\frac{1}{2}\Gamma_\sigma - i\epsilon_{r\sigma}}{2\pi T}\right),\end{aligned} \tag{144}$$

under corresponding simplifications also agrees with that obtained in Refs. [77,134]. Both the stationary value and the decay towards it depend on the spin σ: For spin-independent tunneling $\Gamma_{r\sigma} := \tilde{\Gamma}_r$, this is a consequence of the Zeeman splitting B on the quantum dot. For $B = 0$, however, this is due to nonequilibrium spin accumulation on the quantum dot, $\langle S_z\rangle(t) = \sum_\sigma \langle \sigma n_\sigma\rangle/2 = \sum_\sigma \sigma\,\Phi_\sigma/2$, caused by the spin-dependent tunneling. Only when both $B = 0$ and $\Gamma_{r\sigma} := \tilde{\Gamma}_r$ do we have full spin-rotation symmetry. In this case, the occupancies are equal $\langle n_\uparrow\rangle = \langle n_\downarrow\rangle$, and there is no correction to the longitudinal spin $\langle S_z\rangle(t)$ as given by the $T \to \infty$ value (116): $\langle S_z\rangle(t)$ decays exponentially to zero, in agreement with the spin-rotation symmetry (z axis). The decay rate, $\Gamma_\sigma = \sum_r \tilde{\Gamma}_r$, is identical to the rate $\Gamma/2 = \sum_r \tilde{\Gamma}_r$ of the spin- and electron-pair coherences $\Upsilon_\eta(t)$ and $\Omega_\sigma(t)$, respectively, all of which are temperature independent.

(c) Fermion-parity and two-particle correlations. The full time evolution of the fermion-parity operator expansion coefficient [Eq. (70)] thus reads as follows:

$$\begin{aligned}\Xi(t) &= e^{-\Gamma(t-t_0)}\Xi(t_0) + \sum_\sigma e^{-\Gamma_\sigma(t-t_0)}\\ &\quad\times \sum_r \frac{2\Gamma_{r\sigma}}{\Gamma_{\bar\sigma}}[F^+_{r\bar\sigma}(t-t_0) + F^-_{r\bar\sigma}(t-t_0)]\Phi_\sigma(t_0)\\ &\quad + \frac{1}{2}\vartheta(t-t_0).\end{aligned} \tag{145}$$

This coefficient takes account of the correlations of the occupancies through the average of the fermion-parity operator: $\Xi(t) = \frac{1}{2}\langle e^{i\pi n}\rangle = 2\langle\prod_\sigma(n_\sigma - 1/2)\rangle = 2\langle n_\uparrow n_\downarrow\rangle - \langle n\rangle + 1/2$. The result (145) is valid for an arbitrary initial state of the quantum dot with two-particle correlations: $\langle n_\uparrow n_\downarrow\rangle(t_0) \neq \langle n_\uparrow\rangle(t_0)\langle n_\downarrow\rangle(t_0)$, equivalent to

$$\Xi(t_0) \neq 2\prod_\sigma \Phi_\sigma(t_0). \tag{146}$$

The first contribution to Eq. (145) is the exponential decay determined by the $T \to \infty$ limit. As explained in Sec. III C 2, this part of the time-dependent-decay *never* has any finite-temperature corrections: It is, in fact, independent of all parameters except the sum of all rates $\Gamma = \sum_{r\sigma}\Gamma_{r\sigma}$, even when the interaction is switched on ($U \neq 0$). The second term describes the transient effect of the initial occupancies on the correlations through $\Phi_\sigma(t_0) = \langle n_\sigma\rangle(t_0) - 1/2$. This term decays to zero in an oscillatory fashion, for small temperatures with an exponential envelope $\propto e^{-(\Gamma_{\bar\sigma}/2+\Gamma_\sigma)(t-t_0)}$. Thus, besides the rates encountered so far, there are two additional decay rates:

$$\tfrac{1}{2}\Gamma_{\bar\sigma} + \Gamma_\sigma \quad \text{for} \quad \sigma = \uparrow, \downarrow. \tag{147}$$

When all tunnel rates are spin and reservoir independent and equal to $\Gamma_{r\sigma} = \tilde{\Gamma}$, this rate reduces [135] to $\Gamma_\sigma + \frac{1}{2}\Gamma_{\bar\sigma} = 3\tilde{\Gamma}$, in contrast to the other rates encountered so far, $\Gamma = 4\tilde{\Gamma}$, $\Gamma_\sigma = 2\tilde{\Gamma}$ or $\frac{1}{2}\Gamma_\sigma = \tilde{\Gamma}$. For this simple case this additional energy scale was noted in Ref. [67] and related to the rates of a virtually excited particle-hole pair and an incident particle. Our spin-resolved result (147), written as $(\Gamma_{\bar\sigma} + \Gamma_\sigma)/2 + \Gamma_\sigma/2$, agrees with this. Here, we find that this scale is related to decay of two-particle correlations arising from the initial spin-orbital occupations.

Finally, the coefficient $\vartheta(t - t_0)$ defines the stationary value $\Xi(\infty)$. It is defined exclusively by the stationary two-loop propagator (139) and its nonzero stationary value (140) factorizes into the stationary values $\Phi_\sigma(\infty)$ [see Eq. (144)]:

$$\Xi(\infty) = \tfrac{1}{2}\vartheta(\infty) = 2\prod_\sigma \Phi_\sigma(\infty). \tag{148}$$

This relation simply expresses that the stationary nonequilibrium averages of the total fermion-parity operator factorize into the averages of the fermion parity of the two spin orbitals:

$$\lim_{t\to\infty}\langle e^{i\pi n}\rangle(t) = \lim_{t\to\infty}\prod_\sigma\langle e^{i\pi n_\sigma}\rangle(t). \tag{149}$$

Rewritten using $e^{i\pi n_\sigma} = (1 - 2n_\sigma)$, this is equivalent to the factorization of the correlator of the occupancies, $\lim_{t\to\infty}\langle n_\uparrow n_\downarrow\rangle(t) = \lim_{t\to\infty}\langle n_\uparrow\rangle(t)\cdot\langle n_\downarrow\rangle(t)$, which is expected for the noninteracting limit ($U = 0$): Each spin-σ

"channel" can be averaged independently; see Appendix F. This relation *always* holds in the stationary limit: The initial correlations between the orbital occupancies, expressed by the inequality Eq. (146), are "forgotten" in the long-time limit. For a two-particle correlated initial state on the quantum dot, satisfying Eq. (146), the relation Eq. (149) is violated on time scales $t - t_0 \lesssim \Gamma^{-1}$. This time scale is set by the fermion-parity protected eigenvalue and is therefore independent of all other parameters in the problem, even for nonzero *interaction* U, as discussed in Sec. III C 2. For an initially uncorrelated quantum dot, the relation $\Xi(t) = 2\prod_\sigma \Phi_\sigma(t)$ or equivalently, $\langle n_\uparrow\rangle(t)\langle n_\downarrow\rangle(t) = \langle n_\uparrow n_\downarrow\rangle(t)$ at $t = t_0$, continues to hold for all times $t \geqslant t_0$.

Although the effects of the initial dot state for $U = 0$ have been studied previously [75,77,134,136], all these works are based on spinless electrons or, equivalently, on a single spin-orbital model. For the a single-spin orbital the electron-parity operator practically coincides with the level occupancy operator n_σ: $(-1)^{n_\sigma} \propto n_\sigma - 1/2$. Thus, by the simplicity of this model the effect of the initial two-particle correlators $\langle n_\uparrow n_\downarrow\rangle$ cannot appear. However, for electrons with spin it makes a crucial difference if the dot was initially prepared in the nonfactorizable form, Eq. (146), or not, as our result show. We are not aware of any work presenting an exact analytical result for the nonfactorizing time evolution of this correlator in this limit.

B. Stationary limit

We now illustrate how simplifications arise in Laplace space in the noninteracting limit and directly calculate the exact $U = 0$ *stationary* density operator. This independent calculation is also of more general interest since it involves the direct, explicit calculation of the stationary self-energy $\Sigma(i0)$ and the effective Liouvillian $L(i0) = L + \Sigma(i0)$ for $U = 0$ using the renormalized perturbation theory but now formulated in Laplace space. This independent result was used (but not derived) in Ref. [30] to check that the real-time RG explicitly recovers the noninteracting limit for the stationary current and the corresponding self-energy parts [see Eq. (176)]. Here we provide the derivation of this important benchmark not only for the current, but also for the full density operator and the self-energy.

1. *Frequency space perturbation expansion for the self-energy*

To keep the paper self-contained, we first briefly outline the renormalized perturbation theory in Laplace space which is also valid for $U \neq 0$. Although this theory was formulated in Ref. [30], it was not used to explicitly calculate the $U = 0$ limit, but the RG approach was used instead to analytically verify the current and the relevant self-energy parts in this limit. We proceed in close analogy to the above time-dependent formulation and start with the Laplace transform of the (nonrenormalized) perturbation expansion Eq. (45b) for the time-evolution propagator. Alternatively [30], we transform the general solution Eq. (37) and then expand the resolvent $1/(z - L^{\rm tot})$ in powers of L^V using $\mathop{\rm Tr}_R L^R = 0$:

$$\Pi(z) := \int_{t_0}^{\infty} dt e^{izt}\Pi(t,t_0) = \mathop{\rm Tr}_R \frac{i}{z - L^{\rm tot}}\rho_R = \sum_{k=0}^{\infty} \frac{i}{z - L}\mathop{\rm Tr}_R\left(L^V \frac{1}{z - L^R - L}\right)^k \rho_R. \quad (150)$$

Inserting Eq. (48) for L^V, we have for the mth-order term of the expansion of the Laplace-space resolvent, $\Pi(z) = \sum_{m=0}^{\infty}\Pi_m(z)$ [cf. Eq. (85)]:

$$\Pi_m(z) = i\mathop{\rm Tr}_R\big(J^{q_m}_{\bar m}\cdots J^{q_1}_{\bar 1}\rho^R\big)\frac{1}{z - L}G^{q_m}_m \times \frac{1}{z - L - X_m}\cdots\frac{1}{z - L - X_2}G^{q_1}_1\frac{1}{z - L}. \quad (151)$$

Here we have commuted all J^q to the far right, using $[L^R, J^q_1]_- = \eta(\omega + \mu_r)J^q_1$ and collected all *reservoir* energies $x_k = \eta_k(\omega_k + \mu_k)$ of the $G^{q_k}_k(J^{q_k}_{\bar k})$ originally standing to the left to the resolvent i in $X_i = \sum_i^m x_k$. Evaluating the reservoir average using the Wick theorem (87), we obtain terms that can be represented by the same diagrams as in Fig. 2, where the free propagators connecting vertices stand for $1/(z - L - X_i)$ and the contraction line connecting a pair of vertices $\bar G$-$\bar G$ and $\bar G$-$\tilde G$ stands for the contraction functions (89) and (90), where the line is now assigned a frequency x_k. The irreducible parts of these diagrams [cf. Sec. III C 1] are collected into the superoperator self-energy $\Sigma(z)$, which is just the Laplace transform of $\Sigma(t - t')$ in Eq. (38):

$$\Sigma(z) = \int_0^{\infty} e^{iz\tau}\Sigma(\tau,0)d\tau. \quad (152)$$

After grouping the diagrams into $\Sigma(z)$ blocks, we can resum the resulting geometric series and obtain the Laplace-space solution of the Dyson equation (38)/the kinetic equation (39),

$$\rho(z) = \frac{i}{z - L(z)}\rho(t_0), \quad (153)$$

where the effective Liouvillian in the Laplace representation [the Laplace transform of Eq. (105)] is decomposed as in Eq. (105) [51]:

$$L(z) = L + \Sigma(z). \quad (154)$$

The required expansion for $\Sigma(z)$ thus has the form

$$\Sigma(z) = (-1)^P\Big(\prod\gamma\Big)_{\rm irr}\bar G_m\frac{1}{z - X_m - L}\cdots G^{q_2} \times \frac{1}{z - X_2 - L}G^{q_1}. \quad (155)$$

The causal structure of this expansion [cf. discussion of Eq. (91)] enforces that the leftmost vertex in each contraction is always a *creation* superoperator $\bar G_m$ as a consequence of Eq. (54). We use the same conventions as in Eqs. (91) and (85), suppressing all sums and integrations over reservoir frequencies. Note that unlike in the time representation, these integrals cannot be pulled into the contraction functions; i.e., the $\gamma^q_{i,j}$ are given by Eqs. (89) and (90). This is because in the Laplace transform the frequencies are convoluted with the dot evolution in the propagators $(z - L + X)^{-1}$. The main

advantage of Eq. (155) is that we can now directly work in the stationary limit by taking the limit $z \to i0$ and then calculating the stationary state by finding the right zero eigenvector of $L(i0) = L + \Sigma(i0)$.

Similar to Sec. III B 1 we explicitly work out the WBL by noting that diagrams with a vertex inside a $\tilde{\gamma}$ contraction can be neglected [30] and that one can integrate out the $\tilde{\gamma}$ contractions and the $\tilde{G}$ vertices, incorporating them into the Laplace transform $\tilde{\Sigma}$ of the self-energy $\tilde{\Sigma}(t,t')$ [Eq. (95)], which is simply the time-independent factor given by Eq. (96). What remains is to evaluate the perturbative expansion for $\bar{\Sigma}(z) = \Sigma(z) - \tilde{\Sigma}$, with the simplified diagram rules schematized by

$$\bar{\Sigma}(z) = (-1)^P \left(\prod_i \bar{\gamma}_i\right)_{\text{irr}} \times \bar{G}_m \frac{1}{z - X_m - \bar{L}} \cdots \frac{1}{z - X_2 - \bar{L}} \bar{G}_1, \tag{156}$$

where we sum over irreducible $\bar{\gamma}$ contractions and $\bar{L} = L + \tilde{\Sigma}$ as before [Eq. (98)]. We can now find the stationary state as the right zero eigenvector of $L(i0) = L + \Sigma(i0) = \bar{L} + \bar{\Sigma}(i0)$. Notably, in Eq. (156) we can *set* $z = 0$ since $\bar{L}$ is a *dissipative* Liouvillian which automatically regularizes all propagators [137]. We note how these technical properties neatly tie in with the physical meaning. That the denominators in Eq. (156) contain no zeros was a key point in setting up the real-time RG flow in Laplace space for the calculation of effective Liouvillians, referred to as the "zero-eigenvector problem" [51,138].

2. *Noninteracting limit and super-Pauli principle*

We now work out the simplifications that occur for the self-energy in the limit $U = 0$, in full analogy with the time representation. The part $\tilde{\Sigma}$ is obtained by setting $U = 0$ in Eq. (96) or (112). In the remaining calculation of $\bar{\Sigma}$ [Eq. (156)], using Eq. (118) we commute the $\bar{G}$ through the resolvents: This gives the analog of Eq. (121),

$$\bar{\Sigma}(z) = (-1)^P \left(\prod_i \bar{\gamma}_i\right)_{\text{irr}} \bar{G}_m \cdots \bar{G}_1 \times \frac{1}{z - X_m - E_m - \bar{L}} \cdots \frac{1}{z - X_2 - E_2 - \bar{L}}, \tag{157}$$

where $\bar{L}$ is given by Eq. (114) with $U = 0$ and $E_i = \sum_{k=2}^{i} \epsilon_k$ is the sum over renormalized, single-particle *quantum dot* energies,

$$\epsilon_i = \eta_i \epsilon_{\sigma_i} - i\tfrac{1}{2}\Gamma_{\sigma_i}. \tag{158}$$

These have acquired an imaginary part by the inclusion of broadening of the $T \to \infty$ limit through the self-energy term $\tilde{\Sigma}$ in the renormalized Liouvillian $\bar{L}$. Thus, also in the Laplace representation, the super-Pauli principle (62) directly reveals that in the $U = 0$ limit nonzero terms of the renormalized self-energy of order $m > 4$ [cf. Eq. (63)] cannot appear: $\bar{\Sigma}(z) = \bar{\Sigma}_2(z) + \bar{\Sigma}_4(z)$; cf. Eq. (123).

(a) One-loop self-energy: Stationary occupancies and current. We first calculate the one-loop diagram for $\bar{\Sigma}_2$ by substituting Eq. (129) into

$$\begin{aligned}\bar{\Sigma}_2(i0) &= \sum_{\eta,\sigma,r} \bar{G}_2 \bar{G}_{\bar{2}} \int \frac{d\bar{\omega}\bar{\gamma}(\bar{\omega})}{i0 - \bar{\omega} - \bar{\mu}_2 - \epsilon_{\bar{2}} - \bar{L}} \\ &= \sum_{\eta,\sigma,r} \eta \frac{\Gamma_{r\sigma}}{2\pi} \left[|\chi_\sigma)(Z_L| \int \frac{d\bar{\omega}\tanh(\bar{\omega})}{i0 - \bar{\omega} - \bar{\mu}_2 - \epsilon_{\bar{2}} - \bar{L}} \right. \\ &\quad \left. + |Z_R)(\chi_{\bar{\sigma}}| \int \frac{d\bar{\omega}\tanh(\bar{\omega})}{i0 - \bar{\omega} - \bar{\mu}_2 - \epsilon_{\bar{2}} - \bar{L}} \right] + F.\end{aligned} \tag{159}$$

Here and in the following, we abbreviate $\bar{\omega}_i \equiv \eta_i \omega_i = x$ and $\bar{\mu}_i := \eta_i \mu_{r_i}$ and we write this in the form (omitting the fermionic part)

$$\bar{\Sigma}_2(i0) = -i \sum_\sigma \{\psi_\sigma |\chi_\sigma)(Z_L| + \phi_\sigma |Z_R)(\chi_\sigma|\}. \tag{160}$$

Using $(Z_L|\bar{L} = 0$ and summing over η explicitly, this gives after replacing $x \to -x$ in the second integral the stationary value of the first two coefficients (see Appendix C):

$$\begin{aligned}\psi_\sigma &= -i \sum_r \frac{\Gamma_{r\sigma}}{2\pi} \int dx \left[\frac{\tanh(x/2T)}{i\frac{1}{2}\Gamma_\sigma - x + \epsilon_{r\sigma}} - \frac{\tanh(x/2T)}{i\frac{1}{2}\Gamma_\sigma - x - \epsilon_{r\sigma}} \right] \\ &= -\sum_r \frac{2\Gamma_{r\sigma}}{\pi} \operatorname{Im} \Psi \left(\frac{1}{2} + \frac{\frac{1}{2}\Gamma_\sigma - i\epsilon_{r\sigma}}{2\pi T} \right),\end{aligned} \tag{161}$$

where [cf. Eq. (131)],

$$\epsilon_{r\sigma} = \epsilon + \sigma B/2 - \mu_r. \tag{162}$$

We see that the coefficients (161) of the *one-loop* self-energy $\bar{\Sigma}_2(i0)$ completely determine the stationary current. As a result, the current only shows the usual broadening $\Gamma_\sigma/2 = \sum_r \Gamma_{r\sigma}/2$ due to the cumulative relaxation rate for spin σ.

Analogously, we calculate the remaining coefficients ϕ_σ $(\chi_\sigma|\bar{L} = -2i\Gamma(\chi_\sigma|$, cf. Eq. (114a):

$$\begin{aligned}\phi_\sigma &= -i \sum_r \frac{\Gamma_{r\bar{\sigma}}}{2\pi} \int dx \left[\frac{\tanh(x/2T)}{i\left(\frac{1}{2}\Gamma_{\bar{\sigma}} + \Gamma_\sigma\right) - x + \epsilon_{r\bar{\sigma}}} \right. \\ &\quad \left. - \frac{\tanh(x/2T)}{i\left(\frac{1}{2}\Gamma_{\bar{\sigma}} + \Gamma_\sigma\right) - x - \epsilon_{r\bar{\sigma}}} \right] \\ &= -\sum_r \frac{2\Gamma_{r\bar{\sigma}}}{\pi} \operatorname{Im} \Psi \left(\frac{1}{2} + \frac{\frac{1}{2}\Gamma_{\bar{\sigma}} + \Gamma_\sigma - i\epsilon_{r\bar{\sigma}}}{2\pi T} \right).\end{aligned} \tag{163}$$

This part of the self-energy involves a quite different broadening, $\Gamma_\sigma + \frac{1}{2}\Gamma_{\bar{\sigma}}$ instead of $\frac{1}{2}\Gamma_\sigma$, an energy scale that we noted earlier in Eq. (147). However, we see that the exact $U = 0$ stationary current is not sensitive to this quantity. We note that for $U \neq 0$, it can be shown that this broadening, although modified by the interaction, does enter into the stationary current [139].

(b) Two-loop self-energy: Stationary average fermion parity. The two-loop contribution to $\bar{\Sigma}$ is calculated in close analogy to the two-loop contributions to $\bar{\Pi}_4$

in Eq. (137):

$$\bar{\Sigma}_4(i0) = \sum_{\sigma,r,r'} \frac{\Gamma_{r\sigma}\Gamma_{r'\bar{\sigma}}}{(2\pi)^2} \bar{G}_l \bar{G}_{\bar{l}} \bar{G}_{l'} \bar{G}_{\bar{l}'} \int d\bar{\omega}_l \int d\bar{\omega}_{l'} \frac{\tanh(\bar{\omega}_l/2T)\tanh(\bar{\omega}_{l'}/2T)}{\left[\eta_l \epsilon_{r\sigma} + i\left(\frac{\Gamma_\sigma}{2} + \Gamma_{\bar{\sigma}}\right) - \bar{\omega}_l\right]}$$
$$\times \left[\frac{1}{\left(\eta_{l'}\epsilon_{r'\bar{\sigma}} + i\frac{\Gamma_{\bar{\sigma}}}{2} - \bar{\omega}_{l'}\right)} \frac{1}{\left(\eta_l\epsilon_{r\sigma} + \eta_{l'}\epsilon_{r'\bar{\sigma}} + i\frac{\Gamma}{2} - \bar{\omega}_l - \bar{\omega}_{l'}\right)} \right.$$
$$\left. + \frac{1}{\left(\eta_l\epsilon_{r\sigma} + i\frac{\Gamma_\sigma}{2} - \bar{\omega}_l\right)} \frac{1}{\left(\eta_l\epsilon_{r\sigma} + \eta_{l'}\epsilon_{r'\bar{\sigma}} + i\frac{\Gamma}{2} - \bar{\omega}_l - \bar{\omega}_{l'}\right)} \right] \tag{164a}$$
$$= \sum_{\sigma,r,r'} \frac{\Gamma_{r\sigma}\Gamma_{r'\bar{\sigma}}}{(2\pi)^2} \bar{G}_l \bar{G}_{\bar{l}} \bar{G}_{l'} \bar{G}_{\bar{l}'} \int d\bar{\omega}_l \frac{\tanh(\bar{\omega}_l/2T)}{\left[\eta_l\epsilon_{r\sigma} + i\left(\frac{\Gamma_\sigma}{2} + \Gamma_{\bar{\sigma}}\right) - \bar{\omega}_l\right]} \frac{1}{\left(\eta_l\epsilon_{r\sigma} + i\frac{\Gamma_\sigma}{2} - \bar{\omega}_l\right)} \int d\bar{\omega}_{l'} \frac{\tanh(\bar{\omega}_{l'}/2T)}{\left(\eta_{l'}\epsilon_{r'\bar{\sigma}} + i\frac{\Gamma_{\bar{\sigma}}}{2} - \bar{\omega}_{l'}\right)}. \tag{164b}$$

Here we made use of the fact that for $\bar{\gamma}_{ij}$ the multi-indices are related as $i = \bar{j}$, and we relabeled $4 \to l = \omega_l, \eta_l, r, \sigma$ and $2 \to l' = \omega_{l'}, \eta_{l'}, r', \bar{\sigma}$ for compactness. We also explicitly made use of relation $\sigma_l = \sigma = \bar{\sigma}_{l'}$, which expresses the fact that in the product $\bar{G}_l \bar{G}_{\bar{l}} \bar{G}_{l'} \bar{G}_{\bar{l}'}$ all operators must be different [otherwise the product is zero due to the super-Pauli principle (62) and (63)]. Equation (164a) has two types of contributions, represented by the irreducible parts of the last two diagrams in Fig. 4. To obtain the form (164a), we have anticommuted the field superoperators to have the same order in each type of contribution. This cancels the Wick sign, similar to the rewriting of Eq. (137) into Eq. (138); cf. Fig. 5 and Appendix E. Notably, when combining these two types of contributions in Eq. (164b), the double integral over frequencies $\bar{\omega}_l$ and $\bar{\omega}_{l'}$ becomes factorizable *but only for zero* quantum-dot *frequency* $z = 0$. Therefore, the complete expression (164b) is a sum over factorizable integrals. As in Eqs. (137) and (139), the superoperator structure of (164b) is very simple:

$$\bar{\Sigma}_4(i0) = \zeta |Z_R)(Z_L|. \tag{165}$$

Using $\bar{G}_l \bar{G}_{\bar{l}} \bar{G}_{l'} \bar{G}_{\bar{l}'} = \eta_l \eta_{l'} |Z_R)(Z_L|$ and Eq. (C1) (Appendix C), we obtain

$$\zeta = \sum_{\sigma,r,r'} \frac{4\Gamma_{r\sigma}\Gamma_{r'\bar{\sigma}}}{\pi^2} \left[\operatorname{Im}\Psi\left(\frac{1}{2} + \frac{\frac{1}{2}\Gamma_\sigma + \Gamma_{\bar{\sigma}} - i\epsilon_{r\sigma}}{2\pi T}\right) \right.$$
$$\times \operatorname{Im}\Psi\left(\frac{1}{2} + \frac{\frac{1}{2}\Gamma_{\bar{\sigma}} - i\epsilon_{r'\bar{\sigma}}}{2\pi T}\right)$$
$$- \operatorname{Im}\Psi\left(\frac{1}{2} + \frac{\frac{1}{2}\Gamma_\sigma - i\epsilon_{r\sigma}}{2\pi T}\right)$$
$$\left. \times \operatorname{Im}\Psi\left(\frac{1}{2} + \frac{\frac{1}{2}\Gamma_{\bar{\sigma}} - i\epsilon_{r'\bar{\sigma}}}{2\pi T}\right) \right]. \tag{166}$$

Summarizing, the exact zero-frequency effective dot Liouvillian in the WBL for the noninteracting Anderson model ($U = 0$) is

$$iL(i0) := i[L + \tilde{\Sigma} + \bar{\Sigma}_2(i0) + \bar{\Sigma}_4(i0)]$$
$$= \Gamma |Z_R)(Z_R| + \zeta |Z_R)(Z_L|$$
$$+ \sum_\sigma [\phi_\sigma |Z_R)(\chi_\sigma| + \psi_\sigma |\chi_\sigma)(Z_L|]$$
$$+ \sum_\sigma \Gamma_\sigma |\chi_\sigma)(\chi_\sigma|$$
$$+ \sum_\sigma \left[i\sigma B + \frac{1}{2}\Gamma \right] |S_\sigma)(S_\sigma|$$
$$+ \sum_\eta \left[i\eta(2\epsilon + U) + \frac{1}{2}\Gamma \right] |T_\eta)(T_\eta|, \tag{167}$$

with ψ_σ given by Eq. (161), ϕ_σ given by Eq. (163), ζ given by Eq. (166), and not writing the irrelevant fermionic part.

3. *Stationary density operator*

The stationary state, the unique right zero eigenvector of $L(i0)$, can be determined conveniently using the form (167) of the superoperator. In fact, the complete eigenspectrum of $L(i0)$ can be found in terms of the its coefficients [30]: Generally, the effective Liouvillian written in the basis Eqs. (60) must have the form (ignoring the fermionic part again)

$$iL(i0) = \Gamma |Z_R)(Z_R| + \zeta |Z_R)(Z_L|$$
$$+ \sum_\sigma [\phi_\sigma |Z_R)(\chi_\sigma| + \psi_\sigma |\chi_\sigma)(Z_L|]$$
$$+ \sum_{\sigma,\sigma} \xi_{\sigma,\sigma'} |\chi_\sigma)(\chi_{\sigma'}|$$
$$+ \sum_\sigma E_\sigma |S_\sigma)(S_\sigma| + \sum_\eta M_\eta |T_\eta)(T_\eta|. \tag{168}$$

This form follows from the causal structure, the WBL (fixing the first coefficient to the constant, fermion-parity eigenvalue $-i\Gamma$; cf. Sec. III C 2) [140], and the symmetries of the Anderson model. (Notably, it does *not* require $U = 0$.) As in Ref. [30], we have conservation of the charge and of the spin along the direction of the magnetic field B, even though we now also include spin-dependent tunneling (we assume that the magnetic field B and the polarization vectors are collinear, preserving the spin-rotation symmetry about this axes). The stationary state can be expressed in terms of the effective Liouvillian coefficients [30], and by comparing Eq. (167) with the general form Eq. (168), we obtain in terms of the matrix $\xi_{\sigma,\sigma'} = \Gamma_\sigma \delta_{\sigma,\sigma'}$, and the vectors [Eqs. (161)

and (163)]

$$\rho(\infty) = \frac{1}{2}|Z_L) - \frac{1}{2}\sum_{\sigma,\sigma'}\xi^{-1}_{\sigma,\sigma'}\psi_{\sigma'}|\chi_\sigma) + \frac{1}{2\Gamma}\left(\sum_{\sigma,\sigma'}\phi_\sigma\xi^{-1}_{\sigma,\sigma'}\psi_{\sigma'} - \zeta\right)|Z_R) \quad (169a)$$

$$= \frac{1}{2}|Z_L) + \sum_\sigma \Phi_\sigma(\infty)|\chi_\sigma) + \Xi(\infty)|Z_R), \quad (169b)$$

where the expansion coefficients are

$$\Phi_\sigma(\infty) = \frac{1}{\pi}\sum_r \frac{\Gamma_{r\sigma}}{\Gamma_\sigma}\,\mathrm{Im}\,\Psi\left(\frac{1}{2} + \frac{\frac{1}{2}\Gamma_\sigma - i\epsilon_{r\sigma}}{2\pi T}\right), \quad (170)$$

$$\Xi(\infty) = 2\Phi_\uparrow(\infty)\cdot\Phi_\downarrow(\infty). \quad (171)$$

We note that the additional broadening scale $\frac{1}{2}\Gamma_\sigma + \Gamma_{\bar\sigma}$ that we noted already in Eqs. (147) and (163) is also present in ζ [Eq. (166)] but drops out in the calculation of $\Xi(\infty)$ when one sums over σ. Equation (170) reproduces the stationary spin-orbital occupancies Eq. (144) through $\langle n_\sigma\rangle = \frac{1}{2} + \Phi_\sigma$. Moreover, Eq. (171) confirms the factorization (148) of the *stationary* value $\Xi(\infty)$ into the coefficients $\Phi_\sigma(\infty)$. On the superoperator level, the renormalized two-loop self-energy $\bar\Sigma_4$ does not factorize for *any* frequency z, not even at $z = 0$; see Eqs. (165) and (166). One can verify that to achieve such a factorization a reducible term needs to be added to $\bar\Sigma_4(t,t_0)$. This is precisely what happens in Eq. (125) and produces essentially the Laplace transform of superoperator $\bar\Pi_4(t,t_0)$, which indeed factorizes at any time t by Eq. (138). This shows that for $\bar\Sigma_4(z)$ itself no such factorization is to be expected at any frequency. There are thus advantages of working directly with full propagators in time space in comparison with working with self-energies in Laplace space, when considering the noninteracting limit of the Anderson model and its generalizations. Furthermore, Eqs. (169b) and (171) show the physical importance of the stationary two-loop self-energy superoperator $\bar\Sigma_4(i0)$, i.e., the *quartic* term (164b) appearing in the effective theory despite the absence of two-particle interactions ($U = 0$). To obtain the correct two-particle correlations for $U = 0$ in the stationary limit it is crucial to calculate both the one- and two-loop self-energies, i.e., to work with the effective Liouvillian which is quartic in the fields.

Finally, we note that in the expansion (169b) of the *stationary* state, the terms containing superkets $|S_\sigma)$ and $|T_\eta)$, describing spin- and electron-pair coherence [cf. Sec. II D 3], do not appear since they are forbidden by charge- and spin-rotation symmetry. If such coherences are prepared in the initial state, they must decay to zero in time, in agreement with the central result Eq. (142).

C. Time-dependent current

In this last section of the paper we illustrate that in the calculation of *observable* averages very similar simplifications can be made using the causal field superoperators. We focus on the example of the time-dependent charge current in the noninteracting limit $U = 0$.

1. Current self-energy

We first present considerations which apply generally, i.e., to the interacting Anderson model ($U \neq 0$), and, in fact, to multiorbital generalizations. Generally, an observable A that is not local to the dot requires the calculation of an additional self-energy Σ_A with its own real-time diagrammatic expansion [51]. However, for a quantity which is conserved in the tunneling, such as the current I^r into reservoir r, this is not necessary: It can be obtained by simply keeping track of the part of the self-energy that is related to reservoir r. That is, we decompose $\Sigma = \sum_r \Sigma^r$ by splitting up the interaction $L^V = \sum_r L^{V^r}$ into r contributions $L^{V^r} = [V^r,\bullet]_-$ [cf. Eq. (21)] at the *latest time* t_m in each term of the perturbation series [cf. Eq. (45)]. Then, by rewriting $I^r = -i[H^{\rm tot},n^r] = -i[V^r,n^r] = -iL^{V^r}n^r$ with fixed r, one finds the relation [30]

$$\langle I^r(t)\rangle = -\frac{i}{2}\mathop{\mathrm{Tr}}_D L^{n+}\mathop{\mathrm{Tr}}_R L^{V^r}\rho^{\rm tot}(t) \quad (172a)$$

$$= -\frac{i}{2}\mathop{\mathrm{Tr}}_D L^{n+}\int_{t_0}^t dt'\,\Sigma^r(t,t')\rho(t'), \quad (172b)$$

where $L^{n+} = [n,\bullet]_+$ is the *anti*commutator with the dot particle number operator n. Besides the computational simplification, extended here to the time-dependent case, this result can be used to show very easily [30] nonperturbatively that the *stationary* current at zero bias voltage is always zero (as it should be), something which is not always obvious. This is an obvious physical requirement. However, within the real-time approach (or its equivalent, the Nakajima-Zwanzig approach), designed to deal with strongly interacting models, it is not obvious how to verify explicitly that, in general, this is actually the case, in particular, when going to higher orders in the perturbation theory in Γ or when making nonperturbative approximations in this framework, as, for instance, in Ref. [30]. When properly done, concrete calculations of this type always seem to comply with zero current at zero bias, but why this is so in general has not been clarified before. We found that Eq. (172b) provides this key step in explicitly verifying this physical requirement. We can now again take advantage of the causal structure by decomposing $\Sigma^r = \bar\Sigma^r + \tilde\Sigma^r$ into the $T\to\infty$ part $\bar\Sigma^r$ and the finite-temperature corrections $\tilde\Sigma^r$. The only difference with the analysis in Sec. III C is that one simply does not sum over the reservoir index r of the contraction with the latest field superoperator $\bar G_m$ in the $m/2$-loop renormalized perturbation expansion for $\bar\Sigma$ discussed in Sec. III C 1. To make progress, we first expand the dual supervector $\mathrm{Tr}_D\frac{1}{2}L^{n+} = \frac{1}{2}(Z_L|L^{n+}$, appearing in Eq. (172b), in the dual Liouville-Fock basis (60):

$$\mathop{\mathrm{Tr}}_D\frac{1}{2}L^{n+}\bullet = \sum_\sigma \mathop{\mathrm{Tr}}_D(n_\sigma\bullet) = \sum_\sigma(\chi_\sigma| + 2(Z_L|. \quad (173)$$

When this is inserted into Eq. (172b), it follows from the causal structure of the perturbation theory, $(Z_L|\Sigma^r \propto \mathrm{Tr}_D\Sigma^r = 0$ (*not* from probability conservation) [141], that the current is a sum of projections onto two *doubly excited* superkets $|\chi_\sigma)$

[cf Eq. (60b)]:

$$\langle I^r(t)\rangle = -i\sum_\sigma (\chi_\sigma|[\tilde\Sigma^r(t,t') + \bar\Sigma^r(t,t')]\rho(t') = \tilde I^r(t) + \bar I^r(t). \tag{174}$$

2. Wideband limit and artifacts

The expression for $\bar I^r(t)$ is, in general, rather complicated since it requires the nontrivial part of the self-energy $\bar\Sigma^r$. However, in the WBL $\tilde\Sigma^r = -i\sum_\sigma \frac{1}{2}\Gamma_{r\sigma}\bar G_1\tilde G_{\bar 1}\bar\delta(t-t')$ is just Eq. (95) without the sum over r. The superoperator expansion of $\tilde\Sigma^r$ is given then by Eq. (112), where one has to replace $\Gamma_\sigma \to \Gamma_{r\sigma}, \Gamma \to \sum_\sigma \Gamma_{r\sigma}$. For $\tilde I^r$ this gives (compare with the Green's function result of Ref. [115] and Eq. (30) in Ref. [134])

$$\tilde I^r(t) = -i\sum_\sigma (\chi_\sigma|\int_{t_0}^t dt'\tilde\Sigma^r(t,t')\rho(t') \tag{175a}$$

$$= -\sum_\sigma \Gamma_{r\sigma}\Phi_\sigma(t). \tag{175b}$$

This only depends on the coefficients $\Phi_\sigma(t) = \langle n_\sigma\rangle(t) - 1/2$ of the density operator (68), i.e., the deviations of the average spin-orbital occupations from the stationary, $T\to\infty$ values. In the $T\to\infty$ limit the current is given by the contribution (175b) alone, when substituting for $\Phi_\sigma(t)$ the value $\lim_{T\to\infty}\Phi_\sigma(t) = e^{-\Gamma_\sigma(t-t_0)}\Phi_\sigma(t_0)$ [cf. Eq. (116)]. In the stationary limit, this gives a vanishing current, which is as it should be since the bias voltage is dominated by thermal fluctuations. Note that this holds generally for $U\neq 0$ and nonperturbatively in Γ, as in Sec. III C 3.

For finite temperature, the current requires the calculation of $\bar I^r(t)$ but also $\tilde I^r(t)$ changes since $\Phi_\sigma(t)$ takes another value for finite T [cf. Eq. (175b)], also requiring a calculation [142]. Before we turn to this, we note that the WBL result for (175b) has the disconcerting property that at the initial time t_0 it can give rise to a nonzero total current for a general initial condition $\Phi_\sigma(t_0)$. This is again clear in the $T\to\infty$ limit mentioned above: $\lim_{T\to\infty} I^r(t_0) = \lim_{T\to\infty}\tilde I^r(t_0) = \Phi_\sigma(t_0)$ yields a nonzero value. In the next section, we explicitly show that for the $U=0$ limit this also occurs at finite temperature.

This nonzero current is inconsistent with our initial assumption that the dot and reservoirs are decoupled at $t=t_0$ and is unphysical. This is an artifact of the WBL and raises the question on which time scale (175b) is correct. For the noninteracting [143] case $U=0$ this has been discussed, e.g., in Refs. [76,77,134], and it was shown by explicit calculation for a finite bandwidth D that the current starts from zero at $t=t_0$ as it should, but then on the time scale set by the inverse bandwidth, $1/D$, the result rapidly approaches the WBL result.

The use of causal field superoperators allows us to generalize this qualitative understanding to the interacting case ($U\neq 0$) since the effect of the WBL can be traced explicitly on the level of superoperators. The effect is twofold. First, as explained in Sec. III B, the δ function constraint on time integrations arising from the large bandwidth energy forbids diagrams in which a retarded contraction crosses with any other contraction line. Since experimentally the bandwidth D is usually much larger than any characteristic energy of the dot, temperature, or transport bias, this should be a good approximation. Second, the time-dependent retarded contraction (94), retained in $\tilde\Sigma(t,t')$, is basically the Fourier transform of the function Γ_{1,ω_1}, $\tilde\gamma_{1,2}(t,t') \propto \int d\omega_1\Gamma_{1,\omega_1}e^{-i\eta_1(\omega_1+\mu_{r_1})(t-t')}$. For large, but finite, bandwidth D, this therefore has a characteristic finite time support of order $1/D$. If we now correct for this in Eq. (175a), then the integral over t' starts from zero at t_0, as it should, and only on the time scale $1/D$ does it acquires the WBL value given by Eq. (175b). Note, however, that the times on which this difference is noticeable is below femtoseconds for the typical energies $D\sim 1.0$ eV, which seems to be far below realistic time scales of switching on the tunnel coupling Γ at t_0.

3. Noninteracting current

We now again return to the noninteracting limit $U=0$. In this case, the first contribution $\tilde I^r(t)$ to the current (174) is given by Eq. (175b) with the value of $\Phi_\sigma(t)$ given by the central result (143). We see that $\tilde I^r(t)$ depends on the initial state through $\Phi_\sigma(t_0)$ and decays to a nonzero stationary value. The second contribution $\bar I^r(t)$ can now be simplified for $U=0$ using the super-Pauli principle (62) and (63): In the renormalized perturbation expansion for the finite T corrections only two terms survive, $\bar\Sigma^r(t,t') = \bar\Sigma^r_2(t,t') + \bar\Sigma^r_4(t,t')$, in full analogy to Eq. (123). In addition, by the same principle $(\chi_\sigma|\bar\Sigma^r_4(t,t') = 0$ in Eq. (174) [since $\bar\Sigma^r_4 \propto \bar G_2\bar G_{\bar 2}\bar G_1\bar G_{\bar 1} \propto |Z_R)(Z_L|$], and therefore only the two-loop self-energy $\bar\Sigma^r_2(t,t')$ contributes to the current in this limit (here there is no summation over the r component of the multi-index 2):

$$\bar\Sigma^r_2(t,t') = \sum_2 \bar G_2 e^{-i\bar L(t-t')}\bar G_{\bar 2}\bar\gamma_{2,\bar 2}(t,t') = \sum_{\eta,\sigma} -\frac{\Gamma_{r\sigma}Te^{(i\eta\epsilon_{r\sigma}+\frac{1}{2}\Gamma_\sigma)(t-t')}}{\sinh[\pi T(t-t')]}e^{-i\bar L(t-t')}\bar G_2\bar G_{\bar 2}. \tag{176}$$

Using Eq. (129) together with $(\chi_\sigma|\bar L = (\chi_\sigma|\tilde\Sigma = -i\Gamma_\sigma(\chi_\sigma|$ [cf. Eq. (114a)] and summing over η, one obtains

$$\bar\Sigma^r_2(t,t') = -2i\Gamma_{r\sigma}Te^{-\frac{1}{2}\Gamma_\sigma(t-t')}\frac{\sin[\epsilon_{r\sigma}(t-t')]}{\sinh[\pi T(t-t')]}|\chi_\sigma)(Z_L| + \cdots. \tag{177}$$

The terms not written out give no contribution when inserted in Eq. (174) for the current (either proportional to $|Z_R)(\chi_{\bar\sigma}|$ or to fermionic projectors), and the term shown gives a contribution independent of the initial dot state [since $(Z_L|\rho(t') = 1/2$]. The explicit result in terms of the function (134a) reads as

$$\bar I^r = -\sum_\sigma \Gamma_{r\sigma}T\int_{t_0}^t dt' e^{-\frac{1}{2}\Gamma_\sigma(t-t')}\frac{\sin[\epsilon_{r\sigma}(t-t')]}{\sinh[\pi T(t-t')]} = \sum_\sigma \Gamma_{r\sigma}F^+_{r\sigma}(\Delta), \tag{178}$$

where again $\Delta = t-t_0$.The total average current through reservoir r, written for the case of two reservoirs $r=\pm$,

$\mu_r = rV_b/2$, is then

$$\langle I^r\rangle(t) = \sum_\sigma \frac{\Gamma_{r\sigma}\Gamma_{\bar r\sigma}}{\Gamma_\sigma}[F^+_{r\sigma}(\Delta) - F^+_{\bar r\sigma}(\Delta)] - \sum_{r,\sigma}\frac{\Gamma^2_{r\sigma}}{\Gamma_\sigma}F^-_{r\sigma}(\Delta) - e^{-\Gamma_\sigma\Delta t}\sum_\sigma \Gamma_{r\sigma}\Phi_\sigma(t_0). \quad (179)$$

For the noninteracting case the time-dependent current has already been explicitly calculated in the limit of one spin-orbital, e.g., in Ref. [134] (using the Keldysh Green's function approach), under the assumption that the dot was initially fully unoccupied, and for an arbitrary occupation in Ref. [75] (using the real-time RG for the interacting resonant-level model in the limit of $T \to 0$ and vanishing nonlocal interaction, corresponding the noninteracting Anderson model). We have verified that under the corresponding simplifications our result Eq. (179) agrees with these works. The last two terms in Eq. (179) are not antisymmetric in the reservoir index r and do not vanish as $V_b = 0$. They originate from the current caused the change of the dot charge [$I_{\rm dis} = dn(t)/dt$], the displacement current [134]. The displacement current decays, as it should, to zero in the stationary limit $\Delta \to +\infty$, which follows from the asymptotic relation Eq. (135a). We note the deviation of the results of Ref. [77] from the above body of works [144].

Close to the initial time, $D^{-1} \ll |t - t_0| \ll \Gamma^{-1}_{r\sigma}$ (cf. discussion above),

$$\langle I^r\rangle(t) \approx \tilde I^r(t_0) = \sum_\sigma \Gamma_{r\sigma}\left[\frac{1}{2} - n_\sigma(t_0)\right]; \quad (180)$$

i.e., the total current is dominated by the last term in Eq. (179), the part of the displacement current coming from Eq. (175b). This is again in agreement with the zero-temperature results of Ref. [75] for the spinless, interacting resonant level model in the limit of vanishing nonlocal interaction. This also agrees with the result for the initial current in Ref. [134]; however, in contrast to that work, we take into account arbitrary initial dot level occupancies. The physical picture behind the result (180) again nicely relates to the fundamental importance of the $T = \infty$ limit built into our causal superfermion technique. Extending [145] the discussions in Ref. [134] [cf. Eq. (36) there], it is as follows. The initial current (180) stems form the part (175), which describes the current in the $T \to \infty$ limit [see discussion following Eq. (175)]. Due to the WBL, the processes described by $\tilde\gamma$ [cf. Eq. (94)] are very fast, taking place on the times of order D^{-1} and in the WBL, giving a finite instantaneous current response at $t = t_0$. In contrast, the temperature-induced processes described by $\bar\gamma$ [cf. Eq. (101)] are much slower and do not contribute on such short time scales. The current thus "does not know yet" about the actual temperature of the reservoirs on such time scales and therefore behaves such as if T would be infinite. This is what the physical decomposition (174) of the charge current expresses, which follows naturally on a general level from our formalism. In the concrete result (180) the factors $\langle n_\sigma\rangle(t_0)\rangle - 1/2$ show that a deviation of the initial dot charge from the value $1/2$, the stationary value in the limit $T \to \infty$, determines the response: The empty dot $\langle n_\sigma\rangle(t_0) = 0$ will charge up, $I^r(t_0) = \sum_\sigma \Gamma_{r\sigma}/2$, whereas the filled dot $\langle n_\sigma\rangle(t_0)\rangle = 1$ will discharge, $I^r = -\sum_\sigma \Gamma_{r\sigma}/2$.

The stationary value of the current, attained at much later times $|t - t_0| \gg \Gamma^{-1}_{r\sigma}$, is determined by the first term of Eq. (179), which is antisymmetric in the reservoirs (and thus vanishes at zero bias) [cf. Eq. (135a)]:

$$\langle I^r\rangle(\infty) = \sum_{r',\sigma}\frac{\Gamma_{r\sigma}\Gamma_{\bar r\sigma}}{\pi\Gamma_\sigma}r'\,\mathrm{Im}\,\Psi\left(\frac{1}{2} + \frac{\frac{1}{2}\Gamma_\sigma - i\epsilon_{r'\sigma}}{2\pi T}\right). \quad (181)$$

Expressed in the Fermi function $f(x) = \frac{1}{e^{x/T}+1} = \frac{1}{2} - \frac{1}{2}\tanh(x/2T)$ and using Eq. (C2), this can be rewritten as the more familiar form of a sum of current contributions from the independent spin orbitals, each broadened by $\Gamma_\sigma = \sum_r \Gamma_{r\sigma}$:

$$\langle I^r\rangle(\infty) = \sum_\sigma \frac{\Gamma_{r\sigma}\Gamma_{\bar r\sigma}}{\pi\Gamma_\sigma}\int_{-\infty}^{\infty}\frac{\Gamma_\sigma/2}{(x-\epsilon_\sigma)^2 + (\Gamma_\sigma/2)^2} \times [f(x+\mu_r) - f(x+\mu_{\bar r})]dx. \quad (182)$$

This result coincides with either of Refs. [75,77,134] in the corresponding limits mentioned above. Finally, we note that the stationary current (179), calculated here by explicitly taking the long-time limit, is recovered from our direct calculation of the stationary quantities in Sec. IV B: With the help of Eqs. (172b) and (169a) one can show that the stationary current depends on just two stationary self-energy coefficients [30]:

$$I^r(\infty) = \sum_\sigma \frac{\Gamma_{\bar r\sigma}\psi^r_\sigma - \Gamma_{r\sigma}\psi^{\bar r}_\sigma}{2\Gamma_\sigma}. \quad (183)$$

Inserting the $U = 0$ result for ψ^r_σ by leaving out the r sum in Eq. (161) reproduces Eq. (181). This confirms the result for the current in the $U = 0$ limit obtained in Ref. [30] by a real-time RG calculation of these coefficients. This is another way of seeing that the additional broadening scales $\Gamma_\sigma + \frac{1}{2}\Gamma_{\bar\sigma}$ [Eq. (147)] do not affect the stationary current for $U = 0$since the coefficients ϕ_σ [Eq. (163)] and ζ [Eq. (166)] do not appear in Eq. (183).

The main objective of the above was to illustrate in a tractable example how the causal superfermion technique works for the calculation of an observable, in this case the current. Although we were able to include all possible initial coherences and correlations in the initial density operator locally on the quantum dot, the time-dependent current reduces to the sum over its spin-resolved components. The current is not sensitive to the fermion-parity decay of the quantum-dot mixed state, which can be detected in ways discussed in the introduction [cf. Eq. (1)]. In the noninteracting and WBL the effect of the spin-polarization of the ferromagnetic leads is to merely introduce different decay time scales for different spin states ($\Gamma^{-1}_{r\sigma}$). The situation becomes more interesting when Coulomb interaction is included since this generates of the effective exchange magnetic field [146–150], a nondissipative effect. The time evolution of this field after switching on the tunnel processes between the dot and the ferromagnetic leads is of considerable interest. The method presented in the present paper may serve as a starting point for conveniently addressing how such effects develop, in particular, even for small Coulomb interaction nonperturbatively but strong tunnel coupling ($\Gamma \gg U$). It is advantageous that this can be done in the same formalism which can treat the complementary limit ($\Gamma \ll U$).

V. DISCUSSION AND OUTLOOK

As outlined in the Introduction, the time evolution of strongly interacting quantum dots is of great experimental interest, but analytical theoretical methods struggle to deal with it. Taking an Anderson model description as a starting point, we focused on improving the real-time approach which has already been successfully applied to explain various experiments. The goal of this paper was twofold: We wanted (i) to set up from scratch the real-time approach to time-dependent decay in interacting transport problems, systematically exploiting the causal superfermion technique (Sec. III), and (ii) to highlight its practical advantages by a complete solution of the noninteracting Anderson model describing a quantum dot with spin-dependent tunneling rates $\Gamma_{r\sigma}$ and for an arbitrarily correlated initial mixed state (Sec. IV). We now summarize these two aspects separately, starting with the concrete results (ii)and then turning to the general framework (i). In the process we generalize the concrete results to multiorbital models, in both the interacting and the noninteracting cases. We also comment on the limitations imposed by the few assumptions that we made and provide an outlook on possible further applications which have motivated this work all along.

A. Quantum-dot spin valve: $U = 0$ and interaction corrections

In Sec. IV A we calculated the exact time-evolution propagator of the complete two-fermion density operator in the noninteracting limit ($U = 0$). The exact result, nonperturbative in the tunneling rates $\Gamma_{r\sigma}$, is obtained from a simple *second-order* renormalized perturbation theory, expanding in the Keldysh reservoir correlation function $\bar{\gamma}(\omega) \propto \Gamma_{r\sigma} \tanh(\omega/2T)$ instead of just $\Gamma_{r\sigma}$. Our result (142) includes all possible coefficients of the density operator—spin-orbital occupancies ($\langle n_\uparrow\rangle$, $\langle n_\downarrow\rangle$), transverse spin coherences (e.g., $\langle d_\uparrow^\dagger d_\downarrow\rangle$), and electron-pair coherences (e.g., $\langle d_\downarrow d_\uparrow\rangle$)—but also the two-particle correlations quantified by the nonequilibrium average of the fermion-parity operator $\langle(-1)^n\rangle \sim \langle n_\downarrow n_\uparrow\rangle(t) + \cdots$. The last three arise only due to the initial preparation of the quantum-dot state.

Besides recovering known results for the one-particle quantities, we noted that, in general, the *transient* two-particle correlator does not factorize $\langle n_\downarrow n_\uparrow\rangle(t) \neq \langle n_\downarrow\rangle(t) \cdot \langle n_\uparrow\rangle(t)$ until stationarity is reached, $\langle n_\downarrow n_\uparrow\rangle(\infty) = \langle n_\downarrow\rangle(\infty) \cdot \langle n_\uparrow\rangle(\infty)$. This happens when the quantum-dot state is initially prepared in a two-particle correlated state. In the stationary state these correlations, however, die out [151]. Another, more striking aspect of the decay of these initial correlations on the quantum dot, $\langle(-1)^n\rangle(t) \sim e^{-\Gamma(t-t_0)}\langle(-1)^n\rangle(t_0) + \cdots$, is that the strict exponential form and the decay rate $\Gamma = \sum_{r\sigma}\Gamma_{r\sigma}$ is independent of any other parameter in the problem. Within our superfermion formulation of the real-time approach it is immediately clear that no corrections to this simple "universal" behavior can appear, due to neither finite temperature T (see Sec. III C 2), nor bias voltage V, nor magnetic field B, nor *interaction* U. Notably, Γ depends only on the sum of the spin-dependent rates, i.e., even the spin-polarization of the tunneling drops out, an aspect not addressed in Ref. [30]. This generalizes an earlier conclusion based on perturbation theory [31]: This absence of corrections holds *nonperturbatively* in the tunnel coupling $\Gamma_{r\sigma}$ for the *interacting* Anderson model but also for the decay in multiorbital generalizations, recently studied in Ref. [121]. The key point is that by the fundamental fermion-parity superselection rule, any local quantum-dot Hamiltonian must commute with the operator $(-1)^n$. Therefore, the decay of the initial correlations $\langle(-1)^n\rangle(t_0)$, appearing in the expansion of the density operator, can only come from the tunnel coupling to the reservoirs and has the above mentioned form.

In addition, we found that the time evolution of $\langle(-1)^n\rangle(t) \sim \langle n_\downarrow n_\uparrow\rangle(t) + \cdots$ contains additional oscillatory decaying terms coming from the initial occupations $\langle n_\sigma\rangle(t_0)$ with rate $\Gamma_\uparrow + (\Gamma_\downarrow/2)$ and $\Gamma_\downarrow + (\Gamma_\uparrow/2)$. These unexpected rates were noted earlier for spin- and junction-independent tunnel rates $\Gamma_{r\sigma} = \tilde{\Gamma}$ as an additional broadening scale $3\tilde{\Gamma}$ in the stationary density operator [30] and in related self-energies [67]. Thus, even in this simple limit the time-dependent decay of the density operator of the noninteracting ($U = 0$) Anderson model shows four characteristic decay rates: $\tilde{\Gamma}$, $2\tilde{\Gamma}$, $3\tilde{\Gamma}$, $4\tilde{\Gamma}$.

Finally, in Sec. IV C we illustrated the application of superfermions to the calculation of observable quantities for the time-dependent charge current. We showed that the small-time artifacts of the WBL in the transport current can be discussed on the superoperator level. Also, the $T \to \infty$ limit, built into the field superoperators, naturally appears in the expressions for the displacement current. We furthermore confirmed the RG results for the stationary noninteracting limit in Ref. [30]; in particular, we related the observation made there—that only one-loop self-energy corrections matter for the current—to the super-Pauli principle introduced here.

B. Superfermions in the real-time approach

The results summarized above served to illustrate three general aspects of superfermions—announced in the title of the paper—as applied to the real-time transport theory that we discussed in Sec. III.Therefore, these can be also generalized to multiorbital Anderson quantum dots.

(i) Causal structure of superfermions. Using various examples, we illustrated that physical meaning can be assigned to formal objects appearing in a Liouville-space theory of a strongly interacting, open fermionic system. Although many concepts carry over from the usual Hilbert-Fock space, many others require careful reconsideration, e.g., the role of the super-kets in the expansion of a mixed state [Eq. (68)] or the superfermion number [Eq. (64)]. The crucial feature distinguishing quantum fields in Liouville-Fock space from those in Hilbert-Fock space is what we refer to as the "causal structure." On the one hand, this entails [Eq. (55)]

$$\bar{G}_{\eta\sigma}|Z_R) = 0, \tag{184}$$

where $|Z_R) \sim (-1)^n$ is the fermion-parity operator appearing in the corresponding superselection rule of quantum mechanics. Roughly speaking, this imposes the constraint that "fermions on different Keldysh contours anticommute." [30] On the other hand, the identity [Eq. (54)]

$$(Z_L|\bar{G}_{\eta\sigma} = 0, \tag{185}$$

where the $(Z_L| = \mathrm{Tr}$ represents the trace operation, is involved in the probability conservation of the density operator. As we showed in Sec. III B, the causal structure implies much

more than probability conservation of the dynamics. Whereas the former has received much attention in Green's function formalism, in density operator approaches much less attention seems to have been given to this more fundamental structure.

We emphasized the central importance of the unit operator $|Z_L) \sim \mathbb{1}$ as the Liouville-Fock space vacuum and its physical meaning as the $T \to \infty$ maximally mixed state. We used the $T \to \infty$ limit as a point of reference, not only in the construction of the Liouville-Fock space but also in the calculation of the time-evolution propagator and its self-energy. This may be compared with the limit of infinite bias $V_b = \infty$, which also admits an exact analysis. It has recently been studied by Oguri and Sakano [67] and earlier by Gurvitz [152,153], while the relevance of renormalization corrections at finite bias were pointed out in Ref. [154]. In comparison with this, we emphasize that our formulation using the $T \to \infty$ limit has the important technical advantage that it is provides a unique starting point irrespective of the number of reservoirs. Moreover, it applies irrespective of the asymmetry of the tunnel couplings: The latter spoils the relation between the $V_b \to \infty$ and $T \to \infty$ limits for two electrodes, discussed in Ref. [155].

Another interesting consequence of incorporating the $T \to \infty$ limit is that the unperturbed evolution (i.e., the reference problem for the renormalized time-dependent perturbation theory) is *dissipative* and therefore damped as a function of time. This may prove to be interesting for numerical schemes that aim to calculate memory kernels [25,26,68–72]. This damping depends only on the tunnel couplings, in contrast to the broadening obtained by a recently proposed dressing scheme [38]; cf. also [156], which depends on the quantum-dot energies and is based on a partial resummation of real-time diagrams that serves a different purpose.

Finally, the $T \to \infty$ limit also aids the physical understanding of observables, such as the displacement part of the current (180).

(ii) Fermion-parity protected decay mode. As shown in Sec. III C the striking independence of the key result [Eq. (1)], $\langle(-1)^n\rangle(t) \sim e^{-\Gamma(t-t_0)}\langle(-1)^n\rangle(t_0)+\cdots$, of all remaining parameters including the *interaction* U relates to a formal property of the general theory. Since the causal superfermion approach uses the $T \to \infty$ limit as a reference point, it reveals that finite-temperature corrections to the time evolution only involve *creation* superoperators $\bar{G}$. Clearly then, the time evolution of the superket $|Z_R) \sim (-1)^n$ in Liouville space cannot have any such correction: As expressed by Eq. (184), it is the "most filled" superket and simply cannot accommodate more superfermions. Moreover, it is readily seen that *any interacting* N-spin-orbital Anderson model (orbitals $l = 1,\ldots,N/2$) with quadratic tunnel coupling exhibits exactly this purely exponential decay mode with rate $\Gamma = \sum_{r\sigma,l}\Gamma_{r\sigma,l}$. Finally, it is interesting to note that half of the decay modes that we studied in the noninteracting case ($U = 0$) are, in fact, fixed completely by the $T = \infty$ calculation.

(iii) Super-Pauli principle. The super-Pauli principle (62) states that formal superkets cannot be "doubly occupied":

$$(\bar{G}_{\eta\sigma})^2 = 0. \tag{186}$$

This simple consequence of the causal Liouville-Fock space construction provides useful insights in two directions. First, when applying the real-time approach to noninteracting problems, the super-Pauli principle is the key simplification that keeps the calculations completely tractable on the *superoperator* level. The renormalized perturbation theory is simple to set up, and a *finite-order* N calculation gives the *exact* result for N spin orbitals, including all local N-particle nonequilibrium correlations. The higher-order corrections vanish exactly, not by their scalar magnitude but by their superoperator structure: Generalizing Eq. (63) to the case for N spin orbitals, we have

$$\bar{G}_m \cdots \bar{G}_1 = 0 \quad \text{for } m > 2N, \tag{187}$$

as a direct consequence of the super-Pauli principle. The other major implication of taking the noninteracting limit, Eq. (138), can also be generalized to this case by extending the simple considerations in Fig. 5 to even orders $m = 4,\ldots,2N$: The $m/2$-loop time propagator factorizes into one-loop propagators,

$$\bar{\Pi}_m(t,t_0) = \frac{1}{(m/2)!}\bar{\Pi}_2(t,t_0)e^{i\bar{L}(t-t_0)}\underbrace{\bar{\Pi}_2(t,t_0)\cdots e^{i\bar{L}(t-t_0)}\bar{\Pi}_2(t,t_0)}_{\text{(m/2 times)}}. \tag{188}$$

The superoperator algebraic structure thus carries important physical information, which is naturally revealed by the causal superfermions. We emphasize that these simple general features of the noninteracting limit remain hidden in the real-time approach unless one starts from the renormalized the perturbation theory (99), incorporating the WBL. We furthermore showed that certain observables, such as the charge current, turn out to be insensitive to corrections beyond the one-loop order. This raises a question of practical importance: Given a physical M-particle quantity, to which loop order does one need to calculate the self-energy in order to get the exact noninteracting result?

This leads to the second important insight which is relevant to applications of the real-time RG approach [24,51,75], which aims to provide a good solution in both the strong and the *weak* interaction limits. Our complementary frequency-space calculation of the stationary limit in Sec. IV B confirmed that the real-time RG in the one- plus two-loop approximation [30] correctly reproduces the exact noninteracting limit, in particular, the self-energy part relevant to the current, relating this to the super-Pauli principle. We additionally calculated the stationary state in this limit, obtaining the exact effective Liouvillian by a *two-loop* order calculation. For generalized Anderson models with N spin-orbitals, we inferred above that at least a N-loop calculation in the renormalized perturbation theory will reproduce the exact noninteracting limit. This implies that real-time RG schemes must include *at least* a consistent N-loop RG flow for the Liouvillian together with the corresponding vertex corrections in order to capture the exact noninteracting limit. In view of the complications encountered in Ref. [30], already at the $N = 2$-loop order for the Anderson model, a question becomes practically relevant: Under which conditions may higher loop orders be avoided (e.g., for a given observable or specific density operator component)? Here we should point out that it can be shown that if one is interested in the evolution of single-particle quantities [expressible through two (super)fields] only one-loop diagrams are required for the time-dependent decay in the noninteracting limit. This carries

over to multiparticle quantities only under the condition that initial correlations on the dot are absent; i.e, these factorize at the initial time [see main result Eq. (145); cf. Eqs. (146) and (140)]. When initial correlations are present, however, higher loop evolution does matter. Note that even when the initial density operator contains nonfactorizable correlators, our key result [Eqs. (138) and (188)] shows that the time-evolution superoperator can still be factorized.

We also found that the noninteracting limit becomes most transparent when considering the renormalized two-loop propagator $\bar{\Pi}_4(t,t_0)$ in time space (rather than its Laplace transform), because it factorizes in the limit $U=0$. This seems to have no equally simple counterpart in Laplace space for the two-loop renormalized self-energy $\bar{\Sigma}_4(z)$. The generalized time-space relations (188) allow for a convenient verification on the superoperator level that a real-time RG scheme correctly reproduces the noninteracting limit in all nonvanishing loop orders $m/2=1,2,\ldots,N$.

C. Limitations and further extensions

Our considerations were quite general. We now end with comments on the limitations imposed by our assumptions and provide an outlook on how these may be overcome.

Noninteracting limit ($U=0$). Although we focused in Sec. IV on the noninteracting limit for illustrative purposes, the principles demonstrated here can be applied to interacting problems, as we showed, e.g., in Sec. II D 3 b. This is what has motivated our exhaustive study all along. A more advanced example is our RG study Ref. [30], but other approaches may also be developed. For instance, one may consider expanding the time-evolution propagator Π or its self-energy $\bar{\Sigma}$ in the *nonlinear part* of the Coulomb interaction, i.e., not simply in the parameter U, but in the term $U(-1)^n/2$ in the Anderson Hamiltonian; cf. Sec. II D 3 b. This perturbative expansion then yields an approximate result which is nonperturbative in both U and $\Gamma_{r\sigma}$ [the quadratic term (74a) also depends on U, and this part is treated nonperturbatively]. The coefficients for the mth-order term in this nonlinear interaction can be calculated using our causal superfermion approach through an expansion in the Keldysh correlation function $\bar{\gamma}$, which is truncated as in the noninteracting limit, but now at the $(2+m)$-loop order [157]. Also, here the result simplifies due to the superoperator structure dictated by the super-Pauli principle.

Wideband limit. The WBL is another main simplifying assumption that we made in Sec. III B. However, beyond this limit the number of Keldysh contractions ($\bar{\gamma}$) is still limited to *two* by the super-Pauli principle (62) and (63) in the noninteracting limit ($U=0$). This expresses the general fact that retarded contractions ($\tilde{\gamma}$) always connect a creation and an annihilation superoperator, and thus its contribution does not change the total superparticle number. In contrast, Keldysh contractions $\bar{\gamma}$ always connect two *creation* superoperators, increasing the total superfermion number by two. Since the super-Pauli principle limits the total number of superfermions to four, at most, two Keldysh contractions are allowed. This illustrates how common physical reasoning based on the usual second quantization can be transferred to nonequilibrium problems using our causal superfermions, aiding the solution of physical problems.

Initial system-reservoir factorization. The assumption of factorizing system-reservoir correlations at the initial time is not that restrictive either. Much of the technical and physical conclusions presented can be generalized to apply also to the case of nonfactorizing system-reservoir initial conditions and will be discussed in a forthcoming work [84].

Time-dependent parameters. So far, we have focused on the time evolution of the quantum dot to the new stationary state after the tunnel couplings $\Gamma_{r\sigma}$ experience a sudden change (quench) at $t=t_0$ from $\Gamma_{r\sigma}=0$ to a set of finite values which further remain unchanged for $t>t_0$. Although Refs. [75,77,134] also studied this problem, the main motivation here was to illustrate the advantages of the causal superfermion approach in this most simple setting. However, our formalism can be easily extended to deal with a time dependence of all the parameters involved, i.e., $\epsilon=\epsilon(t)$, $B=B(t)$, $V_b=V_b(t)$, and $\Gamma_{r\sigma}=\Gamma_{r\sigma}(t)$, as we briefly outline. First, we note that once we consider the WBL, Eq. (94) remains valid if the parameters vary much slower than the inverse bandwidth, which always seems to be experimentally given. This allows us to integrate out the retarded reservoir contractions also in this case and obtain an infinite-temperature kernel $\tilde{\Sigma}$ [cf. Eq. (95)], but now with a time-dependent $\Gamma_{r\sigma}(t)$ and a corresponding time-dependent renormalized Liouvillian $\bar{L}(t)=L(t)+\tilde{\Sigma}(t)$; cf. Eq. (98). The interaction-representation vertices (100) now include a time-ordering superoperator T and reduces in the noninteracting case to a result similar to Eq. (119):

$$\bar{G}_j(t)=\mathrm{T}e^{-i\int_{t_0}^{t}d\tau\bar{L}(\tau)}\bar{G}_j(\mathrm{T}e^{-i\int_{t_0}^{t}d\tau\bar{L}(\tau)})^{-1} \tag{189}$$

$$=e^{\int_{t_0}^{t}d\tau[i\eta\epsilon_\sigma(\tau)+\frac{1}{2}\Gamma_\sigma(\tau)]}\bar{G}_1 \quad \text{for} \quad U=0. \tag{190}$$

The main ideas of our approach thus remain the same and apply also to multiorbital extensions without any crucial complications arising. In particular, the super-Pauli principle (62) is also valid for the above field superoperators and causes the perturbation series to terminate at a finite order as in Eq. (122), which is one of the central insights of this paper.

ACKNOWLEDGMENTS

We acknowledge useful discussions with M. Hell, M. Pletyukhov, H. Schoeller, and J. Splettstoesser.

APPENDIX A: FIELD SUPEROPERATORS

In this Appendix, we provide further comments on the construction of field superoperators undertaken in Sec. II D 1. As discussed in Sec. II A, we emphasize the importance of starting this construction from sets of fermionic operators d_1 and b_1 (or a_1) for the quantum dot and the reservoirs respectively, which mutually *commute*. The crucial advantage of using such field operators is that Eq. (54) holds for the *partial* traces of the corresponding dot or reservoir superoperators G_1^q [Eq. (46)] and J_1^q [Eq. (47)]. This allows one to obtain the reduced dynamics of the dot (by integrating out the reservoir degrees of freedom), while preserving the causal properties Eq. (54), which we have shown to bring many computational and physical insights.

If one uses in Eqs. (46) and (47) instead of d_1 and b_1 mutually anticommuting sets of fermion operators d_1' and

$b'_1 = \sqrt{\Gamma_{r\sigma}/2\pi}a'_1$, constructed in Sec. II A, then one obtains the same anticommutation relations (50) and (51) for the resulting field superoperators. However, in this case no definite commutation relations analogous to Eq. (52) are obtained (neither commutation nor anticommutation relations), which is a major disadvantage. In principle, one can introduce other sets of field superoperators which are free of this problem, even though one starts again from the anticommuting fields d'_1 and $b'_1 = \sqrt{\Gamma_{r\sigma}/2\pi}a'_1$. Instead of using Eqs. (46) and (47), one defines

$$\mathfrak{G}^q_1 \bullet = \frac{1}{\sqrt{2}}\left\{d'_1 \bullet + q(-1)^{n+n^R} \bullet d'_1(-1)^{n+n^R}\right\}, \quad \text{(A1)}$$

$$\mathfrak{J}^q_1 \bullet = \frac{1}{\sqrt{2}}\left\{b'_1 \bullet - q(-1)^{n+n^R} \bullet b'_1(-1)^{n+n^R}\right\}. \quad \text{(A2)}$$

Here one uses, in contrast to Eqs. (46) and (47), the *global* fermion-parity operator $(-1)^{n+n^R}$. The field superoperators $\mathfrak{G}_1$ and $\mathfrak{J}_1$ can be checked to satisfy the same anticommutation relations, Eqs. (50) and (51), as G_1, J_1 and the same superadjoint relation. In contrast to Eq. (52), they satisfy instead mutual *anti*commutation relations Eq. (52):

$$[\tilde{\mathfrak{J}}_1, \tilde{\mathfrak{G}}_2]_+ = [\bar{\mathfrak{J}}_1, \bar{\mathfrak{G}}_2]_+ = [\bar{\mathfrak{J}}_1, \tilde{\mathfrak{G}}_2]_+ = [\tilde{\mathfrak{J}}_1, \bar{\mathfrak{G}}_2]_+ = 0. \quad \text{(A3)}$$

However, the disadvantage of this construction is that, instead of the causal property [Eq. (54)], we now have

$$\mathsf{Tr}\bar{\mathfrak{G}}_1 = 0, \ \ \mathsf{Tr}\tilde{\mathfrak{J}}_1 = 0, \quad \text{(A4)}$$

where $\mathsf{Tr} = \underset{D}{\mathsf{Tr}}\underset{R}{\mathsf{Tr}}$ is a *global* trace, while the crucial *local*-trace identities Eq. (54) are not valid anymore:

$$\underset{D}{\mathsf{Tr}}\bar{\mathfrak{G}}_1 \not\equiv 0, \ \ \underset{R}{\mathsf{Tr}}\tilde{\mathfrak{J}}_1 \not\equiv 0. \quad \text{(A5)}$$

This seems to drastically complicate [158] the calculation of the partial reservoir trace required in Sec. III.

APPENDIX B: TIME REPRESENTATION FOR THE KELDYSH CONTRACTION

In the WBL, the explicit form of the time-dependent Keldysh correlation function $\bar{\gamma}_{2,1}(t_2 - t_1)$ [Eq. (90)] can be obtained using the partial fraction expansion for the meromorphic function,

$$\tanh(z) = \sum_{n=-\infty}^{+\infty} [z + i\pi(n+1/2)]^{-1}. \quad \text{(B1)}$$

Closing the contour of integration over ω in the lower half of the complex plane and making use of the residual theorem, we obtain Eq. (101) of the main text as follows:

$$\begin{aligned}\bar{\gamma}_{2,1}(t) &= \frac{\Gamma}{2\pi}\int d\omega e^{-i\eta(\omega+\mu)t}\tanh(\eta\omega/2T)\delta_{2,\bar{1}} \\ &= -i2Te^{-i\eta\mu t}\Gamma\sum_{n=0}^{+\infty} e^{-\pi T(2n+1)t}\delta_{2,\bar{1}} \\ &= \frac{-i\Gamma T}{\sinh(\pi Tt)}e^{-i\eta\mu t}\delta_{2,\bar{1}}. \end{aligned} \quad \text{(B2)}$$

Here, as in Eq. (94), the multi-indices $2, \bar{1}$ in the δ function do not contain the reservoir frequencies.

APPENDIX C: INTEGRALS OF KELDYSH CONTRACTION-DIGAMMA FUNCTION

In Eqs. (161), (166), and (181), we used the following result, obtained from $\mathrm{Im}\,\Psi(z) = -\mathrm{Im}\sum_{n=0}^{+\infty} 1/(n+z)$, the expansion (B1) of $\tanh(z)$, and application of the residual theorem (closing the integration contour in the lower half of the complex plane):

$$\begin{aligned}&\frac{1}{2}\int_{-\infty}^{+\infty} dx \frac{\Gamma\tanh(x/2T)}{\Gamma^2 + (x-\epsilon)^2} \\ &= -\frac{1}{2}\,\mathrm{Im}\int_{-\infty}^{+\infty} dx \frac{\tanh(x/2T)}{i\Gamma + \epsilon - x} \quad \text{(C1)} \\ &= -\frac{1}{2}\,\mathrm{Im}\sum_{n=-\infty}^{+\infty}\int_{-\infty}^{+\infty} dx \frac{1}{x/2T + i\pi(n+1/2)}\frac{1}{i\Gamma + \epsilon - x} \\ &= \frac{1}{2}\,\mathrm{Im}\sum_{n=0}^{+\infty}\frac{2}{n + 1/2 + \frac{\Gamma}{2\pi T} - \frac{i\epsilon}{2\pi T}} \\ &= -\,\mathrm{Im}\,\Psi\left(\frac{1}{2} + \frac{\Gamma - i\epsilon}{2\pi T}\right). \quad \text{(C2)}\end{aligned}$$

APPENDIX D: EVALUATION OF THE FUNCTIONS $F^+_{r\sigma}(t)$ AND $F^-_{r\sigma}(t)$

Here we present the calculation of the function $F^+_{r\sigma}(\Delta t)$ given in Eq. (134a). We use the expansion

$$\frac{1}{\sinh(x)} = \frac{2e^{-x}}{1 - e^{-2x}} = 2\sum_{n=0}^{\infty} e^{-(2n+1)x}, \quad \text{(D1)}$$

which holds for any positive x since $e^{-2x} < 1$ lies inside the convergence radius. We obtain Eq. (134a) as

$$F^+_{r\sigma}(\Delta t) := -\int_0^{\Delta t} d\tau \frac{T\sin(\epsilon_{r\sigma}\tau)}{\sinh(\pi T\tau)}e^{-\Gamma\tau} \quad \text{(D2)}$$

$$\begin{aligned}&= -2T\,\mathrm{Im}\sum_{n=0}^{\infty}\int_0^{\Delta t} d\tau e^{(i\epsilon_{r\sigma}-\Gamma)\tau - \pi T\tau(2n+1)} = 2T\,\mathrm{Im}\sum_{n=0}^{\infty}\frac{1 - e^{(i\epsilon_{r\sigma}-\Gamma)\Delta t - \pi T\Delta t(2n+1)}}{i\epsilon_{r\sigma} - \Gamma - \pi T(2n+1)} = \frac{1}{\pi}\,\mathrm{Im}\,\Psi\left(\frac{1}{2} + \frac{\Gamma - i\epsilon_{r\sigma}}{2\pi T}\right) \\ &+ \mathrm{Im}\left\{\frac{e^{(i\epsilon_{r\sigma}-\Gamma-\pi T)\Delta t}}{\pi}\Phi\left(e^{-2\pi T\Delta t}; 1; \frac{1}{2} + \frac{\Gamma - i\epsilon_{r\sigma}}{2\pi T}\right)\right\}, \end{aligned} \quad \text{(D3)}$$

where $\Psi(z) = -\gamma - \sum_{k=0}^{\infty}[1/(z+k) - 1/(1+k)]$ is the digamma function, and $\Phi(z;s;v) = \sum_{n=0}^{\infty} z^n/(n+v)^s$ is the *Lerch transcendent* (see, e.g., Ref. [131]). Analogously, we obtain for the function $F^{-}_{r\sigma}(t)$ [Eq. (134b)]:

$$F^{-}_{r\sigma}(\Delta t) := e^{-2\Gamma\Delta t}\int_0^{\Delta t} d\tau \frac{T\sin(\epsilon_{r\sigma}\tau)}{\sinh(\pi T\tau)} e^{\Gamma\tau} \tag{D4a}$$

$$= -e^{-2\Gamma\Delta t} 2T \sum_{n=0}^{\infty} \mathrm{Im}\int_0^{\Delta t} d\tau e^{(i\epsilon_{r\sigma}+\Gamma)\tau - \pi T\tau(2n+1)} = -e^{-2\Gamma\Delta t}(F^{+}_{r\sigma}(\Delta t)|_{\Gamma\to-\Gamma})$$

$$= \mathrm{Im}\left\{\frac{e^{(i\epsilon_{r\sigma}-\Gamma-\pi T)\Delta t}}{\pi}\Phi\left(e^{-2\pi T\Delta t};1;\frac{1}{2}-\frac{\Gamma+i\epsilon_{r\sigma}}{2\pi T}\right) + \frac{e^{-2\Gamma\Delta t}}{\pi}\Psi\left(\frac{1}{2}+\frac{-\Gamma+i\epsilon_{r\sigma}}{2\pi T}\right)\right\}. \tag{D4b}$$

Note that the results satisfy the formal relation Eq. (134b). One can think that the function $F^{-}_{r\sigma}(\Delta t)$ can have a pole at $\Gamma = 2\pi Tk$ ($k = 1,2,\ldots$) for $\epsilon_{r\sigma} = 0$, since both $\Psi(\frac{1}{2} + \frac{-\Gamma+i\epsilon_{r\sigma}}{2\pi T})$ and $\Phi(e^{-2\pi T\Delta t};1;\frac{1}{2} - \frac{\Gamma+i\epsilon_{r\sigma}}{2\pi T})$ have it. However, the pole of the Ψ function exactly compensates the pole of the Φ function, giving zero in that case. That this should be the case is already clear from Eq. (D4b) by taking $\epsilon_{r\sigma} = 0$.

APPENDIX E: TWO-LOOP CONTRIBUTIONS TO THE TIME-EVOLUTION

In this Appendix, we write out the proof of the factorization (138), presented diagrammatically in Fig. 5. The manipulations that we apply are analogous to those of Ref. [41] for two-loop calculations. That reference, however, deals with self-energy diagrams for interacting systems in the zero frequency limit. We start from Eq. (137), repeated here for convenience:

$$\bar{\Pi}_4(t,t_0) = e^{-i\bar{L}(t-t_0)} \times \int_{t\geqslant t_4\geqslant t_3\geqslant t_2\geqslant t_1\geqslant t_0} dt_4dt_3dt_2dt_1 \bar{G}'_4(t_4)\bar{G}'_3(t_3)\bar{G}'_2(t_2)\bar{G}'_1(t_1) \times \sum_{\langle i,j,k,l\rangle} (-1)^P \bar{\gamma}_{ij}(t_i-t_j)\bar{\gamma}_{kl}(t_k-t_j). \tag{E1}$$

Here we sum over the following possible contractions: $i,j,k,l = 4,3,2,1$ (reducible) and $4,2,3,1$ and $4,1,3,2$ (both irreducible). First, we relabel the times and multi-indices as indicated in Fig. 5 such that the contraction function is the same for all terms, equal to $\bar{\gamma}_{43}(t_4-t_3)\bar{\gamma}_{21}(t_2-t_1)$. In the irreducible contractions, this changes the order of the vertices from $\bar{G}'_4(t_4)\bar{G}'_3(t_3)\bar{G}'_2(t_2)\bar{G}'_1(t_1)$, but for each of these we can restore this order by anticommuting the creation superoperators [Eq. (120)]. This puts the superoperators connected by a $\bar{\gamma}$ contraction adjacent to each other; i.e., one disentangles the contractions: Therefore, the sign appearing from anticommutation of the creation superoperators precisely cancels the fermionic Wick sign $(-1)^P$. We are left with

$$\bar{\Pi}_4(t,t_0) = e^{-i\bar{L}(t-t_0)}\left[\int_{t\geqslant t_4\geqslant t_3\geqslant t_2\geqslant t_1\geqslant t_0} dt_4dt_3dt_2dt_1 + \int_{t\geqslant t_4\geqslant t_2\geqslant t_3\geqslant t_1\geqslant t_0} dt_4dt_2dt_3dt_1 + \int_{t\geqslant t_2\geqslant t_4\geqslant t_3\geqslant t_1\geqslant t_0} dt_2dt_4dt_3dt_1\right] \times \sum_{4321} \bar{G}'_4(t_4)\bar{G}'_3(t_3)\bar{G}'_2(t_2)\bar{G}'_1(t_1)\bar{\gamma}_{43}(t_4-t_3)\bar{\gamma}_{21}(t_2-t_1). \tag{E2}$$

By duplicating these terms, while compensating by a factor $1/2$, and interchanging the dummy variables $t_1,t_2 \leftrightarrow t_3,t_4$ in the duplicates, we obtain a sum of integrals which can be factorized as Eq. (138) by comparing with the definition of $\bar{\Pi}_2(t,t_0)$ [Eq. (127)]:

$$\bar{\Pi}_4(t,t_0) = \frac{1}{2}e^{-i\bar{L}(t-t_0)} \tag{E3a}$$

$$\times \left[\int_{t\geqslant t_4\geqslant t_3\geqslant t_2\geqslant t_1\geqslant t_0} dt_4dt_3dt_2dt_1 + \int_{t\geqslant t_4\geqslant t_2\geqslant t_3\geqslant t_1\geqslant t_0} dt_4dt_2dt_3dt_1 + \int_{t\geqslant t_2\geqslant t_4\geqslant t_3\geqslant t_1\geqslant t_0} dt_2dt_4dt_3dt_1 + \int_{t\geqslant t_2\geqslant t_1\geqslant t_4\geqslant t_3\geqslant t_0} dt_2dt_1dt_4dt_3 + \int_{t\geqslant t_2\geqslant t_4\geqslant t_1\geqslant t_3\geqslant t_0} dt_2dt_4dt_1dt_3 + \int_{t\geqslant t_4\geqslant t_2\geqslant t_1\geqslant t_3\geqslant t_0} dt_4dt_2dt_1dt_3\right]$$

$$\times \sum_{4321} \bar{G}'_4(t_4)\bar{G}'_3(t_3)\bar{G}'_2(t_2)\bar{G}'_1(t_1)\bar{\gamma}_{43}(t_4-t_3)\bar{\gamma}_{21}(t_2-t_1)$$

$$= \frac{1}{2}e^{-i\bar{L}(t-t_0)}\int_{t\geqslant t_4\geqslant t_3\geqslant t_0} dt_4dt_3 \sum_{43} \bar{G}'_4(t_4)\bar{G}'_3(t_3)\int_{t\geqslant t_2\geqslant t_1\geqslant t_0} dt_2dt_1 \sum_{21} \bar{G}'_2(t_2)\bar{G}'_1(t_1)$$

$$= \frac{1}{2}\bar{\Pi}_2(t,t_0)e^{i\bar{L}(t-t_0)}\bar{\Pi}_2(t,t_0). \tag{E3b}$$

APPENDIX F: SPIN-CHANNEL DECOMPOSITION

In this Appendix we outline the calculation of the propagator by using the noninteracting limit *in the first step* and then setting up the perturbation theory. (In contrast to this, the calculations given in Sec. IV first set up the perturbation theory and make use of the assumption $U = 0$ *in the last step* and rather aim to show how, in a framework applicable to interacting systems, this limit is achieved. The approach we now outline, although shorter, does not make that clear.) In particular, we use that for $U = 0$ the quantum-dot Liouvillian decomposes into single-spin species, $L = \sum_\sigma L_\sigma$. Due to this special property, the total Liouvillian decomposes into commuting spin-resolved parts, $L^{\rm tot} = \sum_\sigma L^{\rm tot}_\sigma$ with $L^{\rm tot}_\sigma = L_\sigma + L^R_\sigma + L^V_\sigma$, since the reservoirs are noninteracting, the tunnel coupling (22) is quadratic, and all spin-dependencies (due the junctions and the magnetic field) are considered to be collinear. Here L_σ, L^R_σ, and L^V_σ are obtained from Eqs. (74), (81), and (48), respectively, by leaving out the sum over the spin-index σ. One now splits the propagator (37) into commuting factors relating to different spins,

$$\Pi(t,t_0) = \operatorname*{Tr}_R\big(e^{-iL^{\rm tot}(t-t_0)}\rho^R\big)\bullet \tag{F1a}$$

$$= \operatorname*{Tr}_R\big(e^{-iL^{\rm tot}_\uparrow(t-t_0)}e^{-iL^{\rm tot}_\downarrow(t-t_0)}\rho^R_\uparrow\rho^R_\downarrow\big)\bullet \tag{F1b}$$

$$= \Pi^\uparrow(t,t_0)\Pi^\downarrow(t,t_0), \tag{F1c}$$

where $\rho^R_\sigma = \prod_r e^{-\frac{1}{T}(H^r_\sigma-\mu^r n^r_\sigma)}Z^r_\sigma$ and

$$\Pi^\sigma(t,t_0) = \operatorname*{Tr}_{R\sigma}\big(e^{-iL^{\rm tot}_\sigma(t-t_0)}\rho^R_\sigma\big)\bullet, \tag{F2}$$

where the trace runs over one spin-degree of freedom. The superoperator $\Pi^\sigma(t,t_0)$ can be again calculated using the renormalized perturbation series, Eq. (122), which the super-Pauli principle now truncates at the one-loop order:

$$\Pi^\sigma(t,t_0) = \bar\Pi^\sigma_0(t,t_0) + \bar\Pi^\sigma_2(t,t_0). \tag{F3}$$

Here $\bar\Pi^\sigma_0(t,t_0) = e^{-i\bar L_\sigma(t-t_0)}$ with $\bar L_\sigma = L_\sigma + \bar\Sigma_\sigma$. In turn, $\bar\Sigma_\sigma$ and $\bar\Pi^\sigma_2(t,t_0)$ are defined by Eqs. (96) and (128), respectively, by leaving out the summation over the spin index, fixing it to the value σ, and in Eq. (128) replacing $\bar L \to \bar L_\sigma$ in the exponential prefactor. Inserting Eq. (F2) into Eq. (F1c) and comparing order by order with the expansion Eq. (122), we obtain

$$\bar\Pi_0(t,t_0) = \bar\Pi^\uparrow_0(t,t_0)\bar\Pi^\downarrow_0(t,t_0) = e^{-i\sum_\sigma \bar L_\sigma(t-t_0)}, \tag{F4a}$$

$$\bar\Pi_2(t,t_0) = \sum_\sigma \bar\Pi^\sigma_0(t,t_0)\bar\Pi^{\bar\sigma}_2(t,t_0), \tag{F4b}$$

$$\bar\Pi_4(t,t_0) = \bar\Pi^\uparrow_2(t,t_0)\bar\Pi^\downarrow_2(t,t_0)$$

$$= \frac{1}{2}\sum_\sigma \bar\Pi^\sigma_2(t,t_0)\bar\Pi^{\bar\sigma}_2(t,t_0)$$

$$= \frac{1}{2}\bar\Pi_2(t,t_0)e^{i\bar L(t-t_0)}\bar\Pi_2(t,t_0), \tag{F4c}$$

where we used in the last step that $[\bar\Pi^\sigma_2(t,t_0)]^2 = 0$ by the super-Pauli principle (62). The last equation is the factorization relation (138) obtained in the main text.

[1] L. P. Kouwenhoven, S. Jauhar, K. McCormick, D. Dixon, P. L. McEuen, Y. V. Nazarov, N. C. van der Vaart, and C. T. Foxon, Phys. Rev. B **50**, R2019 (1994).

[2] M. Switkes, C. M. Marcus, K. Campman, and A. C. Gossard, Science **283**, 1905 (1999).

[3] T. Fujisawa, D. G. Austing, Y. Tokura, Y. Hirayama, and S. Tarucha, J. Phys. Cond. Mat. **15**, R1395 (2003).

[4] J. M. Elzerman, R. Hanson, L. H. W. van Beveren, B. Witkamp, L. M. K. Vandersypen, and L. P. Kouwenhoven, Nature (London) **430**, 431 (2004).

[5] R. Hanson, L. H. Willems van Beveren, I. T. Vink, J. M. Elzerman, W. J. M. Naber, F. H. L. Koppens, L. P. Kouwenhoven, and L. M. K. Vandersypen, Phys. Rev. Lett. **94**, 196802 (2005).

[6] J. Gabelli, G. Fève, J.-M. Berroir, B. Plaçais, A. Cavanna, B. Etienne, Y. Jin, and D. C. Glattli, Science **313**, 499 (2006).

[7] G. Fève, A. Mahé, J.-M. Berroir, T. Kontos, B. Plaçais, D. C. Glattli, A. Cavanna, B. Etienne, and Y. Jin, Science **316**, 1169 (2007).

[8] S. Amasha, K. MacLean, I. P. Radu, D. M. Zumbühl, M. A. Kastner, M. P. Hanson, and A. C. Gossard, Phys. Rev. Lett. **100**, 046803 (2008).

[9] R. Hanson, L. P. Kouwenhoven, J. R. Petta, S. Tarucha, and L. M. Vandersypen, Rev. Mod. Phys. **79**, 1217 (2007).

[10] F. A. Zwanenburg, A. S. Dzurak, A. Morello, M. Y. Simmons, L. C. L. Hollenberg, G. Klimeck, S. Rogge, S. N. Coppersmith, and M. A. Eriksson, Rev. Mod. Phys. **85**, 961 (2013).

[11] B. Roche, R.-P. Riwar, B. Voisin, E. Dupont-Ferrier, R. Wacquez, M. Vinet, M. Sanquer, J. Splettstoesser, and X. Jehl, Nat. Commun. **4**, 1581 (2013).

[12] K. K. Likharev, Proc. IEEE **87**, 606 (1999).

[13] S. Kurth, G. Stefanucci, E. Khosravi, C. Verdozzi, and E. K. U. Gross, Phys. Rev. Lett. **104**, 236801 (2010).

[14] O. Zarchin, M. Zaffalon, M. Heiblum, D. Mahalu, and V. Umansky, Phys. Rev. B **77**, 241303(R) (2008).

[15] T. Delattre, C. Feuillet-Palma, L. G. Herrmann, P. Morfin, J.-M. Berroir, G. Fève, B. Plaçais, D. C. Glattli, M.-S. Choi, C. Mora, and T. Kontos, Nat. Phys. **5**, 208 (2009).

[16] Y. Yamauchi, K. Sekiguchi, K. Chida, T. Arakawa, S. Nakamura, K. Kobayashi, T. Ono, T. Fujii, and R. Sakano, Phys. Rev. Lett. **106**, 176601 (2011).

[17] J. Basset, A. Y. Kasumov, C. P. Moca, G. Zaránd, P. Simon, H. Bouchiat, and R. Deblock, Phys. Rev. Lett. **108**, 046802 (2012).

[18] F. B. Anders and A. Schiller, Phys. Rev. Lett. **95**, 196801 (2005).

[19] A. Hackl, D. Roosen, S. Kehrein, and W. Hofstetter, Phys. Rev. Lett. **102**, 219902(E) (2009).

[20] D. Lobaskin and S. Kehrein, Phys. Rev. B **71**, 193303 (2005).

[21] P. Wang and S. Kehrein, Phys. Rev. B **82**, 125124 (2010).

[22] A. Goker, B. A. Friedman, and P. Nordlander, J. Phys.: Condens. Matter **19**, 376206 (2007).

[23] C. Jung, A. Lieder, S. Brener, H. Hafermann, A. C. B. Baxevanis, A. N. Rubtsov, M. I. Katsnelson, and A. I. Lichtenstein, Ann. Phys. **524**, 49 (2012).

[24] M. Pletyukhov, D. Schuricht, and H. Schoeller, Phys. Rev. Lett. **104**, 106801 (2010).

[25] G. Cohen, E. Gull, D. R. Reichman, A. J. Millis, and E. Rabani, Phys. Rev. B **87**, 195108 (2013).

[26] S. Weiss, J. Eckel, M. Thorwart, and R. Egger, Phys. Rev. B **77**, 195316 (2008).

[27] F. B. Anders and A. Schiller, Phys. Rev. B **74**, 245113 (2006).

[28] R. Härtle, G. Cohen, D. R. Reichman, and A. J. Millis, Phys. Rev. B **88**, 235426 (2013).

[29] G. Cohen, E. Gull, D. R. Reichman, and A. J. Millis, Phys. Rev. Lett. **112**, 146802 (2014).

[30] R. B. Saptsov and M. R. Wegewijs, Phys. Rev. B **86**, 235432 (2012).

[31] L. D. Contreras-Pulido, J. Splettstoesser, M. Governale, J. König, and M. Büttiker, Phys. Rev. B **85**, 075301 (2012).

[32] J. Splettstoesser, M. Governale, J. König, and M. Büttiker, Phys. Rev. B **81**, 165318 (2010).

[33] J. Schulenborg, J. Splettstoesser, M. Governale, and L. D. Contreras-Pulido, Phys. Rev. B **89**, 195305 (2014).

[34] R. B. Saptsov, M. R. Wegewijs, and A. Cottet (unpublished).

[35] S. Andergassen, V. Meden, H. Schoeller, J. Splettstoesser, and M. Wegewijs, Nanotechnology **21**, 272001 (2010).

[36] H. Schoeller and G. Schön, Phys. Rev. B **50**, 18436 (1994).

[37] J. König, H. Schoeller, and G. Schön, Phys. Rev. Lett. **78**, 4482 (1997).

[38] J. Kern and M. Grifoni, Eur. Phys. J. B **86**, 384 (2013).

[39] B. Kubala and J. König, Phys. Rev. B **73**, 195316 (2006).

[40] M. Leijnse and M. R. Wegewijs, Phys. Rev. B **78**, 235424 (2008).

[41] S. Koller, M. Grifoni, M. Leijnse, and M. R. Wegewijs, Phys. Rev. B **82**, 235307 (2010).

[42] R. Schleser, T. Ihn, E. Ruh, K. Ensslin, M. Tews, D. Pfannkuche, D. C. Driscoll, and A. C. Gossard, Phys. Rev. Lett. **94**, 206805 (2005).

[43] A. K. Hüttel, B. Witkamp, M. Leijnse, M. R. Wegewijs, and H. S. J. van der Zant, Phys. Rev. Lett. **102**, 225501 (2009).

[44] A. S. Zyazin, J. W. van den Berg, E. A. Osorio, H. S. van der Zant, N. P. Konstantinidis, F. May, M. Leijnse, W. Hofstetter, M. R. Wegewijs, C. Danieli, and A. Cornia, Nano Lett. **10**, 3307 (2010).

[45] A. Eliasen, J. Paaske, K. Flensberg, S. Smerat, M. Leijnse, M. R. Wegewijs, H. I. Jørgensen, M. Monthioux, and J. Nygård, Phys. Rev. B **81**, 155431 (2010).

[46] C. Stevanato, M. Leijnse, K. Flensberg, and J. Paaske, Phys. Rev. B **86**, 165427 (2012).

[47] O. Klochan, A. P. Micolich, A. R. Hamilton, D. Reuter, A. D. Wieck, F. Reininghaus, M. Pletyukhov, and H. Schoeller, Phys. Rev. B **87**, 201104 (2013).

[48] M. Governale, M. G. Pala, and J. König, Phys. Rev. B **77**, 134513 (2008).

[49] M. Schmutz, Z. Phys. B **30**, 97 (1978).

[50] U. Harbola and S. Mukamel, Phys. Rep. **465**, 191 (2008).

[51] H. Schoeller, Eur. Phys. J. Spec. Top. **168**, 179 (2009).

[52] T. Prosen, New. J. Phys. **10**, 043026 (2008).

[53] D. Kosov, J. Chem. Phys. **131**, 171102 (2009).

[54] A. A. Dzhioev and D. S. Kosov, J. Phys.: Condens. Matter **24**, 225304 (2012).

[55] J. König, H. Schoeller, and G. Schön, Phys. Rev. Lett. **76**, 1715 (1996).

[56] J. König, J. Schmid, H. Schoeller, and G. Schön, Phys. Rev. B **54**, 16820 (1996).

[57] A. Dzhioev and D. Kosov, J. Chem. Phys. **134**, 044121 (2011).

[58] A. Kamenev and A. Levchenko, Adv. Phys. **58**, 197 (2009).

[59] S. G. Jakobs, M. Pletyukhov, and H. Schoeller, J. Phys. A: Math. Theor. **43**, 103001 (2010).

[60] G. C. Wick, A. S. Wightman, and E. P. Wigner, Phys. Rev. **88**, 101 (1952).

[61] For instance, it was shown that the proof of the Liouville-space Wick theorem for fermions [51] simplifies greatly when using causal superfermions, reducing to the standard proof by Gaudin [114]. Moreover, the causal structure [58] of the reservoir Green's functions in the WBL was shown to lead to an exponential reduction of the number of diagrams contributing to the self-energy. Also, an algebraic term-by-term proof of the bandwidth-independence of the perturbation theory was suggested, relating it to the completeness of the basis used for the reduced system.

[62] F. Reckermann, Ph.D. thesis, RWTH-Aachen University, 2010.

[63] M. Hell, Master's thesis, RWTH-Aachen University, 2011.

[64] N. Gergs, Master thesis, RWTH-Aachen University, 2013.

[65] M. Hell, S. Das, and M. R. Wegewijs, Phys. Rev. B **88**, 115435 (2013).

[66] J. Splettstoesser, M. Governale, and J. König, Phys. Rev. B **86**, 035432 (2012).

[67] A. Oguri and R. Sakano, Phys. Rev. B **88**, 155424 (2013).

[68] G. Cohen and E. Rabani, Phys. Rev. B **84**, 075150 (2011).

[69] G. Cohen, E. Y. Wilner, and E. Rabani, New. J. Phys. **15**, 073018 (2013).

[70] D. Segal, A. J. Millis, and D. R. Reichman, Phys. Rev. B **82**, 205323 (2010).

[71] D. Segal, A. J. Millis, and D. R. Reichman, Phys. Chem. Chem. Phys. **13**, 14378 (2011).

[72] M. Kulkarni, K. Tiwari, and D. Segal, New. J. Phys. **15**, 013014 (2013).

[73] H. Schoeller, *Mesoscopic Electron Transport* (Kluwer, Dordrecht, 1997), p. 291.

[74] H. Schoeller, *Interactions and Transport Properties* (Springer, Berlin, 1999), p. 137.

[75] S. Andergassen, M. Pletyukhov, D. Schuricht, H. Schoeller, and L. Borda, Phys. Rev. B **83**, 205103 (2011).

[76] J. Maciejko, J. Wang, and H. Guo, Phys. Rev. B **74**, 085324 (2006).

[77] J. Jin, M. W.-Y. Tu, W.-M. Zhang, and Y. Yan, New. J. Phys. **12**, 083013 (2010).

[78] C. Caroli, R. Combescot, P. Nozieres, and D. Saint-James, J. Phys. C **4**, 916 (1971).

[79] D. C. Langreth and P. Nordlander, Phys. Rev. B **43**, 2541 (1991).

[80] Y. Aharonov and L. Susskind, Phys. Rev. **155**, 1428 (1967).

[81] N. N. Bogolubov, A. A. Logunov, A. I. Oksak, and I. T. Todorov, *General Principles of Quantum Field Theory* (Nauka, Moscow, 1987) [in Russian; English translation, Kluwer Academic, Dordrecht, 1989].

[82] C. W. Gardiner, Opt. Commun. **243**, 57 (2004).

[83] L. D. Landau and E. M. Lifshitz, *Quantum Mechanics: Non-relativistic Theory* (Butterworth-Heinemann, Oxford, UK, 1977).

[84] R. B. Saptsov and M. R. Wegewijs (unpublished).

[85] The operators n_σ and $\mathbf{S}$ have the same form in terms of d_1 operators as in terms of d_1'; see discussion after Eq. (29).

[86] Although the multi-indices of the reservoirs contain additional variables, we use the same notation for them. No confusion should arise since it is always clear from the context to which type of operator (dot, reservoir) the given multi-index belongs.

[87] For models with particle nonconserving terms, additional signs may however appear which change the *form* of the model Hamiltonian expressed in terms of the new variables. This is only a change of variables and the change of the Hamiltonian form does not alter the physics.

[88] C. Timm, Phys. Rev. B **77**, 195416 (2008).

[89] C. Emary, Phys. Rev. B **80**, 235306 (2009).

[90] M. Pletyukhov and H. Schoeller, Phys. Rev. Lett. **108**, 260601 (2012).

[91] C. Karrasch, S. Andergassen, M. Pletyukhov, D. Schuricht, L. Borda, V. Meden, and H. Schoeller, Eur. Phys. Lett. **90**, 30003 (2010).

[92] C. B. M. Hörig, D. Schuricht, and S. Andergassen, Phys. Rev. B **85**, 054418 (2012).

[93] A. Thielmann, M. H. Hettler, J. König, and G. Schön, Phys. Rev. B **68**, 115105 (2003).

[94] A. Braggio, J. König, and R. Fazio, Phys. Rev. Lett. **96**, 026805 (2006).

[95] C. Flindt, T. Novotný, A. Braggio, M. Sassetti, and A.-P. Jauho, Phys. Rev. Lett. **100**, 150601 (2008).

[96] C. Flindt, T. Novotný, A. Braggio, and A.-P. Jauho, Phys. Rev. B **82**, 155407 (2010).

[97] H.-P. Breuer and F. Petruccione, *The Theory of Open Quantum Systems* (Oxford University Press, Oxford, U.K., 2002).

[98] J. Splettstoesser, M. Governale, J. König, and R. Fazio, Phys. Rev. Lett. **95**, 246803 (2005).

[99] J. Splettstoesser, M. Governale, J. König, and R. Fazio, Phys. Rev. B **74**, 085305 (2006).

[100] O. Kashuba, H. Schoeller, and J. Splettstoesser, Eur. Phys. Lett. **98**, 57003 (2012).

[101] L. D. Landau and E. M. Lifshitz, *Statistical Physics* (Pergamon, Oxford, 1980), Part 2.

[102] E. Fick and G. Sauermann, *The Quantum Statistics of Dynamic Processes*, Springer Series in Solid-State Sciences (Springer-Verlag, Berlin, 1990).

[103] U. Fano, Rev. Mod. Phys. **29**, 74 (1957).

[104] S. Mukamel, *Principles of Nonlinear Optical Spectroscopy* (Oxford University Press, Oxford, UK, 1995).

[105] M. Esposito, U. Harbola, and S. Mukamel, Rev. Mod. Phys. **81**, 1665 (2009).

[106] The definitions $G^\pm$ in Eq. (46) and $J^\pm$ in (47) differ from those in Ref. [30] [Eqs. (51) and (52), respectively] by using the opposite convention for the sign of q. This is effected by placing the field operators d_1 and b_1 to the right of the operators $(-1)^n$ and $(-1)^{n^R}$ in Eqs. (46) and (47), respectively. In contrast to Eqs. (51) and (52) in Ref. [30], we here explicitly write the superoperators $p^{L^n}\bullet = p^n \bullet p^n$, $(p=\pm,\ p^{2n}=1)$. However, the definitions of $\bar{G}$ and $\tilde{G}$ Eq. (49) coincide with those of Ref. [30]. Here we favor $q=+$ for "creation" $(G^+=\bar{G})$ and $q=-$ for "destruction" superoperators $(G^-=\tilde{G})$ [but opposite in the reservoirs, cf. Eq. (47)], tying in better with the discussion of second quantization to Liouville space. The opposite convention used in Ref. [30] agrees better with that used for "quantum" and "classical" fields obtained by the Keldysh rotation in the path integral approach of Kamenev *et al.* [58].

[107] Although one should in general carefully distinguish between Hermitian and super-Hermitian conjugation, we use the same notation $\dagger$ for both since it is always clear from the context whether we deal with a super- or usual operator.

[108] Here, we insert $(-1)^n$ for the argument of Eq. (56a) (the bullet $\bullet$) and make use of $(-1)^n(-1)^n = 1$.

[109] R. B. Saptsov and M. R. Wegewijs (unpublished).

[110] The fermion-parity guarantees orthogonality, $(\alpha_1^+|\alpha_2^-) \propto \mathrm{Tr}_D d_1^\dagger(-1)^n d_2 = \mathrm{Tr}_D(-1)^n d_2 d_1^\dagger = 0$, since $\mathrm{Tr}_D[(-1)^n\bullet] = \sum_{n_\uparrow n_\downarrow}(-1)^{n_\uparrow+n_\downarrow}\langle n_\uparrow n_\downarrow|\bullet|n_\uparrow n_\downarrow\rangle = 0$ for any one-particle operator since the matrix element is independent of $n_\uparrow$ or $n_\downarrow$ (or both).

[111] This connects to the other possible construction of the Liouville-Fock space, starting from the fermion-parity operator $|Z_R) = \frac{1}{2}(-1)^n$ as the vacuum state, which is annihilated by the creation operator $G_1^+ = \bar{G}_1$ by the fundamental relation (55): $\bar{G}_{\eta\sigma}|Z_R) = 0$. See Ref. [30], Appendix E, for a systematic discussion.

[112] Note that the total superoperator $\sum_{\eta,\sigma}\mathcal{N}_{\eta\sigma}$ counting the occupation of the basis superkets Eqs. (60) and (61) does *not* equal the superoperator defined by the commutator with the particle number operator, $[n,\bullet]$.

[113] In Eq. (76) all free dot propagators $e^{-iL(t_{k+1}-t_k)}$ between the vertices $G_{k+1}^{q_{k+1}}$ and $G_k^{q_k}$ for $k \neq 2$ are denoted as ellipsis "..." for compactness.

[114] M. Gaudin, Nucl. Phys. **15**, 89 (1960).

[115] A.-P. Jauho, N. S. Wingreen, and Y. Meir, Phys. Rev. B **50**, 5528 (1994).

[116] Also here one must be careful with physically interpreting the expressions: The action of a field superoperator G_1^q results in a Liouville-space superposition of terms with a definite Keldysh contour index. Only the latter can be identified with a "process" generated by the total Hamiltonian H^{tot} [Eq. (32)].

[117] See Secs. II 3b and II 3c in Ref. [30] for a corresponding argument in frequency space.

[118] See Ref. [30] for a Laplace space argument.

[119] L. Levitov and A. Shytov, *Green's Functions: Theory and Practice* (FizMatLit, 2002) [only in Russian], www.mit.edu/~levitov/book/

[120] C. Timm, Phys. Rev. B **83**, 115416 (2011).

[121] J. Schulenborg, Master thesis, RWTH-Aachen University, 2013.

[122] For the full expression for Eq. (113b) see Eq. (135) in Ref. [30].

[123] The $T \to \infty$ self-energy $\tilde{\Sigma}$ is quadratic in general due to the WBL. Therefore, the Liouville-Fock basis Eqs. (60) and (61) is an eigenbasis, also when generalized to multiorbital Anderson models. However, when including more general interaction terms in L for such models, it may be that the bosonic blocks of L and $\tilde{\Sigma}$ do not commute and have no common eigenbasis. In this case, the diagonalization of $\bar{L}$ may be less simple.

[124] Note that *fermionic* basis superkets are *not* supereigenkets of L for $U \neq 0$, due to Eq. (77)]; see Ref. [30].

[125] For finite temperature *and* $U \neq 0$ the fermionic part of $\bar{L}$, not given in Eq. (114), is needed to describe virtual intermediate renormalized time evolution; see the discussion of Eq. (76). In the $U = 0$ illustrations in this paper, it is not needed.

[126] To obtain Eqs. (124) and (125), (i) insert the finite expansions Eq. (122) and (123) into the renormalized Dyson equation (104); (ii) use that $\bar{\Sigma}_2$ and $\bar{\Sigma}_4$ commute with $\bar{\Pi}_0$ up to unimportant c-number factors; and (iii) use that—ignoring $\bar{\Pi}_0$—by Eq. (62): $(\bar{\Sigma}_2)^\alpha(\bar{\Sigma}_4)^\beta = 0$ when it contains $2\alpha + 4\beta \geqslant 4$ superfields, leaving only four combinations $(\alpha,\beta) = (0,0),(1,0),(2,0),(1,1)$.

[127] For $U \neq 0$ Eq. (121) is no longer valid. In this case, nonzero terms arise beyond the second order in the general expansion Eq. (99b). The reason is that if one tries to commute $\bar{L} = L + \bar{\Sigma}$ to the left—containing a quartic term [Eq. (74)]—this generates terms containing destruction superoperators $\tilde{G}_1$, which are not required to vanish by the super-Pauli principle. We note that by our discussion of Eq. (76) (taking $q_4 = q_3 = q_2 = q_1 = +$) this effect of the quartic terms in L is restricted to only half of the propagators in virtual intermediate states.

[128] As pointed out in Ref. [30], for selected quantities such as the charge current a one-loop RT-RG approximation already includes the noninteracting limit. A recent perturbative study indicates that for thermoelectric transport such fortuitous simplifications are absent [64].

[129] Here "quartic" refers to the total power of field operators $\bar{G}_1'(t)$ in the (renormalized) interaction picture [Eq. (100)]. For $U = 0$ this is proportional to the original creation superoperator $\bar{G}_1$ [Eq. (119)]. However, for $U \neq 0$ explicit calculation of $\bar{G}_1'(t)$ shows it additionally contains destruction superoperators $\tilde{G}$. In this case, the super-Pauli principle cannot truncate the perturbation series after the second order.

[130] Alternatively, one can make use of the explicit basis expansion of the creation superoperator $\bar{G}$ defined by Eq. (118) and Eq. (120) in Ref. [30].

[131] A. Erdély, W. Magnus, F. Oberhettinger, and F. Tricomi, *Higher Transcendental Functions* (McGraw-Hill, New York, 1953), Vol. 1.

[132] Note that the stationary contributions to $\rho(t)$ are generated by terms in $\Pi(t,t_0)$ [Eq. (141)] of the form $|A(t))(Z_L|$: since by probability conservation any possible $\rho(t_0)$ contains $\frac{1}{2}|Z_L)$ in its expansion [see Eq. (68) with $t = t_0$], we have $|A(t))(Z_L|\rho(t_0)) = \frac{1}{2}|A(t))$, independent of $\rho(t_0)$.

[133] This can be seen from Eq. (151) in Ref. [30].

[134] T. L. Schmidt, P. Werner, L. Mühlbacher, and A. Komnik, Phys. Rev. B **78**, 235110 (2008).

[135] For spin-independent tunneling $\Gamma_{r\sigma} = \tilde{\Gamma}$, this $3\tilde{\Gamma}$ decay rate already appeared as the imaginary part of one of the eigenvalues of the noninteracting Anderson model ($U = 0$); see Eq. (244) of Ref. [30]. This eigenvalue was found [30] to drop out of the calculation of the stationary current and the single-level occupancies. Note that in Ref. [30] Eq. (244) does not follow from RG considerations, but rather directly from the renormalized perturbation theory, in particular Eq. (163) there. It also does not make use of the $T \to 0$ limit. See also Sec. IV B 2 a.

[136] A. Komnik, Phys. Rev. B **79**, 245102 (2009).

[137] That, indeed, no zero can appear in the denominator is related to the causal structure Eq. (156) and to the stationary properties of the infinite-temperature self-energy discussed in Sec. III C 3. By the causal property Eq. (54), the creation superoperators $\bar{G}_1$ have a left zero eigenvector $(Z_L|$ which is *unique*, as mentioned in Sec. III C 2. At the same time, $|Z_L)$, the stationary $T \to \infty$ density operator, is the *unique* right zero eigenvector of $\bar{L} = L + \bar{\Sigma}$, even when accounting for the both the bosonic and the fermion diagonal blocks [30]. Therefore, when inserting a complete set of superkets in the superoperator expressions $(z - \bar{L} + X_k)^{-1}\bar{G}_1$ the only zero of $\bar{L}$, occurring for $|Z_L)$, is canceled by the vanishing of the projection $(Z_L|\bar{G}_1$. Finally, one could worry that insertion of $|Z_L)(Z_L|$ could generate a zero in the leftmost expression $\bar{G}_1(z - \bar{L} + X_k)^{-1}$ in Eq. (156), since for the $T \to \infty$ limit the superadjoint $|Z_L)$ is the corresponding right zero eigenvector of the effective Liouvillian $\bar{L}$ [cf. discussion in Sec. III C 3]. However, this zero is canceled as well by the adjacent creation superoperator on the right: $\bar{G}_1|Z_L)(Z_L|(z - \bar{L} + X_k)^{-1}\bar{G}_2 = \bar{G}_1(z + X_k)^{-1}|Z_L)(Z_L|\bar{G}_2 = 0$.

[138] T. Korb, F. Reininghaus, H. Schoeller, and J. König, Phys. Rev. B **76**, 165316 (2007).

[139] That the rate $3\tilde{\Gamma}$ drops out for $U = 0$ was shown in Ref. [30], Sec. III C 3, due to the vanishing of a propagator supermatrix element, Eq. (246) of that reference. For $U \neq 0$, this matrix element does not vanish, and as a result the RG flow is affected by this decay rate.

[140] The limit considered in Ref. [30] corresponds to the case: $\Gamma_{r\sigma} = \tilde{\Gamma}$ for all r,σ. The coefficient before the first term in Eq. (168) is then $\Gamma = \sum_{r,\sigma}\Gamma_{r\sigma} = 4\tilde{\Gamma}$. This Γ [from (168)] should not be confused with one used in Ref. [30], the latter corresponds to the $\tilde{\Gamma}$ in the present notations.

[141] $\mathsf{Tr}_D\,\Sigma^r = 0$ does *not* follow from probability conservation, which only requires $\mathsf{Tr}_D\sum_r \Sigma^r = 0$. The causal structure is a stronger constraint.

[142] Note that although $\tilde{\Sigma}^r(t,t')$ is the (reservoir-resolved) $T \to \infty$ self-energy, $\tilde{I}^r(t)$ is *not* simply the $T \to \infty$ current.

[143] In Ref. [134], also the first-order expansion in U as well as Monte Carlo simulations for an arbitrary U were discussed.

[144] The results of Ref. [77] seem to be at variance with other known solutions [75, 134] and with ours. These authors used a Feynman path integral to derive a convolutionless master equation. We have carefully checked our result against theirs by using the identity $T/\sinh(\pi T\tau) = i\int_{-\infty}^{+\infty} e^{-i\omega\tau}\tanh(\frac{\omega}{2T})\frac{d\omega}{2\pi}$ to rewrite our explicitly evaluated current Eq. (179) in the form of an unevaluated ω integral, as is done in Ref. [77]. We find that our result, Eq. (179) (and therefore that of others [75, 134]), can only be recovered by adding by hand a term to Eq. (35) of Ref. [77] that seems to be missing: $\Gamma_{r\sigma}e^{-(\Gamma_\sigma/2)\Delta}\int\frac{d\omega}{2\pi}\{\frac{(\Gamma_\sigma/2)\cos[(\omega-\epsilon)\Delta]}{(\omega-\epsilon)^2+(\Gamma/2)^2} - \frac{(\omega-\epsilon)\sin[(\omega-\epsilon)\Delta]}{(\omega-\epsilon)^2+(\Gamma/2)^2}\}|$, considering only one spin orbital σ, as has been done in Ref. [77]. The result for the initial current in Ref. [77], $-\Gamma_{r\sigma}n_\sigma(t_0)$, also deviates from the results of other works and our Eq. (180), by missing the term $\Gamma_{r\sigma}/2$ (resulting from the preceding equation for $\Delta = 0$, and writing again fixed spin σ). As a consequence, the result of Ref. [77] also does not seem to fit in the intuitive physical picture sketched in Ref. [134] after Eq. (36) and here after Eq. (180). It is puzzling why, despite these differences, the result of Ref. [77] for the average dot occupation number does coincide with that of other works [75, 134] and with our Eq. (143). The authors of Ref. [77], discussing their results for the current, Eqs. (38) and (39a) in Ref. [77], only mention that that "some of their results [for the the current] were also obtained using nonequilibrium Green function technique [134]" without mentioning or investigating the discrepancy with Ref. [134]. The results of the present paper and of Ref. [75] confirm the results of Ref. [134] without

using the $t_0 \to -\infty$ limit which can thus not be used to explain the difference with the results Ref. [77]. The use of this limit, commonly assumed in Keldysh Green's function techniques, was criticized in Ref. [77] and distinguishes their method from that of Ref. [134].

[145] In Ref. [134] the artificial instantaneous current due to the WBL was physically related to the infinite*bias* limit $V_b \to +\infty$. In Ref. [155] it was shown that for symmetric tunnel coupling this is equivalent to the $T \to \infty$ limit. Here we discuss spin- and reservoir-dependent tunneling for which no such equivalence seems be known [67]. Still, the $T \to \infty$ limit provides the essential physical starting point. Moreover, our analysis simply extends to an arbitrary number of reservoirs.

[146] J. König and J. Martinek, Phys. Rev. Lett. **90**, 166602 (2003).

[147] J. Martinek, M. Sindel, L. Borda, J. Barnaś, J. König, G. Schön, and J. von Delft, Phys. Rev. Lett. **91**, 247202 (2003).

[148] M.-S. Choi, D. Sánchez, and R. López, Phys. Rev. Lett. **92**, 056601 (2004).

[149] M. Braun, J. König, and J. Martinek, Phys. Rev. B **70**, 195345 (2004).

[150] J. Martinek, M. Sindel, L. Borda, J. Barnaś, R. Bulla, J. König, G. Schön, S. Maekawa, and J. von Delft, Phys. Rev. B **72**, 121302 (2005).

[151] Formally, for $U = 0$ the stationary state has a form that allows for a Wick theorem on the *quantum dot*, although with *unknown* nonequilibrium parameters $\Phi_\sigma(\infty) = \langle n_\sigma \rangle(\infty) - 1/2$. This is especially clear in terms of superfermions: There is a formal analogy between the nonequilibrium dot stationary state Eq. (169b), which can be written as $\rho(\infty) = \frac{1}{2}\exp[2\sum_\sigma \Phi_\sigma(\infty)\bar{G}_{+\sigma}\bar{G}_{-\sigma}]|Z_L)$, and the thermal-equilibrium state, written as $\rho_{\rm eq} = \exp(-\epsilon_\sigma n_\sigma/T)/Z = \frac{1}{2}\exp[-\sum_\sigma \tanh(\epsilon_\sigma/2T)\bar{G}_{+\sigma}\bar{G}_{-\sigma}]|Z_L)$. The nonequilibrium analog of the fluctuation-dissipation relation Eq. (88) for the dot then reads as $\tilde{G}_1\rho(\infty) = -2\eta\Phi_\sigma\bar{G}_1\rho(\infty)$. The Wick theorem for the dot in this case can be proven in full analogy with the equilibrium reservoir Wick theorem [30], although the dot Keldysh contraction functions are not, in general, expressible via $\tanh(\epsilon/2T)$: $\bar{\gamma}_{\rm dot} = \langle \tilde{G}_1\tilde{G}_2\rangle \propto -\eta_1\Phi_{\sigma_1} \not\propto \tanh(\eta_1\epsilon/2T)$. Before stationarity is reached ($t_0 < t < \infty$), this analogy does not apply unless one starts at t_0 from a quantum-dot state without two-particle correlations.

[152] S. A. Gurvitz and Y. S. Prager, Phys. Rev. B **53**, 15932 (1996).

[153] S. A. Gurvitz, Phys. Rev. B **56**, 15215 (1997).

[154] B. Wunsch, M. Braun, J. König, and D. Pfannkuche, Phys. Rev. B **72**, 205319 (2005).

[155] A. Oguri, J. Phys. Soc. Jpn. **71**, 2969 (2002).

[156] M. Marthaler, Y. Utsumi, D. S. Golubev, A. Shnirman, and G. Schön, Phys. Rev. Lett. **107**, 093901 (2011).

[157] This is because the superoperator expansion of the nonquadratic part of the Liouvillian, Eq. (74b), always contains a term *decreasing* the number of superparticles by two: The first term in Eq. (74b), $\bar{G}_{\eta\sigma}\tilde{G}_{\bar{\eta}\sigma}\tilde{G}_{\eta\bar{\sigma}}\tilde{G}_{\bar{\eta}\bar{\sigma}}$, contains one creation superoperator $\bar{G}_{\eta\sigma}$ and three destruction superoperators $\tilde{G}_{\bar{\eta}\sigma}\tilde{G}_{\eta\bar{\sigma}}\tilde{G}_{\bar{\eta}\bar{\sigma}}$ and thus decreases the total number of superfermions by two. In contrast, each pair of Keldysh contracted creation superoperators always *increases* this number by two. Since the total number of superfermions cannot exceed four by super-Pauli principle, the terms with more than $(2 + m)$ loops are identically equal to zero for given m.

[158] One can, in principle, formulate the problem in terms of $\mathfrak{J}$ and $\mathfrak{G}$ superoperators, separate $\mathfrak{G}$ and $\mathfrak{J}$, and then project the $\mathfrak{G}$ defined in the global reservoir-dot Liouville space onto the local superoperators G, Eq. (46). This involves, however, unnecessary complications.